Compartmentalised modulation of cardiac cAMP by β-adrenergic receptor antagonists

Brandon Shu Huang Low

Balliol College

University of Oxford

A thesis submitted for the degree of

Master of Science (Research)

Trinity 2026

Abstract

Compartmentalisation of 3',5'-cyclic adenosine monophosphate (cAMP) enables spatially restricted signalling pools to govern cardiac function in a stimulus-specific manner. These subcellular nanodomains are regulated by A-kinase anchoring proteins (AKAPs) and local phosphodiesterases (PDEs). However, a less characterised aspect of spatial organisation is how receptor and ligand identity shape this specificity. This question is integral to the β-adrenergic receptors (β-ARs) that generate cardiac cAMP in response to catecholamines and the antagonists that target them.

β-blockers are a mainstay of heart failure (HF) therapy, yet their clinical effects are heterogeneous. Only three agents have been FDA-approved for chronic heart failure, and how individual agents engage spatial cAMP signalling is incompletely understood. This thesis investigates how different β-AR blockers shape downstream cAMP compartmentalisation.

Fluorescence resonance energy transfer (FRET) based biosensors were targeted to defined subcellular compartments, including the cytosol, plasmalemma (AKAP-79), sarcoplasmic reticulum (AKAP-18δ) and myofilament (Troponin I). The cAMP responses to carvedilol, bucindolol and metoprolol were measured in neonatal rat ventricular myocytes, alone or in combination with isoproterenol. All three β-blockers suppressed isoproterenol-stimulated cAMP, but the degree of antagonism varied across compartments.

Carvedilol and bucindolol behaved as partial agonists with distinct, compartment-specific intrinsic sympathomimetic activity (ISA). Selective β1- and β2-AR blockade revealed that carvedilol's ISA is predominantly β2-AR-mediated

whereas bucindolol is β1-AR-mediated. Notably, the AKAP-18δ signalosome at the SERCA/PLB complex was insensitive to carvedilol's partial agonism but responsive to bucindolol's. By sparing this diastolic calcium-handling domain, this exclusion may contribute to carvedilol's clinical superiority in HF, where diastolic function and myocardial energetics are already compromised. Altogether, these findings identify subcellular location as an exploitable facet for future GPCR-targeted therapeutics aimed at improving signalling specificity and reducing off-target effects.

Declaration

I hereby declare that the work reported in this thesis is my own unless stated otherwise. Any work completed by a third party will be duly acknowledged. The content of this work has not been submitted for any other degree or qualification.

Acknowledgements

This research would not be possible without the support of many integral and exceptional individuals and groups. First and foremost, I would like to thank my supervisor Professor Manuela Zaccolo for her steadfastness, reassurance, support and scientific guidance since the start of my project. Her encouragement and discussions have been an extraordinary drive towards my development as a researcher. Thank you for giving the chance to the then year 2 medical student, who emailed deciding to apply to Oxford on an Easter holiday. I am forever grateful; for this and all the opportunities you have provided from symposiums to conferences.

To the members of the Zaccolo Group during my time – Alex, Yvette, Inky and Rahul – thank you for your assistance and kindness in the lab. I want to thank Alex for showing me the ropes when I first began and answering the many, many questions I had along the way. His patience and natural gift for teaching are deeply appreciated. Special mention should also be given to Yvette, without whom I would not have been able to complete this 1–2-year degree under my 10-month time constraint. Her teaching has given me, a medical student with no prior research experience, both the confidence and foundation to develop a deeper appreciation for lab protocols and skills. I wish them all the best in their continued journey beyond the lab. Outside the group, I want to thank the GSDS team and group for their supplementary support in shaping me as a researcher. Moreover, I would want to thank my college advisor, Dr Robin Choudhury, for our insightful discussions and his support towards all my endeavours beyond research.

I want to express gratitude to the Department of Physiology, Anatomy and Genetics for their sponsorship of various studentships including my conference travel grant. Furthermore, to the generous donors of Balliol College for providing research support but also allowing me to explore my interests in artificial intelligence and entrepreneurship. Only from this was I able to explore my passions in computing, participating in my first few hackathons and entrepreneurial fellowships. My year would not have been the same without all my college friends (Ahmad, Alvin, Emil, Kazu, Merlin, Roy and many more to name) for our lovely meal-time conversations, hangouts and travels – making my time at Oxford much more enjoyable. I want to thank my closest friends at University of Birmingham Medical School for their lively visits to Oxford and continued communication with me in preparation for my return to clinical medicine.

Most of all, I am incredibly grateful to my family. My parents (Andy and Michelle) and sister (Britney) have not only provided me with financial support but emotional faith, love and a place to call home during the holidays. To my dog, Bobo, who always makes me smile.

Lastly, I would like to express my deepest gratitude and admiration to Joey for her understanding and unwavering moral support over the past four years since medical school. Her encouragement has profoundly altered the course of my academic, professional and personal journey.

Contents

Abstract 2

Declaration 4

Acknowledgements 5

List of Figures 11

List of Tables 13

List of Abbreviations 14

Chapter 1 19

Background 19

1.1 G-protein Coupled Receptors 19

1.1.1 Structure of a GPCR 20

1.1.2 Activation of the Signal 22

1.1.3 The Ending of the Signal 26

1.1.4 Biased Agonism 30

1.2 Cyclic AMP Signalling 33

1.2.1 Adenylyl Cyclase and Phosphodiesterase 34

1.2.2 Signalling Effectors 35

1.2.3 A-Kinase Anchoring Protein (AKAP) 37

1.2.4 cAMP Nanodomain Signalling 40

1.3 Optical Imaging of cAMP 42

1.3.1 Principles of FRET 42

1.3.2 Sensors for Secondary Messengers 43

1.3.3 The Epac-S^{H187} Sensor 44

1.3.4 CUTie Sensors 45

1.4 The Heart and the β-adrenoceptor 48

1.4.1 Receptor-AKAP Relationship 50
1.4.2 β-adrenoceptor Dysfunction in Cardiovascular Disease 53
1.4.3 Intracellular β-adrenergic signalling 54
1.5 β-blockers in cardiovascular disease 56
1.5.1 Pharmacological heterogeneity beyond competitive antagonism 57
1.5.2 Carvedilol 59
1.6 Thesis Aims 61
Chapter 2 64
Methodology 64
2.1 Materials 64
2.1.1 Reagents 64
2.1.2 Genetic Constructs and Biosensors 66
2.1.3 FRET sensor characteristics 69
2.2 Experimental Methods 70
2.2.1 CHO Cell Culture 70
2.2.2 Primary Neonatal Rat Ventricular Myocyte Isolation and Culture 70
2.2.3 Transfection and Infection Procedures 72
2.2.4 Fluorescence Resonance Energy Transfer (FRET) 74
2.2.5 Immunofluorescence 76
2.2.6 Data and Statistical Analysis 77
Chapter 3 79
Results 79
3.1 Differential antagonistic activity of β-AR antagonists at nanodomains 79
3.1.1 β-AR antagonists differentially inhibit ISO-stimulated cAMP across ECC nanodomains 80

3.2 Carvedilol and bucindolol have partial agonist activity in cardiac myocytes 87
3.2.1 Partial agonist behaviour exhibited by carvedilol persists at lower concentrations 89
3.2.2 Carvedilol and bucindolol elicit distinct, compartment-specific cAMP responses 91
3.2.3 A nanodomain restricted interaction between carvedilol and ISO occurs at AKAP-79 93
3.2.4 ISA-exhibiting β-AR antagonists show distinct engagement kinetics 96
3.3 Selective receptor antagonism identifies that partial agonist activity is β-AR specific 97
3.3.1 β-AR subtype dependence is observed across ECC related nanodomains 99
3.4 The AKAP-18δ signalosome identifies a confined and distinct cAMP nanodomain at the SR 104
3.4.1 β-blocker antagonism at the SR-facing cAMP pool is attenuated 105
3.4.2 Carvedilol elicits a measurable cAMP response at the SR membrane 106
3.5 Preliminary findings for a Golgi associated cAMP pool in cardiac myocytes 108
3.5.1 Bucindolol and carvedilol elicit divergent cAMP responses at the Golgi 109
Chapter 4 112
Discussion 112
4.1 Classification and pharmacology of carvedilol and bucindolol 112
4.2 Compartmentalisation of cAMP by β-adrenergic antagonists 118
4.3 β1 and β2-AR contributions to compartment-specific cAMP 123
4.4 The emerging role of intracellular receptors 128

4.5 Clinical and therapeutic implications 131
4.6 Limitations and future directions 134
Chapter 5 139
Conclusions 139
Appendix 142

List of Figures

Figure 1.1: 22

Figure 1.2:. 24

Figure 1.3: 30

Figure 1.4: 40

Figure 1.5: 47

Figure 3.1: 80

Figure 3.1.1: 82

Figure 3.1.2: 84

Figure 3.1.3: 85

Figure 3.1.4: 87

Figure 3.2.1: 89

Figure 3.2.2: 91

Figure 3.2.3: 93

Figure 3.2.4: 95

Figure 3.3.1: 98

Figure 3.3.2: 101

Figure 3.3.3: 102

Figure 3.3.4: 103

Figure 3.4.1: 106

Figure 3.4.2: 107

Figure 3.5.1: 109

Figure 3.5.2: 111

Figure S1: 142

Figure S2: 143

Figure S3:..... 144

Figure S4:..... 145

Figure S5:..... 146

List of Tables

Table 1.1: 25

Table 1.2: 38

Table 2.1: 65

Table 2.2: 66

Table 2.3: 68

Table 2.4: 69

Table 2.5: 77

Table 4.1: 114

List of Abbreviations

7TMR: 7-transmembrane receptor

AAV: Adeno-associated virus

AC: Adenylyl cyclase

AKAP: A-kinase anchoring protein

AMP: Adenosine monophosphate

ANOVA: Analysis of variance

AR: Adrenergic receptor

AT1: Angiotensin II receptor type 1

ATP: Adenosine triphosphate

β_1AR: β_1 adrenergic receptor

β_2AR: β_2 adrenergic receptor

β_3AR: β_3 adrenergic receptor

bPAC: Bacterial photoactivatable adenylyl cyclase

cAMP: 3',5'-cyclic adenosine monophosphate

cGMP: 3',5'-cyclic guanosine monophosphate

CaM: Calmodulin

CaMKII: Calcium/calmodulin-dependent kinase II

CCPs: Clathrin-coated pits

CFP: Cyan fluorescent protein

CGP-20712A: 2-hydroxy-5-[2-[[2-hydroxy-3-[4-[1-methyl-4(trifluoromethyl)-1H-imidazol-2-yl]phenoxy]propyl]amino]ethoxyl]-benzamide, monomethanesulfonate

CHF: Chronic heart failure

CHO: Chinese hamster ovary

CNBD: Cyclic-nucleotide binding domain

CNS: Central nervous system

CNGC: Cyclic nucleotide-gated channel

CREB: cAMP-response element-binding protein

CRISPR: Clustered regularly interspaced palindromic repeats

CUTie: Cyclic nucleotide Universal Tag for imaging experiments

D1R: Dopamine D1 Receptor

DAD: Delayed afterdepolarisations

DAG: Diacylglycerol

DNA: Deoxyribonucleic acid

ECC: Excitation contraction coupling

EGFR: Epidermal growth factor receptor

EL2: Extracellular loop 2

Epac: Exchange protein activated by cAMP

ER: Endoplasmic reticulum

ERK: Extracellular signalling-related kinase

FSK: Forskolin

FLIM: Fluorescence lifetime imaging microscopy

FRET: Fluorescence/Förster resonance energy transfer

GalT: Galactosyltransferase

GAPs: GTPase-activating proteins

GDP: Guanosine Diphosphate

GEF: Guanine nucleotide exchange factor

GM130: Golgi matrix protein 130

GPCR: G protein-coupled receptor(s)

GRK: G-protein receptor kinase

GTP: Guanosine triphosphate

HEK: Human embryonic kidney

HF: Heart failure

HFpEF: Heart failure with preserved ejection fraction

HFrEF: Heart failure with reduced ejection fraction

HR: Heart rate

IBMX: 3-isobutyl-1-methylxanthine

ICI-118551: ethyl-(S*, S*)-1[2, 3-(Dihydro-7-methyl-1H-inden-4-yl)oxy]-3[(1-methylethyla)amino]-2-butanol hydrochloride

IP_3: Inositol 1,4,5-triphosphate

IPSC: Induced pluripotent stem cells

ISA: Intrinsic sympathomimetic activity

ISO: Isoproterenol

JNK: c-Jun N-terminal kinases

KCNQ1: Potassium voltage-gated channel subfamily Q member 1

LPA: Lysophosphatidic acid receptor

LTCC: L-type Ca^{2+} channel

M2: Muscarinic type 2 acetylcholine receptor

MAPK: Mitogen-activated protein kinases

MOI: Multiplicity of infection

MRAPs: Melanocortin 2 receptor accessory proteins

MyBP-C: Myosin binding protein-C

NC-IUPHAR: Nomenclature Committee of the International Union of Basic and Clinical Pharmacology

NFAT: Nuclear factor of activated T-cells

NMR: Nuclear magnetic resonance

NRVM: Neonatal rat ventricular myocytes

OCT: Organic cation transporter

PARs: Protease-activated receptors

PBS: Phosphate buffered saline

PDE: phosphodiesterase

PFA: Paraformaldehyde

PIP_2: phosphatidylinositol 4,5-bisphosphate

PLB: Phospholamban

PLC: Phospholipase C

PNS: Parasympathetic nervous system

PKA: Protein kinase A

PKC: Protein kinase C

PKD: Protein kinase D

POPDC: Popeye domain containing protein

PP1/2: Protein phosphatase

R: PKA regulatory subunit

RAMPs: Receptor activity modifying proteins

RAS: Rat sarcoma

RET: Resonance Energy Transfer

RGS: Regulator of G-protein signalling

RT: Room temperature

RYR2: Ryanodine receptor

SD: Standard deviation

SEM: Standard error of the mean

SERCA: Sarcoplasmic endoplasmic reticulum calcium ATPase

SNS: Sympathetic nervous system

SOICR: Store-overload-induced calcium release

SR: Sarcoplasmic reticulum

Src: Proto-oncogene tyrosine-protein kinase

TD: Targeting domain

TnI: Troponin I

TnT: Troponin T

TP: Thromboxane receptor

TPSA: Topological polar surface area

TSH: Thyroid stimulating hormone

WT: Wild type

YFP: Yellow fluorescent protein

Chapter 1

Background

1.1 G-protein Coupled Receptors

The heart is a highly specialised muscular organ responsible for maintaining systemic circulation to deliver oxygen and nutrient-rich blood to tissues and remove waste. Cardiac performance exists in a dynamic state through fluctuating physiological demands, such as during exercise or stress. This adaptability is primarily mediated by the autonomic nervous system, which is made up of two branches: sympathetic (SNS) and parasympathetic (PNS). The sympathetic branch increases heart rate, conduction velocity and contraction force through the release of catecholamines. On the other hand, the parasympathetic branch exerts opposing effects through its release of acetylcholine.

At the molecular level, these effects are mediated through cell surface receptors belonging to the G-protein coupled receptor (GPCR) superfamily. The GPCR superfamily is the largest class of membrane receptors in humans, encoded by ~800 genes, and mediates various neurohormonal functions in the body [1]. They are key pharmacological targets, forming the mechanistic basis of ~36% of

approved drugs [2]. Among these targets are the β-adrenoceptors (β-ARs), the central focus of this work. Antagonists of these receptors (known as β-blockers) are the cornerstone of therapy for heart failure, a disease affecting over 55 million people worldwide [3]. However, the outcomes of individual agents from the same family markedly differ in the clinic for reasons that remain mechanistically unexplained [4–8]. This chapter addresses this problem by first introducing the molecular principles of GPCR signalling, with a focus on the mechanisms that enable spatially restricted (compartmentalised) cAMP signalling, before turning to the pharmacology of the relevant β-AR antagonists.

Building on recent evidence, my research examines whether individual β-blockers engage distinct receptor conformations that shape cardiac cAMP signalling with distinct effects at the subcellular level [9].

1.1.1 Structure of a GPCR

A GPCR is an integral membrane protein built from seven α-helical transmembrane domains (7TMRs) connected by three intracellular and three extracellular loops [10]. The NC-IUPHAR recognises six GPCR classes, divided by sequence homology reflecting evolutionary conservation (**Figure 1.1**) [11]. These are: class A (rhodopsin-like), class B1 (secretin-like) and B2 (adhesion receptors), class C (metabotropic receptor-like), class D (fungal mating

pheromone receptor-like), class E (cyclic AMP receptor-like) and class F (Frizzled/Taste2) [12,13]. A receptor's class dictates its structural interaction with ligands. Most GPCRs, including the cardiac β-AR, fall under class A [14].

Diversity of GPCRs is required for receptor recognition and response to a variety of ligands (photons, ions, odorants, neurotransmitters, large peptide hormones, glycoprotein hormones etc.) [11]. This is achieved by mechanisms such as post-translational modifications and alternative splicing [12]. Signal transduction is initiated through the binding of an extracellular ligand that elicits a conformational change in the receptor, enabling G-protein activation [12,15,16]. Impairment of these processes is implicated in pathology across multiple organ systems.

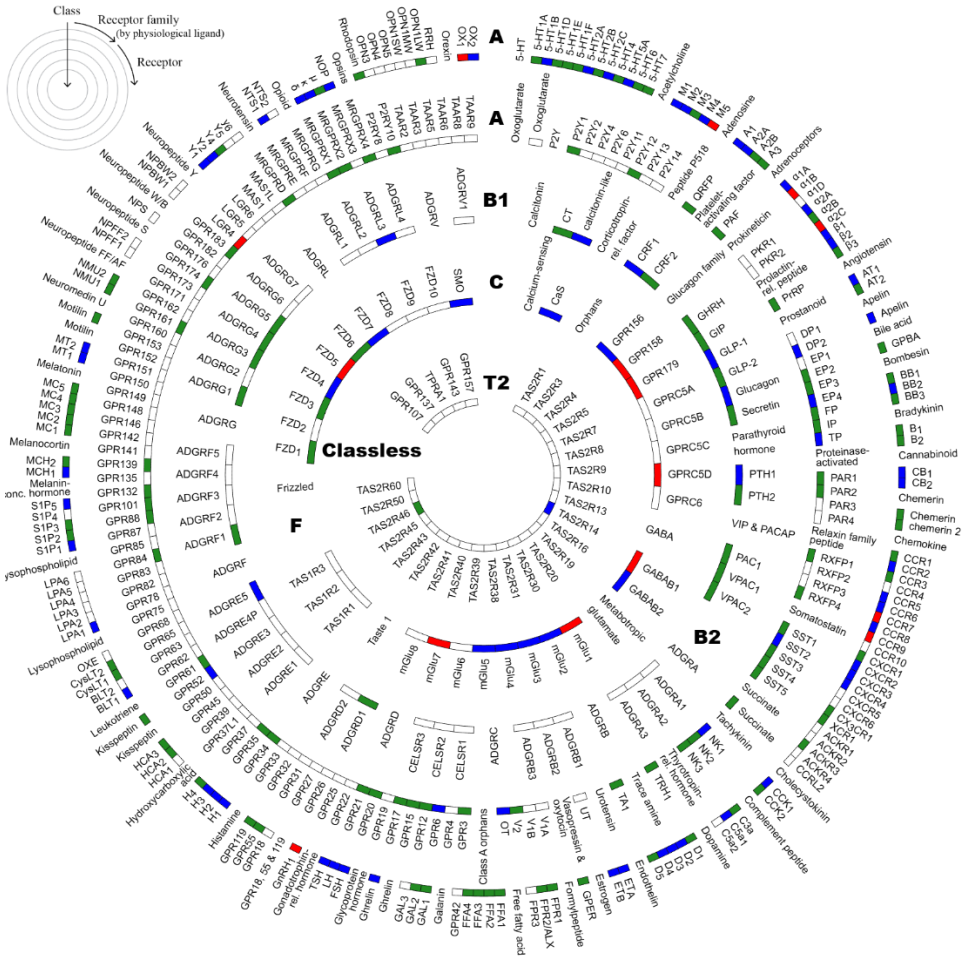


Figure 1.1: Classification of GPCR subfamilies.
Classification of GPCR subfamilies by protein name generated via GPCR.db (November 2025). Structure coverage is grouped by colour. Green = active receptor, Red = inactive and Blue = both [17].

1.1.2 Activation of the Signal

The steps of GPCR transduction prefigure the compartmentalised downstream effects that are central to this thesis. GPCR signal transduction proceeds through a multi-step pathway in which G-proteins engage the receptor, generating soluble secondary messengers that act on downstream effectors [18,19]. These G-proteins may differ in structure and size, ranging from the first monomeric (small) G-protein *ras* to the heterotrimeric configuration of G-proteins [16,20].

Heterotrimeric G-proteins are structured by three distinct subunits (α, β and γ) which themselves are derived from multigene families (16 Gα, 5 Gβ, 12 Gγ), diversifying signalling specificity and allowing over 1300 possible permutations of the complex [21,22]. The functional diversity of these permutations is determined principally by the Gα subunit.

The four major Gα families (G_s, $G_{i/o}$, $G_{q/11}$ and $G_{12/13}$) stimulate or inhibit different secondary messengers such as 3'-5'-cyclic adenosine monophosphate (cAMP), inositol 1,4,5-triphosphate (IP_3) and Ca^{2+} [12]. In the resting state, inactive Gα remains tightly coupled to Gβγ and bound to GDP, whose intrinsically low off rate maintains this stable and inactive configuration. Activation of signal transduction upon ligand binding begins from catalysis of GDP release from Gα and the binding of GTP. The active GPCR acts as a guanine nucleotide exchange factor (GEF), inducing a conformational change in the Gα nucleotide binding pocket that lowers its affinity for GDP to allow GTP to bind in its place. This process dissociates Gα from the Gβγ dimer, forming a Gα-GTP complex; both Gα-GTP and the free Gβγ dimer are then able to modulate effector proteins (**Figure 1.2**) [10,12,16,18]. Gα-GTP may activate or inhibit adenylyl cyclase (AC), ion channels and PLC depending on the G-protein type, ligand and other factors

[16]. AC generates the secondary messenger cAMP, whose actions are examined in the following section (**1.2**).

The heterotrimeric G-proteins, their respective effector proteins and secondary messengers are represented in **Table 1.1** [23].

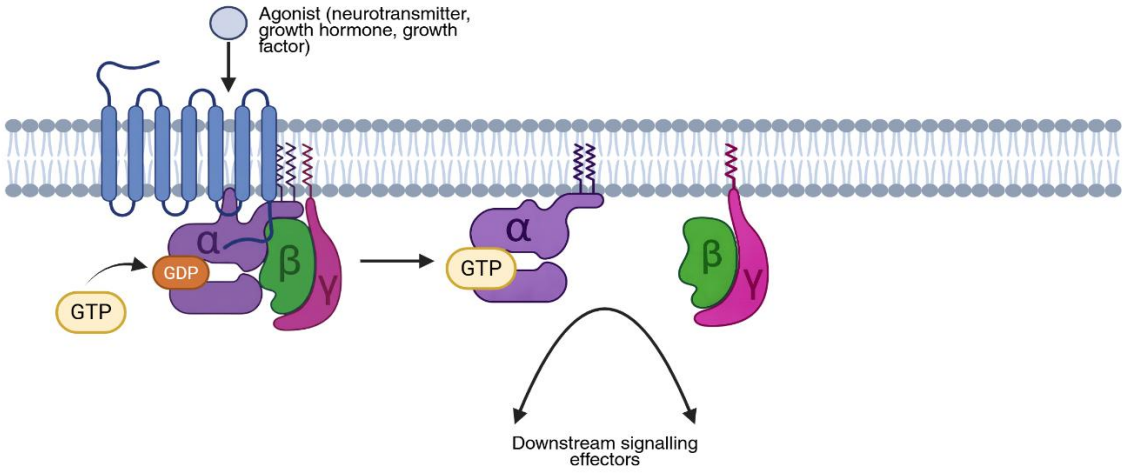


Figure 1.2: Activation of a seven-transmembrane G-protein coupled receptor.
Seven-transmembrane receptor (7TMR) G-protein coupled receptor activation. A binding agonist induces a conformational change to the GPCR, which triggers the activation of the heterotrimeric G-protein complex. When bound to GDP, the complex is in an inactive state. Activation leads to the exchange and displacement of GDP to GTP. Both Gα and Gβγ complexes can activate their distinct downstream effectors. Figure generated using BioRender (2026).

Family/Subunit	Receptor	Effector(s)/Role	Distribution
G_s:	β-adrenergic,	↑ Adenylyl cyclase	Ubiquitous
$\alpha_{s(s)}$	TSH, glucagon,	↑ Ca^{2+} channel	
$\alpha_{s(l)}$	others		
α_{olf}	Odorant receptor, D1R, others	↑Adenylyl cyclase Opens cyclic-nucleotide gated cation channel	Olfactory epithelium
G_i (α_i):	M2, α2-	↑IP_3, DAG, Ca^{2+},	Ubiquitous
α_{i1}	adrenergic, others	arachidonic acid	
α_{i2}		↓Adenylyl cyclase	
α_{i3}			
α_{O1A}	Met-enkephalin,	Variable	Brain, others
α_{O1B}	α_2-adrenergic, others		
α_{t1}	Rhodopsin	↑cGMP-phosphodiesterase	Retinal rods Retinal cones
α_{t2}	Cone opsin		
α_g	Taste receptors	↓Adenylyl cyclase	Taste buds
α_z			Brain, adrenal, platelet, pancreas
G_q	M_1, α_1-adrenergic	↑PLCβ1, PLCβ2,	
α_q	receptor, others	PLCβ3	Ubiquitous
α_{11}			Ubiquitous
α_{14}	Several receptors		Lung, kidney, liver
α_{15}		↑PLCβ1, PLCβ2,	B-cell, myeloid
α_{16}		PLCβ3	T-cell, myeloid
G_{12}	LPA, AT1,	RhoGEF	Ubiquitous
α_{12}	PARs, TP, others	activation, ↑RhoA	Ubiquitous
α_{13}			

Table 1.1: Families and subunits of mammalian G-proteins.

Adapted and modified from Medical Physiology (3rd Ed), by W. F. Boron & E. L & Boulpaep, 2017, Elsevier. Showing families/subunits of mammalian G-proteins. Abbreviations: TSH = Thyroid stimulating hormone; D1R = Dopamine D1 receptor; M2 = Muscarinic type 2 acetylcholine receptor; PLC = Phospholipase C; LPA = Lysophosphatidic acid receptor; AT1 = Angiotensin II receptor type 1; PARs = Protease-activated receptors; TP = Thromboxane receptor

A single GPCR can activate two or more G-protein subfamilies (**Table 1.1**), with distinct kinetics and efficacies (**Figure 1.3**) [24]. $G\alpha_s$ (the focus of this work) activates AC to generate cAMP and $G\alpha_i$ inhibits AC to inhibit production of cAMP. The $G\alpha_q$ family activates PLC-β to hydrolyse phosphatidylinositol 4,5-bisphosphonate (PIP_2) to diacylglycerol (DAG) and IP_3, to elevate cytosolic Ca^{2+} through IP_3 receptor-mediated release from the sarcoplasmic reticulum (SR).

Termination of signalling occurs when the GTPase activity of the Gα-subunit hydrolyses bound-GTP to GDP re-forming the inactive heterotrimer as Gβγ re-associates with the Gα subunit. GTP hydrolysis can be accelerated by regulators of G-protein signalling (RGS) which act as GTPase-activating proteins (GAPs) for Gα [25]. GTP hydrolysis resets the G-protein, but the receptor itself must also be switched off. This longer-term desensitisation, mediated by G-protein coupled receptor kinases (GRKs) and β-arrestin, is discussed next.

1.1.3 The Ending of the Signal

Signal termination prevents sustained signalling and overstimulation. GRKs and β-arrestin regulate this process and the events that follow, including receptor internalisation.

The molecular basis of GPCR desensitisation was first established in studies of rhodopsin and β-adrenoceptors, which revealed that this process begins with a phosphorylation step by proteins known as GRKs, such as rhodopsin kinase (GRK1) and βARK (GRK2-3). These phosphorylate the C-terminus and/or the third intracellular loop of the agonist-occupied receptor, promoting β-arrestin recruitment. Canonically, β-arrestin binding sterically limits further coupling of the receptor to its cognate G-protein and contributes to receptor desensitisation. However, β-arrestins can also adopt signalling-active conformations and participate in more complex interactions with GPCRs and G-proteins [26–28].

Of the four mammalian arrestin proteins, β-arrestin-1 and β-arrestin-2 are ubiquitously expressed and interact with both class A and B GPCRs, showing a high specificity for the β2-AR [18,27,29,30]. Structurally, a clathrin-binding domain at residues 370–380 is essential for a process known as clathrin-mediated internalisation [42].

The arrestins help mediate important processes in GPCR signalling:

1. *Desensitisation* – when the response of a receptor to an agonist diminishes over time i.e. becomes refractory to continued stimuli.

2. *Internalisation* – where the cell-surface receptor is internalised via endocytosis. In this case, arrestin uncouples the GPCR from its cognate G-proteins to promote internalisation.
3. *Downregulation* – the reduction in the number of cell-surface receptors after prolonged stimulation i.e. total cellular receptors decrease.

The action of β-arrestin can be dependent on or independent of the associated GPCR (**Figure 1.3**). β-arrestin is first recruited to the cytoplasmic side of the GPCR and physically competes with G_s for the receptor. This is an observation characteristic of desensitisation for almost all 7TMRs. These events lead to steric occlusion of the receptor's intracellular binding pocket. However, parts of the β-arrestin molecule remain exposed, leaving other effectors free to interact with its central crest region [29,32,33].

GPCRs are internalised and trafficked from the plasma membrane to clathrin-coated endocytic vesicles. Most GPCRs internalise through the formation of clathrin-coated pits (CCPs), with β-arrestin acting as a molecular bridge between the receptor and endocytic machinery [34]. Following internalisation, some GPCRs can still activate G-proteins from within the endosomal compartment by assembling a "megaplex" comprising the receptor, β-arrestin and a G-protein, as evidenced by cryo-electron microscopy (cryo-EM) studies [18,35–37]. Earlier

studies established that β-arrestin adopts two receptor-bound conformations: a "tail" conformation, in which it binds only the receptor C-terminus, and a fully engaged "core" conformation, where it additionally inserts into the transmembrane core [35,38]. The "tail" conformation may explain the formation of the megaplex, whereby a G-protein may still be able to bind to the GPCR due to availability of the receptor's intracellular core [37].

Internalised receptors are then targeted for lysosomal degradation, recycled through the Golgi apparatus, or returned directly to the plasma membrane for re-sensitisation [18,31]. Internalised receptors may also signal from endosomal compartments, where conformationally active receptor complexes generate cAMP distinct from the plasmalemma [39]. This observation has challenged the classical view that GPCR signalling arises solely at the plasma membrane, and carries pharmacological significance discussed in **1.4.3**.

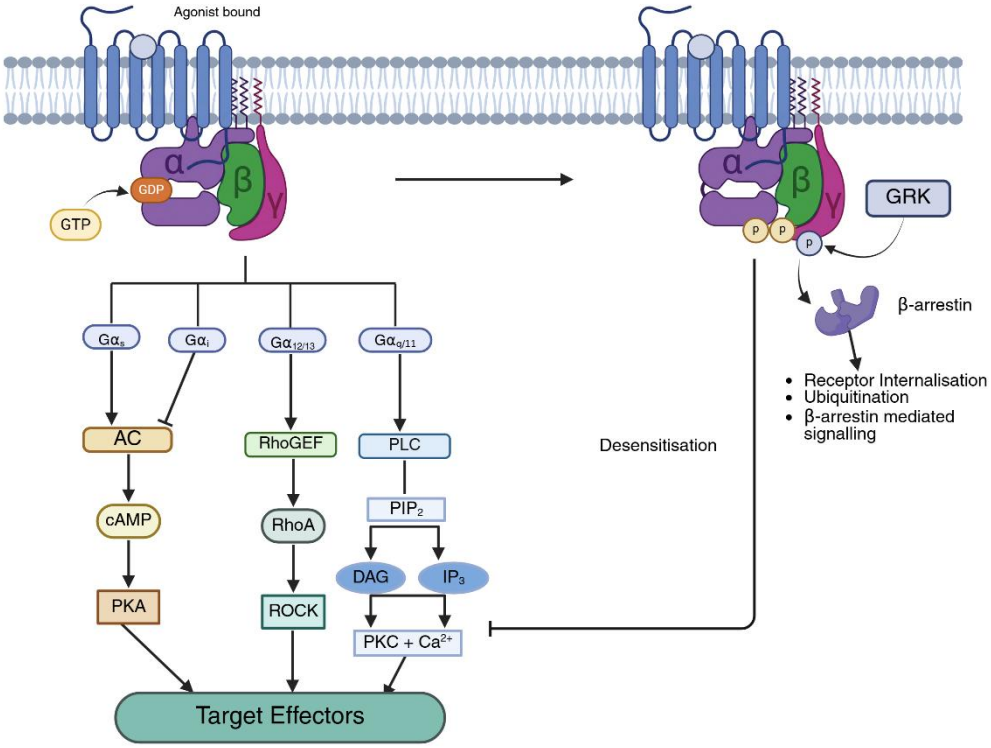


Figure 1.3: Downstream signalling and desensitisation of GPCRs.
Upon agonist binding, G-proteins undergo GTP-GDP exchange on the alpha subunit leading to dissociation and activation of multiple downstream effectors. Pathways from each subunit family engage in a diverse range of cellular responses. Signal termination is mediated by complementary desensitisation mechanisms. Secondary messenger activated kinases such as PKA and PKC phosphorylate the receptor, attenuating G-protein coupling (heterologous desensitisation). GRKs phosphorylate agonist-occupied receptor, promoting β-arrestin recruitment facilitating receptor internalisation, ubiquitination and acts as scaffolds for alternative signalling pathways.

1.1.4 Biased Agonism

Beyond the canonical G_s-AC-cAMP cascade described above (**1.1.2**), studies have identified non-canonical pathways in which β-arrestin activates mitogen-activated protein kinases (e.g. ERK1/2, JNK) following β2-AR stimulation [32,40,41]. These represent examples of what is characterised as biased agonism.

Biased agonism describes an agonist's capacity to activate a specific subset of a receptor's downstream signalling effectors [12]. Canonically, most output of GPCR function is attributed to G-proteins, but biased agonism is a model that explicates how GPCRs can couple to other effectors. The two best-characterised modes are G-protein-biased and β-arrestin-biased (G-protein-independent) signalling, although these are not always mutually exclusive in practice [42].

Several mechanisms may explain biased agonism. A ligand may stabilise specific receptor conformations that preferentially promote either G-proteins or β-arrestin. In turn, these conformations may induce distinct conformational changes in scaffolding proteins such as β-arrestin, activating downstream cascades including MAPK (**1.1.3**). Finally, different ligands may induce conformational changes in G-proteins that alter GEF efficiency, changing the rate of GTP/GDP exchange [43].

In β-arrestin-biased signalling, β-arrestin acts as a signal transducer in its own right, scaffolding other proteins to organise both G-protein-independent and G-protein-dependent signalling [32]. For example, β-arrestin-2 can bind components of the extracellular signal-regulated kinase (ERK1/2) cascade, enabling mitogen-activated protein kinase (MAPK) activation and subsequent regulation of nuclear transcriptional programmes [29,32,44]. Similarly, β-arrestin-1 can recruit Src (c-

Src) to the β2-AR, forming a complex that drives receptor-dependent ERK activation [45].

This concept is directly relevant to cardiac pharmacology as several ligands traditionally classified as β-AR antagonists, have been reported to engage these non-canonical signalling pathways. Carvedilol is the most prominent example, proposed to activate ERK1/2 signalling in this manner [41]. Other β-AR antagonists, including propranolol and ICI-118551, have also been implicated in activating ERK1/2 independently of heterotrimeric G-proteins [46]. The literature on β-blockers, particularly around the debates surrounding carvedilol, is discussed in detail in **section 1.5.2**.

Although biased agonism provides an important framework for understanding ligand-specific GPCR signalling, its clinical translation has been challenging. One explanation is that drug behaviour is often simplified into efficacy (the ability of a drug to trigger a response upon binding) and affinity (ability of a drug to bind to a receptor). In practice, observed drug responses reflect not only intrinsic ligand-receptor interactions but also scaffold proteins, receptor expression, effector availability and the broader cellular context. Signalling bias is also relative and assay-dependent, varying according to which pathway and the reference ligand used for comparison [47]. Therefore, binary classifications for a

ligand (such as “agonist” or “antagonist”) do not accurately represent the range of signalling behaviours a ligand can elicit.

In the context of G_s-coupled β-ARs, biased signalling necessitates precise control of downstream secondary messengers.

1.2 Cyclic AMP Signalling

Cyclic-adenosine 3’,5’-monophosphate (cAMP) is a ubiquitous small hydrophilic molecule implicated in a large number of functions across organisms, and was the first intracellular secondary messenger to be identified by Sutherland and Rall in 1958 [48]. cAMP is controlled by two enzymatic regulators: adenylyl cyclase (AC), which synthesises it, and cyclic nucleotide phosphodiesterase (PDE), which degrades it. Although the synthesis and catabolism of cAMP underpin its diverse cellular function, the mechanisms by which this second messenger elicits highly selective signalling responses remained unsolved for decades following its discovery. The current understanding is that this specificity arises through compartmentalised signalling, whereby spatial and temporal regulation of cAMP is achieved through the coordinated actions of enzymes that synthesise and degrade cAMP (**1.2.1**), its downstream effectors (**1.2.2**) and scaffold proteins that organise the signalling components (**1.2.3**) resulting in the formation of signalling “nanodomains” that confer signalling specificity (**1.2.4**).

1.2.1 Adenylyl Cyclase and Phosphodiesterase

ACs are the enzymes that synthesise cAMP, catalysing the conversion of ATP into cAMP. Nine transmembrane isoforms are expressed in mammals (abbreviated as AC1-9) [49]. The general expression of AC in tissues has been well-characterised. For instance, cardiac tissue exhibits high expression of AC4-7, with additional expression of AC1 [50]. Each isoform is known to have distinct regulatory properties on G-protein subunits.

In the heart, most cAMP is produced downstream of sympathetic activation of β-ARs, which raise cAMP to modulate heart rate (chronotropy), relaxation (lusitropy) and muscular contraction (inotropy). This is usually facilitated by interactions with the α-subunit of G_s, but the βγ subunit is also known to stimulate certain AC isoforms [51]. Subsequently, cAMP is degraded via hydrolysis by PDEs into 5'-AMP thus shutting down the signal and maintaining the basal concentration of cAMP.

The PDE superfamily includes 11 families, encoded by 21 genes, generating over 100 isoforms in mammals. In the heart, eight PDE families have been identified (PDE1-5 and PDE8-10) [52]. These isoforms are not functionally equivalent. To illustrate, experiments in neonatal rat ventricular myocytes (NRVMs) have found

the PDE4 family to exert the greatest control during β-adrenergic stimulation [53–55].

1.2.2 Signalling Effectors

The cascade of effects stimulated by cAMP is coordinated through its effector proteins. There are three main effectors of cAMP: protein kinase A (PKA), exchange protein activated by cAMP (Epac), and cyclic-nucleotide-gated ion channels (CNGC). More recently, the Popeye domain containing protein (POPDC) family have been identified as a fourth effector class [56]. Although their role remains incompletely understood, mutational analysis in animal models suggests a role in membrane trafficking [57].

Of these effectors, the holoenzyme PKA is the best understood. It is a heterotetramer composed of two regulatory and two catalytic subunits. There exist two binding sites for cAMP on the R subunit (CNB-A and CNB-B), which cause dissociation from the C subunit when activated [51]. There are two isoforms of PKA, types I and II, that contain regulatory subunits (RIα/β, RIIα/β) and the catalytic subunits (Cα, Cβ or Cγ). Hence, PKA is divided by its regulatory subunit into PKAI and PKAII [58].

PKA modulates cardiac function through its roles in stress adaptation and excitation-contraction coupling (ECC) via regulation of calcium signalling. It

does this through phosphorylating multiple proteins in the cardiomyocyte to control the electrical state of the cell and sarcomere function. These include, for example, PKA-mediated phosphorylation of the L-type calcium channel (LTCC), ryanodine receptor (RyR) and phospholamban (PLB) that lead to positive chronotropic and inotropic effects [59]. On the other hand, PKA-dependent phosphorylation of troponin I (TnI) and myosin-binding protein-C results in positive lusitropic effects [60]. PKA also cross-activates other signalling pathways including MAP kinases and transcription factor cAMP-response element-binding protein (CREB)[51,61].

The second major effector, Epac, exists as two identified isoforms (Epac1 and Epac2) and acts independently of PKA as a GEF for the Ras-family GTPases Rap1 and Rap2 [59,62]. Epac1 and Epac2 are predominant isoforms in the adult and neonatal myocardium respectively. Similar to PKA, Epac contains an N-terminus CNB domain that mediates activation by cAMP [59]. It modulates cardiac calcium handling and remodelling in a context-dependent manner. Contractility is stimulated when Epac enhances PLC–CaMKII signalling, driving RyR2 phosphorylation and SR-mediated Ca^{2+} release independently of LTCC and PKA. Similarly, Epac has a role in augmenting myocyte shortening through activation of PKC phosphorylation of TnI and MyBP-C [51,63].

1.2.3 A-Kinase Anchoring Protein (AKAP)

Effectors act locally, and specific proteins are needed to tether them close to their target substrate. A-kinase anchoring proteins (AKAPs) fulfil this role by assembling PKA and other effectors alongside their substrates [64]. These scaffolds provide this specificity through a conserved PKA-binding domain [65]. There are over 50 AKAP families in humans, with at least 4–6 major cardiac members that target PKA to different intracellular sites (**Table 1.2**) [58,66]. They also associate with GPCRs, GTPases, PDEs and cytoskeletal components within microdomains, confining local signalling complexes and minimising signal spill-over. This tethering increases both efficiency and specificity of signal transduction [67].

AKAPs	Alternative names/variants	Associated protein(s)	Functionality
mAKAP	AKAP-6	PKA, NFATc3, RyR2, ERK5, NCX1, PP2A, PDE4D3, Calcineurin	Hypertrophy in heart failure, cardiac arrhythmic regulation
AKAP-Lbc	AKAP-13, Ht31, Brx-1	PKA, PKC, Rho, PKD	Hypertrophy in heart failure, inhibition of cardiomyocyte apoptosis
AKAP-7	AKAP-18, AKAP-15	PKA, PLB, PP2B, SERCA2, CaMKII, CaV1.2	Cardiac contraction and regulation of heartbeat
AKAP9	Yotiao, AKAP-350, AKAP-450	PKA, AC, PDE4D3, KCNQ1, PP1	Regulation of cardiac arrhythmia
AKAP-5	AKAP-79, AKAP-150, AKAP-75	PKA, PLB, SERCA2a, Calcineurin, NFATc3, CaMKII, RyR2, PKC	Apoptosis, contraction and relaxation, regulation of cardiac arrhythmia, blood pressure regulation

Sarcomeric AKAPs	N/A	PKA, TnT, synemin	Cardiac contraction and relaxation

Table 1.2: Major cardiac AKAPs, their partner proteins and functions. *Modified from Mauban et al. (2009) [68], Zhang (2025) [58] and Kritzer (2012) [69]. Abbreviations: NFAT = Nuclear factor of activated T-cells; RyR2 = ryanodine receptor 2; NCX = sodium-calcium exchanger; PP2A/B = protein phosphatase 2A/B; PKD = Protein kinase D; CaMKII = calcium/calmodulin-dependent protein kinase II; CaV1.2 = voltage-gated calcium channel type 1.2; KCNQ1 = potassium voltage-gated channel subfamily Q member 1; TnT = troponin T*

The interaction of AKAP and PKA happens through binding of the D/D domain at the N-terminus of the PKA R subunit (1.2.2) [61]. Through anchoring PKA to defined locations, AKAPs enable the formation of localised cAMP domains. In this context, the human AKAP-79 and AKAP-18δ, which localise to the plasmalemma and SR respectively, are of relevance. These proteins have been exploited to develop fluorescence resonance energy transfer (FRET) based cAMP sensors that report compartment-specific dynamics [70,71]. Both have been utilised as sensor targets in this work, together with TnI, owing to their involvement in excitation-contraction coupling (**Figure 1.4**).

The AKAP5 gene product, otherwise known as AKAP-79 in humans, is critical as a scaffold protein in cardiomyocytes. It aids cAMP, calcium and phospholipid signalling through their respective effectors such as PKA and PKC [69]. AKAP-79, among the best-characterised AKAPs, associates mainly with the plasma membrane and with the β2-AR [72]. In the heart, AKAP-79 localises to caveolin-

3-associated submembrane nanodomains, where it scaffolds the β-adrenoceptor. It may directly bind to AC5/6, thus coupling local cAMP production to anchored PKA activity [69]. Consistent with this model, AKAP-79 targeted sensors show predominant localisation to the plasmalemma [70].

On the other hand, AKAP-18δ is a long isoform of AKAP-18 (encoded by AKAP7) that regulates excitation-contraction coupling by modulating SERCA2a-mediated calcium uptake into the SR, setting the rate of diastole. AKAP-18δ binds PLB and plays a role in the activation of SERCA2a by promoting PKA-dependent PLB phosphorylation [69]. Thus, a distinct binding sequence localises AKAP-18δ to the SR, positioning AKAP-18δ to anchor PKA close to SERCA2a and PLB [73]. In terms of functionality, studies have demonstrated that AKAP-18δ contains two distinct regions (NH_2- and COOH-terminal) that inversely and positively regulate CaMKII, respectively [71].

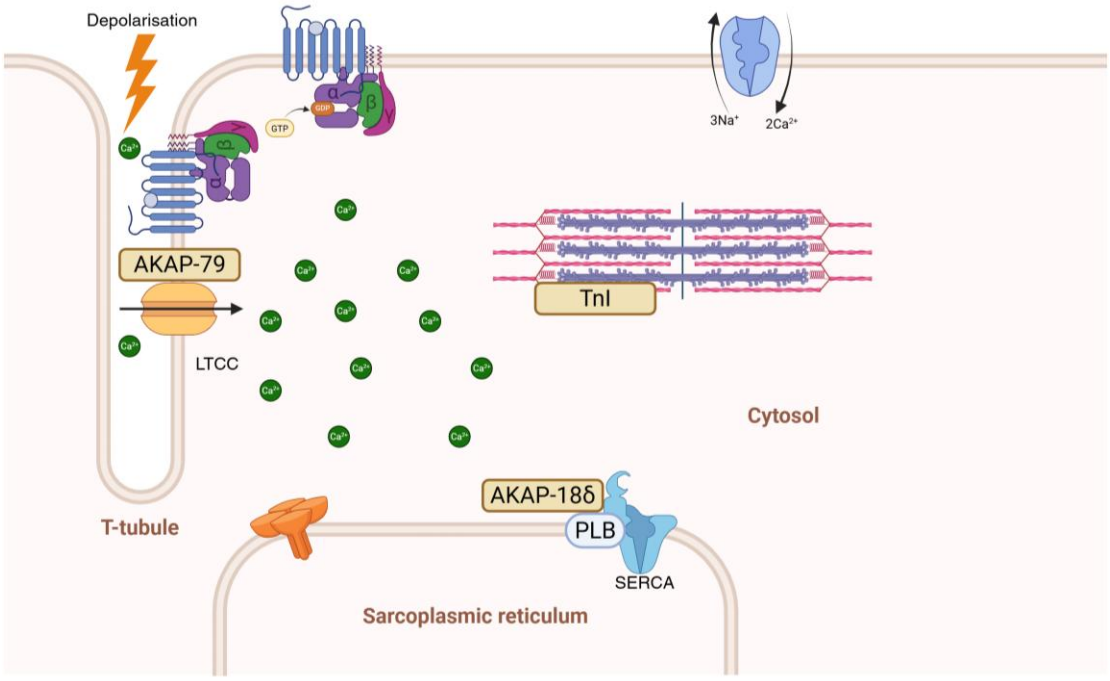


Figure 1.4: AKAP-organised nanodomains along the excitation-contraction coupling axis.
AKAP-organised nanodomains along the excitation-contraction coupling axis in cardiomyocytes. Membrane depolarisation propagating along the T-tubules activates LTCC to enable Ca2+ influx into the dyadic cleft. AKAP-79 is tethered at the sarcolemma in proximity to the LTCC where it may scaffold proteins such as PKA, PKC and calcineurin to regulate β-adrenergic modulation of Ca2+ entry. Cytosolic Ca2+ engages the myofilament, where TnI plays a role in actin-myosin crossbridge formation. AKAP-18δ anchors PKA to the SERCA/PLB complex. These three locations act as targets in this thesis used to resolve β-adrenergic compartmentalised signalling (1.2.3, 1.3.4).

1.2.4 cAMP Nanodomain Signalling

As established, cAMP signalling is spatiotemporally restricted through the formation of small unit multimolecular complexes ("signalosomes") by AKAPs. Signalosome formation reflects the coordinated contribution of localised cAMP synthesis, targeted degradation by PDEs and diffuse barriers imposed by cellular architecture. These mechanisms collectively give rise to spatially restricted cAMP signalling hubs ("nanodomains") that enable compartment-specific regulation.

This framework represents a paradigm shift from the notion of cAMP being a freely diffusible molecule [74].

The classical nanodomain is thus defined by the coordinated actions of localised ACs, PDEs that degrade cAMP, a cAMP effector (e.g. PKA) and scaffold proteins such as AKAP that tether PKA in proximity to defined substrates. Compartmentalised PDEs keep cAMP concentrations below the PKA activation threshold under basal conditions. Upon receptor-mediated activation, enhanced AC activity increases local cAMP production to levels that transiently exceed the degradative capacity of resident PDEs leading to a signalling cascade (**1.1.3, 1.2.1, 1.2.2**). Negative feedback then leads to phosphorylation on PDEs (e.g. long isoforms PDE4 and PDE3) to restore basal cAMP levels [75].

Two models have been proposed to explain how nanodomains emerge: the barrier and sink theories. The first theory posited that PDEs act as enzymatic walls to prevent diffusion of cAMP between compartments, forming a protective perimeter [53,75]. On the other hand, the sink theory explains this using concentration gradients due to apparent kinetic and thermodynamic limitations in PDEs maintaining a basal cAMP concentration [76,77]. In this current model, PDEs create localised zones of low cAMP, through differential hydrolysis of the second messenger at different locations, which relies on the distinct enzymatic

properties of the resident PDEs [78]. In this context, the question this project aims to address is whether a β-blocker acts by lowering bulk cellular cAMP or whether it may vary according to the specific subcellular location.

1.3 Optical Imaging of cAMP

The development of optical tools and biosensors has enabled the visualisation of spatially restricted cAMP pools in living cells, providing compelling evidence that cAMP signalling is compartmentalised. In particular, the introduction of genetically encoded FRET-based cAMP reporters made it possible for the first time to monitor cAMP compartmentalisation in real-time [74,79]. These biosensors largely exploit resonance energy transfer (RET), a phenomenon based on non-radiative dipole–dipole coupling between donor and acceptor molecules. Among RET-based approaches, this work employs fluorescence resonance energy transfer (FRET) [80]. FRET-based biosensors enable continuous real-time measurement of cAMP and can be targeted to defined intracellular structures.

1.3.1 Principles of FRET

In FRET, an excited donor transfers energy to a fluorescent acceptor via dipole-dipole coupling when the emission spectrum of the donor overlaps with the excitation spectrum of the acceptor fluorophore. Transfer efficiency is inversely proportional to the sixth power of the donor-acceptor distance [81]:

$$E = \frac{1}{1 + \left(\frac{r}{R_0}\right)^6}$$

where E is the FRET efficiency (the likelihood that an excited donor undergoes energy transfer to an acceptor), r is the donor-acceptor separation distance and R_0 represents the distance at which the energy transfer efficiency is 50%. Capturing cAMP signalling therefore requires the donor and acceptor to be close (<10 nm) [80]. In this thesis, the principle is applied to cAMP biosensors designed to report the small, spatially restricted changes in intracellular cAMP that accompany β-adrenergic stimulation [80,82].

1.3.2 Sensors for Secondary Messengers

Many class A and class B GPCRs (**1.1.1**) signal through G_s and G_i, therefore utilising the cAMP pathway. The prototype cAMP FRET sensor, FICRhR ('flicker'), used rhodamine- and fluorescein-labelled PKA subunits [83]. In the inactive holoenzyme, the fluorophores must lie close enough for efficient FRET. Upon cAMP binding, as FICRhR is a "loss-of-FRET' sensor, there is a reduction in FRET intensity [83].

Genetically encoded unimolecular FRET-based cAMP sensors have now largely replaced PKA-based sensors for studying compartmentalised signalling. The major sensors used are Epac-based (**1.2.2**), which use a CNBD backbone

sandwiched between donor and acceptor fluorophores [84]. The most extensively used sensors of this class include the Epac1-camps developed by Nikolaev *et al.* (2004) and the reoptimised Epac-S^{H187}, which uses a truncated regulatory domain [85,86].

Epac sensors offer several advantages. As single-chain constructs they eliminate stoichiometric variability and report cAMP levels directly with superior signal-to-noise ratios independent of PKA catalytic activity [85–87]. Furthermore, as there is only a single functional CNBD, Epac sensors do not exhibit the cooperative binding (sigmoidal responses) seen with PKA-based sensors and produce more linear FRET changes. Their improved spatiotemporal resolution is integral to reporting rapid cAMP signal propagation (~40 μm/s) following β-adrenergic receptor stimulation [85].

1.3.3 The Epac-S^{H187} Sensor

Epac-S^{H187} is the fourth-generation Epac1-camps biosensor, refined for detecting compartmentalised cAMP signalling (**Figure 1.5**). It employs a fluorescent donor based on mTurquoise2, a very bright and bleach-resistant donor [86]. The enhanced photostability compared to its predecessors allows prolonged imaging times, especially relevant in investigations requiring sustained GPCR stimulation [88,89].

The acceptor is a tandem pair of cp^{173}Venus fluorophores. This is a circularly permuted Venus where the original N- and C-termini are fused and new termini are artificially created at position 173, an arrangement that improves energy-transfer efficiency by favouring the required dipole orientation [86]. Like FICRhR, Epac-S^{H187} operates as a loss-of-FRET sensor, where a conformational change that increases the distance between donor-acceptor pairs occurs upon cAMP binding. This translates experimentally as a decrease in acceptor/donor emission ratio (tantamount to an increase in donor/acceptor ratio) proportional to cAMP concentration. The sensor is therefore well-suited for time-lapse experiments and capturing rapid cAMP transients that noise might otherwise mask.

1.3.4 CUTie Sensors

Older-generation FRET sensors could not resolve nanoscopic cAMP at discrete intracellular locations, prompting development of the CUTie sensor (Cyclic nucleotide Universal Tag for imaging experiments) by Surdo *et al.* (2017), which can be targeted to a variety of macromolecular complexes and allows comparison at local subcellular sites [82]. Thus, this sensor has been targeted to the key protein complexes regulating ECC: AKAP-79 for the LTCC complex at the plasmalemma, AKAP-18δ for the SERCA/PLB complex at the SR, and TnI at the myofilament regulating Ca^{2+} sensitivity (**1.2.3**). In ventricular cardiomyocytes

these structures lie in close proximity: up to ~1 μm between the sarcolemma and myofilament, and as little as 300 nm between the sarcomere and SR [90]. Targeted CUTie sensors were able to detect cAMP signals at these sub-microscopic levels [82].

The CUTie architecture was achieved through a mix of computational methods and molecular dynamics simulations, identifying the optimal positioning of the FRET pair relative to the CNBD [82,91]. It uses a CFP-YFP FRET pair positioned on either side of a CNBD derived from the PKA-RIIβ regulatory subunit, which serves as the cAMP binding moiety (**Figure 1.5**). Upon cAMP binding, the CNBD undergoes a subtle conformational change that reorients the fluorophores just enough to produce a measurable shift in FRET efficiency. In contrast to the Epac-camp sensors, where CFP-YFP donor-acceptor pairs are fused at opposing termini, the CFP is fused to the C-terminus of the CNBD and the YFP to an external loop of the CNBD. This arrangement allows the CNBD to be fused directly to a targeting domain and makes the sensor less sensitive to steric hindrance from fusion partners. In contrast, attaching a targeting sequence to an Epac-based sensor may compromise its response through steric hindrance, making CUTie better suited to localised nanodomain investigation [82,90].

CUTie sensors operate as gain-of-FRET sensors. When cAMP is unbound, the CFP donor and YFP acceptor are at a distance that produces a low baseline FRET signal. When cAMP is bound to the CNBD, the sensor undergoes the described conformational arrangement to bring the fluorophores closer together. This is the inverse of what occurs with Epac-based sensors, where the larger hinge-like opening movement increases the distance between fluorophores and decreases FRET (**1.3.3**).

CUTie sensors complement the use of Epac-S^{H187}: the latter captures bulk cytosolic dynamics, whereas CUTie resolves signals at defined nanodomains.

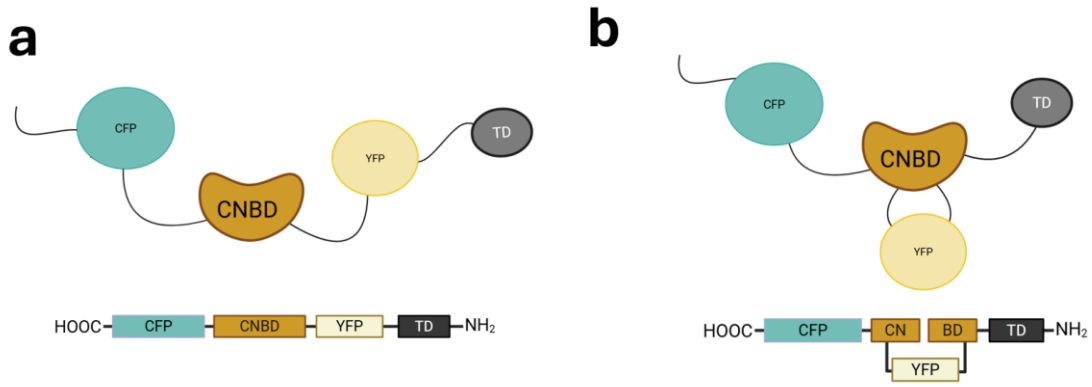


Figure 1.5: *Architecture of FRET biosensors in this work. (a) Epac-SH187 is a single-chain construct; cAMP binding increases donor (CFP) and acceptor (YFP) separation, resulting in decreased FRET efficiency to report rising cAMP. (b) Showing a CUTie sensor, where the CNBD is formed from PKA-RIIβ flanked by CFP/YFP and fused to a targeting domain (TD) which anchors the sensor to a defined nanodomain. cAMP binding causes the donor and acceptor separation to decrease and increase FRET efficiency.*

1.4 The Heart and the β-adrenoceptor

The sympathetic system of the heart exerts its influence through the β-ARs expressed on the surface of cardiomyocytes. Through cAMP-dependent signalling, β-ARs regulate processes such as excitation-contraction coupling. The β1-AR is the predominant subtype, occupying ~75-80% of total β-AR density, while the β2-AR makes up around 20-25%. Smaller populations of β3 have also been identified [92,93]. β-ARs exhibit intrinsic basal activity even in the absence of a bound ligand.

Functionally, the β1-AR is classically associated with positive chronotropic and inotropic effects through $G\alpha_s$-dependent activation of AC and cAMP generation. Meanwhile, the β2-AR produces lesser but modest chronotropic effects and less potent increases of contractile force. These subtype-specific effects are further shaped by differences in endogenous ligand engagement. Norepinephrine (NE), released from nerve terminals of the SNS, has a higher binding affinity for the β1-AR, while adrenaline produced from the adrenal medulla has a more stable binding affinity across β-AR subtypes [93,94].

Nevertheless, the traditional view that β-AR signalling operates solely through cAMP-PKA to regulate ECC has been increasingly challenged. It has been established that persistent activation of β1-AR causes a shift to CaMKII-

dependent signalling, a pathway implicated in maladaptive responses such as adverse cardiac remodelling and arrhythmogenesis [93,95,96]. This pathway switch is indicated in disease states characterised by elevated endogenous catecholamines such as chronic heart failure (CHF) and hypertension and may provide mechanistic insight for potential therapeutics. Consistent with this, recent evidence showed that CaMKII inhibition restored β-adrenergic reserves and improved relaxation, contraction and calcium handling in a mouse model of advanced HF [97].

A further layer of complexity arises from the spatial organisation of β-AR signalling. Although all β-AR subtypes can couple to G_s, β1-AR and β2-AR generate different patterns of cAMP propagation. The β1-AR is considered predominantly coupled to G_s producing a relatively diffuse cAMP signal throughout the cytoplasm and reaching distal targets such as PLB at the SR and other myofilament-associated proteins [98]. This broad signalling profile is supported by the distribution of β1-ARs throughout both caveolae and non-raft domains in the plasmalemma [99].

On the other hand, the β2-AR is primarily enriched within caveolae/lipid rafts and induces local cAMP responses [98]. Although β2-AR stimulation increases LTCC activity and contraction, it fails to phosphorylate PLB or enhance

lusitropy under normal conditions due to such functional compartmentalisation [100].

Uniquely, the β2-AR is also coupled to G_i and has been demonstrated to be dependent on both PKA and GRK phosphorylation [98,101–103]. In contrast to the cardiotoxic effects associated with sustained β1-AR signalling, β2-ARs may switch to G_i signalling and ERK1/2, activating survival pathways that successfully attenuate the cardiotoxic effects of sustained catecholamine stimulation (**1.1.4**) [95,103]. This has contributed to the hypothesis that β-arrestin-dependent signalling is beneficial for the heart. However, this remains complicated by a therapeutic paradox. GRK upregulation, an established feature and causal factor of HF, can enhance β2-AR phosphorylation and promote pathological G_i-biased signalling. This has been reported to exacerbate cardio-depression by impairing contractile reserve [104]. Further investigation is therefore required to delineate the precise signalling events that distinguish adaptive from maladaptive responses.

1.4.1 Receptor-AKAP Relationship

Stimulation of β1-AR produces a markedly larger cAMP response (approximately two-fold) compared to β2-AR, allowing it to create a cAMP gradient across the cell [105]. Both receptor localisation and cAMP maintenance by specific PDEs

and receptor microdomains shape these spatial kinetics (**1.2.2, 1.2.3, 1.2.4**). Scaffold proteins such as AKAPs partake in bringing signalling components (e.g. PKA) in proximity to the receptor and its confinement to the plasmalemma respectively.

Evidence from genetic knockout studies supports an important role for AKAP-79 in coordinating β-adrenergic stimulation of calcium handling. Loss of AKAP-79 in mice uncouples β-AR stimulation from Ca^{2+} transients, despite preserved global influx of Ca^{2+} through the LTCC [106,107]. This suggests that the defect does not just reflect impaired calcium entry, but rather disruption of local PKA-mediated phosphorylation events required for SR calcium release. Although further research is needed to define the precise molecular interactions involved, these findings indicate that AKAP-79 is an important orchestrator of sympathetic regulation of Ca^{2+} in adult cardiomyocytes [106].

Further support for this role comes from biosensor imaging experiments showing that deletion of AKAP5/79 sensitises the β1-AR to isoproterenol (ISO), leading to enhanced cAMP responses and increased contraction rate [108]. This implies that AKAP-79 may act as a constraint that restricts receptor signalling, as well as a scaffold for local signalling.

On the other hand, AKAP-79 also interacts with the β2-AR. Biochemical studies have shown that AKAP-79 can co-precipitate with and directly interact with the β2-AR as part of a signalling complex involving PKA, PKC and calcineurin [109]. Whether all β2-ARs in the cardiomyocyte couple to AKAP-79 remains unclear. However, this coupling provides a plausible mechanism by which β2-AR signalling is confined to specific membrane nanodomains. AKAP-79-associated kinases can promote receptor phosphorylation following agonist stimulation, facilitating the switch from G_s to G_i signalling and subsequent ERK/MAPK activation (**1.4**). Lastly, unlike AKAP-79, AKAP-18δ is currently not known to interact with the β-AR directly.

The receptor and scaffold relationship has direct relevance to β-blocker pharmacology. Ligands with partial or intrinsic sympathomimetic activity may activate specific receptor AKAP nanodomains, depending on subtype and the signalling complex engaged. This can have profound therapeutic implications, particularly when considering the use of β-blockers with ISA, whose downstream effects may depend on where β-AR-derived cAMP is generated [9,110,111].

1.4.2 β-adrenoceptor Dysfunction in Cardiovascular Disease

The clinical relevance of β-AR signalling is most apparent in cardiovascular disease, where chronic dysregulation of the receptor contributes to pathological remodelling and disease progression.

Heart failure is the prototypical example of this. CHF may stem from systolic dysfunction (heart failure with reduced ejection fraction, HFrEF) or diastolic dysfunction (heart failure with preserved ejection fraction, HFpEF). Despite different clinical phenotypes, sustained neurohormonal activation is a common feature of disease progression (hypertrophy, fibrosis, altered calcium signalling). This is characterised by increased plasma levels of norepinephrine, angiotensin II, vasopressin and others [112]. At the receptor level, this sustained stimulation induces cardiac β1-AR phosphorylation, desensitisation and selective downregulation. Although these adaptations may initially protect the myocardium from excessive catecholamine exposure, they ultimately contribute to impaired β-adrenergic reserve and contractile dysfunction in CHF [113].

Heart failure also disrupts the spatial organisation of β-AR signalling. β2-ARs may also redistribute from T-tubules to cell crests during disease, converting normally restricted cAMP signals into diffuse responses [114]. More recent work by Kwan *et al.* [115] further suggests that this remodelling may vary to different

degrees according to disease stage and contribute to impaired adrenergic responsiveness, as both β1 and β2-AR mRNA were observed to distribute to the cell periphery.

These pathological processes underpin the grounds for β-blocker therapy. By attenuating catecholamine stimulation, β-blockers may restore β-AR densities, rebalance receptor coupling and ultimately restore basal compartmentation [116]. This has functional consequences as physiological cAMP compartmentalisation is re-established, thereby preserving haemodynamic function. Importantly, their therapeutic benefit may extend beyond simply reducing total cAMP production (**1.5**).

1.4.3 Intracellular β-adrenergic signalling

As introduced in 1.1.3, β-AR signalling can originate intracellularly. Early evidence of this stemmed from the finding that cAMP signalling persisted following receptor internalisation in thyroid-stimulating hormone receptors and parathyroid hormone receptors.

β1-ARs resident at the Golgi apparatus are capable of generating cAMP distinct from the plasma membrane [39]. To characterise functionality, a study by Nash *et al.* suggested that β1-ARs on the Golgi can generate functionally distinct cAMP pools [117]. It was found that Golgi-localised β1-ARs may activate Epac-

PLCε responses associated with a pro-hypertrophic phenotype in cardiomyocytes, offering an explanation to how pathological cardiac remodelling is promoted [118]. β2-ARs have similarly been identified on early endosomes, where they couple to G_s and contribute to cAMP signalling following internalisation [119].

A third intracellular compartment, the SR, contains cAMP pools shown to contribute to ECC [82]. For example, resident β1-ARs at the SR have also been identified to form a physical complex with SERCA2, allowing for the precise activation of PKA-mediated phosphorylation of PLB and TnI at the myofilament [120].

Together, these findings argue that canonical GPCR signalling receives distinct spatial and functional cAMP contributions from receptors independently located from the plasma membrane. How individual β-blockers engage these spatially distinct receptor populations remains largely unknown, and it is to their pharmacology that the chapter now turns. This likely depends on factors such as membrane permeability and ligand transport, with highly lipophilic agents such as carvedilol expected to access these compartments more readily than hydrophilic β-blockers such as atenolol (**Table 2.2**) [121].

1.5 β-blockers in cardiovascular disease

Pathological remodelling of β-AR signalling underpins the need for therapeutic β-blockade. β-blockers are widely used across cardiovascular and systemic indications including hypertension, myocardial infarction, heart failure, arrhythmias, vascular disease and endocrine abnormalities. They remain one of the most prescribed drug classes globally [122]. In CHF, where there is excess endogenous catecholamines, their benefit derives from antagonising maladaptive β-AR mediated inotropic and chronotropic stimulation.

Although all clinically used β-blockers act as competitive antagonists at β-ARs, their clinical effects are not uniform. β-blockers fall into three generations: non-selective (first-generation prototype, e.g. propranolol), β1-selective ("cardio-selective"; e.g. metoprolol, bisoprolol) and third-generation "vasodilating" agents with ancillary properties (e.g. carvedilol, nebivolol) [123]. These distinctions are clinically relevant, as receptor selectivity influences both efficacy and adverse effects. For example, non-selective agents such as nadolol can cause bronchoconstriction through unwanted β2-AR blockade in airway smooth muscle.

Only a limited subset of β-blockers has shown efficacy and mortality benefit in chronic HFrEF. Bisoprolol, carvedilol and sustained release metoprolol succinate have demonstrated unequivocal benefit in landmark trials including CIBIS-II [7],

COPERNICUS [124] and MERIT-HF [125]. However, these breakthrough results were not uniformly achieved across the drug-class. Structurally related antagonists such as bucindolol have failed to replicate clinical advantage [5]. This divergence argues against the notion that β-blockers act solely as interchangeable orthosteric antagonists.

1.5.1 Pharmacological heterogeneity beyond competitive antagonism

The clinical heterogeneity of many β-blockers suggests that their action is beyond simple antagonism. Several agents including carvedilol, bisoprolol and metoprolol have been reported to exhibit low levels of inverse agonism, which has been proposed to contribute to their clinical efficacy in congestive failure [126].

A further layer of complexity is biased signalling (**1.1.4**). Carvedilol, propranolol, alprenolol and nebivolol have been characterised as β-arrestin biased at the β2-AR and recruit ERK1/2 signalling [41,46,127]. Subsequent work extended this profile to HEK-293 cells and EGFR transactivation (**1.5.2**) [128]. At the β1-AR, carvedilol has been reported to stabilise a distinct receptor conformation that switches coupling from Gαs to Gαi, enabling β-arrestin recruitment and downstream signalling that has been implicated in cardio-protection [129,130].

Beyond biased signalling, certain β-antagonists act as weak partial agonists, eliciting low-level G_s activity termed intrinsic sympathomimetic activity (ISA)

[9,110–112]. The clinical significance of ISA remains contentious; β-blockers with known ISA are traditionally contraindicated in the clinic. An important example is xamoterol, a β1-AR partial agonist contraindicated in CHF due to associated harmful increases in heart rate [4,131]. For the same reason, pindolol's notable ISA may exacerbate congestive HF, and has been linked to arrhythmias and sudden cardiac death [132]. These observations, together with the failure of other cAMP-elevating agents such as milrinone, indicate that sustained drug-induced increases in cAMP appear harmful in the long-term, despite being initially beneficial for contractility [133].

However, the interpretation of ISA is not clear-cut. The adverse profile of some ISA-containing drugs does not necessarily imply that all residual agonist activity is harmful. In patients prone to myocardial depression, such as the elderly, weak G_s activity may theoretically preserve beneficial β-AR activity [134]. Accordingly, agents with ISA were predicted to produce less nodal depression and bronchoconstriction than pure antagonists [122]. In a study of stress-induced cardiac dysfunction in rats, celiprolol (β-blocker with ISA) attenuated left ventricular systolic dysfunction, partially improving contractility [134].

These uncertainties are exemplified by carvedilol, whose superior clinical outcomes remain mechanistically unexplained, with proposed contributors

including β-arrestin biased signalling (**1.1.4**), ancillary properties, inverse agonism and possible ISA [101,120]. In the COMET trial, carvedilol even showed extended survival relative to the β1-selective metoprolol tartrate, reinforcing its distinctiveness [6].

1.5.2 Carvedilol

Carvedilol is of particular interest because its clinical benefit over other β-AR antagonists has been difficult to explain. Its favourable profile was initially attributed to its mixed selectivity and ancillary properties: antioxidant, anti-inflammatory, anti-ischaemic and anti-arrhythmic effects [135–137]. This has prompted investigation into whether carvedilol engages distinct signalling mechanisms downstream of the β-AR.

A major contribution came from studies proposing carvedilol as a β-arrestin-biased ligand at the β2-AR [41]. In the experiment, HEK-293 cells were stably transfected with a mutant β-arrestin that does not couple to G-proteins. Carvedilol promoted GRK mediated phosphorylation of the receptor, subsequently recruiting β-arrestin and phosphorylating ERK1/2. Knockdown of β-arrestin 2 abolished ERK1/2 phosphorylation, supporting the notion that carvedilol may be one of 16 β-blockers that preferentially activate β-arrestin-dependent pathways [41,138]. Further studies have also shown carvedilol and

atenolol could induce β1-mediated transactivation of epidermal growth factor receptor (EGFR), in a β-arrestin dependent manner, and that this provides cardio-protection in mice subject to chronic catecholamine stimulation [128,130].

In more recent attempts, the picture is contradictory. Notably, a study by Benkel *et al.* utilised an engineered HEK-293 cell-line lacking functional G-proteins and failed to reproduce the β-arrestin dependent signalling mechanism of carvedilol [9]. Instead, carvedilol produced low level $G\alpha_s$ signalling at the β2-AR when $G\alpha_s$ was reintroduced by transient transfection. This signalling persisted in β-arrestin knockout models, and was further supported by FRET studies in the bulk cytosol that show an explicit rise in cAMP [9]. This approach has reframed the scientific debate against established clinical pharmacology of carvedilol, backed by decades of data from landmark trials and pre-clinical studies [110,111,124,139,140]. Whether carvedilol possesses ISA could not be resolved, especially when considering its superior clinical outcomes compared to ISA and non-ISA antagonists in HFrEF trials [124,125,131,141].

The conflict in literature likely reflects differences in experimental systems and measured endpoints. Specifically, the Lefkowitz group criticised that transfection by Benkel *et al.* of cDNAs encoding the β2-AR leads to expression levels up to 100-fold higher than endogenous expression [9]. At more physiological levels of

expression in HEK-293, carvedilol has not been reported to induce elevation of cAMP [142]. Furthermore, the 10 μM carvedilol used by Benkel *et al.* and others has been criticised as well above clinically achieved plasma levels [139,143]. These are important considerations because weak partial agonism may only be apparent when receptor reserve is high, or when ligand concentrations exceed those relevant *in vivo*.

Nevertheless, carvedilol's ISA cannot be discounted, as older studies report it raising cAMP in human explants [111] and other overexpression systems [40,144–146]. It can be said, however, that reports are inconsistent, suggesting incongruencies and limitations in experimental design and background (**4.1**).

1.6 Thesis Aims

Although β-blocker therapy is empirical in CHF management, the molecular basis underlying the divergent clinical profiles of individual β-blockers is incompletely understood. Several mechanisms have been proposed to explain the unique effects of distinct β-blockers and certain cardioprotective effects. Biased agonism is one theory that may account for this but has traditionally been examined through the lens of G-protein versus β-arrestin coupling (**1.1.4**). Its potential to also shape the subcellular location at which cAMP is generated has not been investigated. Other reasons for differences in clinical outcomes include ligand selectivity,

ancillary properties and partial agonist effects. For example, carvedilol's mixed selectivity towards α-receptors and its carbazole moiety promote vasodilatory properties and antioxidant activity respectively [136]. No research, however, has addressed variation in downstream cAMP signalling or its compartmentalisation.

In experiments that do investigate cAMP, measurements have relied on bulk cytosolic levels, homogenate cAMP assays, AC activity assays or contractility measurements in isolated muscle preparations [111,137,140]. While informative, these approaches are conceptually incompatible with the underlying physiology of cAMP signalling in signalosomes (**1.2**).

This high experimental heterogeneity has led to debate, exemplified by the Benkel–Lefkowitz disagreement on carvedilol's classification as an arrestin-biased or ISA-associated ligand [9,139,147]. Given the unresolved accounts, carvedilol was therefore selected as the β-blocker of interest in this study.

I hypothesise that β-blockers produce compartment-specific cAMP signals that are not predicted by their bulk-cAMP profiles. The primary aims of the experiments presented are to:

i) Investigate whether the β-blocking effect of carvedilol, bucindolol and metoprolol is compartmentalised.

ii) Characterise compartment-specific responses due to ISA using carvedilol, bucindolol (established ISA), metoprolol (negative control) and isoproterenol (full agonist).

iii) Determine whether compartment-specific signals are due to differential β1- versus β2-AR engagement.

Chapter 2

Methodology

2.1 Materials

2.1.1 Reagents

Reagents were obtained from listed commercial suppliers and were used without further purification. Forskolin (FSK), 3-isobutyl-1-methylxanthine (IBMX) and isoproterenol hydrochloride (ISO) were from Sigma-Aldrich. β-adrenergic ligands: bucindolol, carvedilol, metoprolol (succinate), CGP-20712A, ICI-118551 were obtained from Cayman Chemical. Highly selective β1 (CGP-20712A) and β2 (ICI-118551) antagonists have selectivity ratios of more than 500-fold and are widely used as pharmacological dissectors [148,149]. Binding affinities of each agent employed are listed (**Table 2.1**) and membrane permeability (**Table 2.2**).

Enzymes used for primary cardiomyocyte isolation included collagenase A from Roche, and pancreatin (porcine) from Sigma-Aldrich. The adhesion substrate, laminin (mouse), was from Gibco (Thermo Fisher Scientific). Cell culture reagents used were Dulbecco's Modified Eagle Medium (DMEM; high glucose, HEPES), Ham's F-12 nutrient mixture, horse serum (HS), Medium-199 (M199),

newborn calf serum (NCS), L-glutamine, phosphate-buffered saline (PBS) and penicillin-streptomycin (1000 U/mL), all obtained from Invitrogen (Thermo Fisher Scientific).

Transfection was performed using kits from jetPRIME (Polyplus/Sartorius) and Transfectin (Bio-Rad) in line with manufacturer protocols.

Table 2.1: *Receptor selectivity of ligands utilised in this work. For isoproterenol, a functional pEC50 was recorded based on cAMP accumulation in the cell line. Binding affinities (pKi) at β-adrenoceptors were obtained from radioligand competition binding assays.*

Compound	Class	pK_i (β1)	pK_i (β2)	β1/ β2 selectivity ratio	pEC_{50}	Assay	Reference
Isoproterenol	Non-selective β-agonist	6.1-7.0	6.4-6.6	~1	8.2-8.6 (β1 and β2)	Whole cell [^{3}H]-CGP12177, CHO; [^{125}I]-iodocyanopindolol, ICYP	[144,150,151]
Carvedilol	Non-selective β-antagonist/α1 antagonist	8.8-9.8	9.4-10.6	β2 preferring	N/A	Whole cell [^{3}H]-CGP12177, CHO	[144,152]
Bucindolol	Non-selective antagonist, weak partial agonist	8.79-9.3	8.92	~1	N/A	Whole cell [^{3}H]-CGP12177, CHO	[144,153]
Metoprolol	β1-selective antagonist	7.0-7.9	6.3-6.9	β1 preferring	N/A	Whole cell [^{3}H]-CGP12177, CHO	[144,152,154]
CGP-20712A	β1-selective antagonist (tool)	7.8-9.6	N/A	501.2 (β1 selective)	N/A	Whole cell [^{3}H]-CGP12177, CHO	[144,152,154, 155]
ICI-118551	β2-selective antagonist (tool)	N/A	9.1-9.4	660.7 (β2 selective)	N/A	Whole cell [^{3}H]-	[144,146,154]

	CGP12177, CHO

Table 2.2: *Predicted lipophilicity and topological polar surface area (TPSA) of ligands used in this study, as proxies for passive membrane permeability. Octanol-water partition coefficients (Log Po/w) were calculated using the atom contribution method (WLOGP) [156] and TPSA by the Ertl (2009) fragment-based method [157]. Parameters were obtained from SwissADME using canonical SMILES retrieved from PubChem. Å² = Square Angstrom (1Å = 10-10 m)*

Compound	Log $P_{o/w}$ (WLOGP)	TPSA (Å²)	References
Isoproterenol	0.80	72.72	[156–159]
Carvedilol	3.74	75.74	[156–159]
Bucindolol	3.39	81.07	[156–159]
Metoprolol	1.61	50.72	[156–159]
CGP-20712A	3.47	131.86	[156–159]
ICI-118551	2.61	41.49	[156–159]

2.1.2 Genetic Constructs and Biosensors

In CHO cell experiments, plasmids of the β2-AR (Snap-β2AR) were provided by Dr Paulo Annibale from the University of St. Andrews. Co-transfection with FRET biosensor was performed based on manufacturer's protocol using jetPRIME (Polyplus/Sartorius) kit.

A panel of genetically encoded FRET sensors was used to monitor intracellular cAMP dynamics (**Table 2.3**). These included untargeted and targeted cAMP reporters. The series of reporters used throughout this work (CUTie and Epac-based) were selected for their structural properties and dynamic range (1.3.2), allowing comparisons to be more reliably interpreted.

Targeted sensors include the CUTie sensors, where the CFP is bound to the C-terminus and YFP is integrated in the external loop of the CNBD preserving the N-terminus for conjugation of a targeting domain (**1.3.4**). Due to structural similarity, the sensors exhibit comparable kinetic properties; thus, different responses observed between each sensor can be interpreted confidently as reflecting subcellular location rather than intrinsic differences of the sensors themselves [82]. Untargeted cytosolic cAMP reporters included Epac-S^{H187}, the latest generation of Epac-based sensors with the largest dynamic range (**1.3.3**) [86]. This makes it ideal in experiments to detect small differences in cAMP concentrations. Each reporter can be described as gain or loss of FRET, determined by the conformational change bringing the fluorophores together (**1.3.3, 1.3.4**).

CUTie sensors used in this work included those that localise to the plasmalemma (AKAP-79 CUTie), sarcoplasmic reticulum (AKAP-18δ CUTie) and myofilament (TnI CUTie) [82] (**Table 2.3**). In addition to previously characterised sensors, this study employed two novel genetically encoded plasmids. Firstly, a Golgi-targeted CUTie sensor was designed to enable investigation into receptor internalisation and endomembrane signalling. GalT-CUTie was generated in-house by another member using beta 1,4-galactosyltransferase (GalT), a commonly used trans-

Golgi marker, as a targeting domain. GalT was subcloned from pCMV-GalT-mCherry, a gift from Shinya Tsukiji (Addgene plasmid #214271; http://n2t.net/addgene:214271; RRID:Addgene_214271) [160]. Secondly, an Epac-based endoplasmic reticulum-targeted cAMP reporter (ER-cyto-H90) was generated in previous unpublished work from the laboratory by Dr Miguel Lobo. The construct is derived from an Epac based reporter (H90) and targeted by fusion of cytochrome p450 2C1 N-terminal sequence to the sensor. The sensor reports cAMP changes in the ER-proximal cytosolic nanodomain rather than within the ER lumen.

Constructs were expressed either via transient transfection or adeno-associated viral (AAV) transduction. AAVs carrying desired constructs were generated by Vector BioLabs (Malvern, PA, USA).

Table 2.3: *List of FRET sensors used. All sensors were generated within the laboratory except Epac-S^{H187}.*

Name	Gain or Loss of FRET	Vector	Localisation	Reference
AKAP18δ-CUTie	Gain	Adenoviral	PLB/SERCA (SR)	[82]
AKAP79-CUTie	Gain	Adenoviral	Plasmalemma	[82]
TnI-CUTie	Gain	Adenoviral	Myofilament	[82]
GalT-CUTie	Gain	Plasmid	Galactosyltransferase	[160]
Epac-S^{H187}	Loss	Adenoviral	Cytosolic	[86]
ER-Cyto-H90	Loss	Plasmid	Cytosolic SR	Unpublished

2.1.3 FRET sensor characteristics

Genetically encoded FRET biosensors differ in biochemical and functional characterisation particularly in their affinity and dynamic range (the maximum change in fluorescence signal that a biosensor can produce). Interpretation of these results therefore require careful consideration in terms of the dynamic range, given the potential influence on the magnitude of detected responses. A summary of the reported characteristics of biosensors is shown (Table 2.4). It should be noted that GalT CUTie and ER-Cyto-H90 have not underwent formal biochemical characterisation, and such characterisation was beyond the scope of this work.

Table 2.4: *Biochemical and functional characteristics of FRET-based cAMP biosensors. EC50 and Hill coefficients were determined from cAMP concentration-response curves in stable CHO cells. Dynamic range is expressed as the percentage change in FRET emission ratio relative to baseline (R0) as reported in previous studies.*

Name	**EC_{50}** (μM)	**Hill coefficient**	**Dynamic Range** (% $\Delta R/R_0$)	**Reference**
AKAP18δ-CUTie	7.14	1.04	~164%	[77,82,161]
AKAP79-CUTie	7.17	1.23	~23%	[77,82,161]
TnI-CUTie	7.24	1.15	~23%	[77,82,161]
Epac-S^{H187}	7.41	1.75	~23%	[77,86,161]

2.2 Experimental Methods

2.2.1 CHO Cell Culture

Chinese hamster ovary (CHO) cells were maintained and cultured in Ham's F-12 medium supplemented with 10% (v/v) foetal bovine serum (FBS), 1% (v/v) penicillin-streptomycin and 1% (v/v) L-glutamine. Cells were cultured at 37°C and kept in a humidified incubator with 5% CO_2.

2.2.2 Primary Neonatal Rat Ventricular Myocyte Isolation and Culture

All animal procedures conform to the guidelines from Directive 2010/63/EU on the protection of animals used for scientific purposes. Primary neonatal rat ventricular myocytes (NRVMs) were isolated from 2 to 3 days-old Sprague-Dawley pups (supplied by Charles River) as described previously [162].

Briefly, neonatal rats were sacrificed by cervical dislocation and exsanguination followed by decapitation with sterile scissors. The chest was opened along the sternum for hearts to be extracted and transferred immediately into ice-cold ADS buffer (1.2 mM NaCl, 0.05 mM KCl, 0.18 HEPES, 0.008 mM NaH_2PO_4, 0.06 mM glucose, 0.004 mM $MgSO_4$). The atria and major vessels were removed from each heart. Remaining ventricular tissue was washed in fresh cold ADS buffer and

transferred into a 60mm dish with ice-cold ADS to be minced into small fragments.

Tissue fragments were initially transferred to 5 mL of digestion buffer (0.45 mg/mL collagenase A, 1.25 mg/mL pancreatin in ADS buffer) and incubated under continuous agitation with a magnetic stirrer at 37°C for 5 minutes. The supernatant was then discarded for the tissue to undergo four serial digestions. In each successive digestion, the tissue was incubated this time at 37°C in continuous agitation in 9 mL digestion buffer for 20 minutes. After each digestion, the supernatant was collected and added to 1 mL NCS. This solution was then centrifuged at 1250 rpm for 5 minutes; the pellet was resuspended in 2 mL NCS and incubated at 37°C. Remaining tissue was used in the subsequent digestion steps. After four digestions, NCS cell suspensions were pooled and centrifuged again for 5 minutes at 1250 rpm. The pellet was then resuspended in M1 medium (4.5 g D-glucose/L DMEM (with 25 mM HEPES) supplemented with 17.5% M199, 10% (v/v) HS, 5% (v/v) NCS, 200 mM L-glutamine, 100 U/mL penicillin, and 100 µg/mL streptomycin). The suspension was pre-plated on two 100 mm dishes and incubated in a humidified incubator again at 37°C and 5% CO_2 for 2 hours. This is to reduce non-myocyte contamination, allowing fibroblasts to adhere while cardiomyocytes remained in suspension. The cardiomyocyte

enriched fraction was subsequently collected from the dishes and centrifuged at 1250 rpm for 5 minutes. The supernatant was discarded and the pellet resuspended in 1 mL M1 medium per heart.

For viral transduction and/or plasmid infection, 150 µL of cardiomyocyte suspension was seeded on 24 mm laminin-coated glass coverslips in 6 well plates at a density of 20000-60000 cells per well. Cells were first incubated for another two hours and wells were topped up with 2 ml M1 medium, then incubated overnight at 37°C with 5% CO_2. After 18 hours, cultures were washed with ADS buffer and culture medium was replaced with M2 medium (DMEM (with 25 mM HEPES) supplemented with 17% (v/v) M199, 5% (v/v) HS, 0.5% (v/v) NCS, 200 mM L-glutamine, 100 U/mL penicillin and 100 µg/mL streptomycin). Cells were incubated for a minimum of 2 hours under standard culture conditions, as described, prior to transduction or transfection.

2.2.3 Transfection and Infection Procedures

CHO cells were seeded onto 24mm coverslips from day 0, transfected in accordance with manufacturer instructions using Polyplus jetPRIME transfection reagent on day 1, then imaged on day 3. Where viral transduction was performed, imaging was performed on day 2 instead.

NRVMs were seeded onto 24mm coverslips from day 0, infected (and transfected) on day 1 and imaged on day 2 or 3. In viral transduction, cardiomyocytes were prepared as described above and maintained in M2 medium. AAVs containing the relevant biosensors were used to achieve efficient gene delivery to NRVMs. A defined volume of culture medium (200 µL) was first removed from each well and mixed with the appropriate viral vector to achieve the desired multiplicity of infection (MOI) in range from 10-100. The viral medium was then returned directly and uniformly to the cells. Cells with the viral preparation were incubated under standard culture conditions (37°C , 5% CO_2). For FRET reporters transduced with AAVs, imaging was performed 24 hours following infection, except for AKAP-79 CUTie, for which imaging was performed 48 hours after infection.

DNA transfection in NRVMs was performed using Transfectin reagent (Bio-Rad) according to a modified protocol optimised for primary cardiomyocytes. For each well, two separate solutions were prepared. Briefly, in the first tube, plasmid DNA (2.5 µg per well) was diluted in M199 (250 µL per well) and vortexed. In a second tube, 7.5 µL of Transfectin reagent per well was diluted in M199 (250 µL per well) and vortexed. Diluted DNA and Transfectin solutions were then combined and vortexed once more to ensure homogenous mixing. The solution was

incubated for 20 minutes at room temperature (RT) to allow formation of DNA-reagent complexes. Next, 500 µL of the transfection mixture was added dropwise to seeded NRVMs. Cells were imaged 48 hours post-transfection and were maintained in a humidified incubator at standard culture conditions.

2.2.4 Fluorescence Resonance Energy Transfer (FRET)

The principles of FRET are outlined in **section 1.3**. General structure of Epac and CUTie sensors are described in **section 1.3.3 and 1.3.4**. Sensors employed in this work were introduced in **Table 2.3**. In short, binding of cAMP to the CNBD of the biosensor induces a conformational shape change that alters the spatial relationship between fluorophores. This translates into a measurable signal due to changes in FRET efficiency, manifesting as either a gain or loss of FRET. FRET-based biosensors have been extensively utilised to characterise GPCR signalling [70,82,86,163].

Live-cell imaging was conducted at RT in a modified Ringer's solution (125 mM NaCl, 5 mM KCl, 1 mM Na_3PO_4, 1 mM $MgSO_4$, 20 mM HEPES, 5.5 mM glucose, 1 mM $CaCl_2$, pH 7.4) after pre-incubation for 10 minutes at RT. Imaging was obtained on an inverted microscope (Olympus IX71) using a PlanApoN, 40X, NA 1.42 oil immersion objective (Olympus, UK) and equipped with a CoolSNAP HQ2 CCD camera (Photometrics) and a DV2 beam-splitter (MAG Biosystems,

Photometrics). Acquisition and processing were done using Metafluor 7.1 software (Meta Imaging Series, Molecular Devices) (RRID:SCR_014294). Changes in FRET were measured as a change in background-subtracted fluorescence emission intensity ratio upon excitation and expressed as F/F_0, where F is the ratio at any given time (t) and F_0 is the initial mean baseline ratio before stimulation. Excitation was performed at 430 nm, and emission intensities were collected at 480 nm (donor) and 545 nm (acceptor). Pharmacological agents, such as β-blockers and isoproterenol, were then added during imaging. FRET time courses were normalised to F_0 for easy comparison of different FRET curves. For comparison across different experiments, quantification of curves was performed through normalising responses to the maximal signal obtained following application of a saturating stimulus (FSK (25 µM) and IBMX (100 µM)). FRET change is expressed as a percentage of this maximum response. Analysis was achieved using Microsoft Excel (RRID: SCR_016137) and GraphPad Prism version 10.6.1 (RRID: SCR_002798).

Additionally, the kinetics of cAMP accumulation were analysed by quantifying the initial rate of FRET change of the maximum (ΔFRET/time) following agonist stimulation. This was achieved by fitting a linear regression to the first 20 seconds of the response immediately after administration of the ligand. This

parameter provides a sensitive measure to discriminate between ligands in their rates of activation despite comparable steady-state effects.

2.2.5 Immunofluorescence

Immunofluorescence staining was performed to validate the localisation of the GalT-CUTie sensor. NRVM cells were washed three times with PBS in polystyrene dishes prior to fixation. For immunofluorescence, NRVMs were fixed in 4% (w/v) paraformaldehyde (Thermo Scientific) in PBS for 15 minutes at RT. Following fixation, PFA-solution was removed and cells were washed with PBS. For storage of cells, 1 mL PBS with 0.01% sodium-azide and penicillin/streptomycin (10 µl/ml) was applied. Cells were stored at 4°C.

Following storage, cells were first washed twice with PBS and permeabilised with 0.1% Triton X100 (Thermo Scientific) in PBS for 5 minutes and washed with PBS again. Non-specific binding was blocked by incubating cells at RT with 1% bovine serum albumin (BSA; fraction V Roche) in PBS. All antibodies were diluted in the same solution. Primary antibodies were applied for 1 hour at RT, followed by 3-5 washes with PBS. Next, fluorophore-conjugated secondary antibodies were applied for 1 hour at RT then washed 3-5 times with PBS.

Coverslips were mounted using mounting media with DAPI (Ibidi) and sealed with nail varnish. Imaging was done using a confocal laser scanning microscope

(Leica TCS SP5 II) equipped with a 60x immersion objective. Images were acquired using NDP software (Hamamatsu) (RRID:SCR_025177) and processed using Fiji (ImageJ).

Table 2.5: *List of antibodies used*

Type	Target	Species	Dilution	Company
Primary	GOLGA2/GM130	mouse	1:500	proteintech
Secondary	Alexa Fluor 568 IgG (H+ L)	anti-mouse	1:500	Thermo Fisher Scientific

2.2.6 Data and Statistical Analysis

Image processing was completed using Fiji (ImageJ), Prism (GraphPad) for statistical analyses and Excel for FRET data collection.

Data presented on graphs are displayed as means ± standard deviation (SD) unless otherwise stated. All data presented in the figures were obtained from at least three separate NRVM isolations for reproducibility and mitigation of batch effects. Each dot in the figure represents one cell. Preliminary findings from CHO cells were acquired from at least two different passages (**S5**).

For FRET data analysis, each data point represents a measurement from a single cell or defined subcellular regions. Observations from separate cells were treated independently. This assumption was supported by preliminary experiments

demonstrating that identical stimuli produced heterogeneous responses in neighbouring cells on the same coverslip, validating independence of observations.

Prior to statistical analyses, data distribution was assessed for normality using the Shapiro-Wilk test for small samples ($n<50$). Data were considered normally distributed if the p-value was greater than 0.05. For normally distributed datasets with equal variances, comparisons between multiple groups were undertaken using a one-way analysis of variance (ANOVA) with a Bonferroni correction for multiple comparisons. Otherwise, if data did not meet assumptions for normality, non-parametric analyses were performed. For multiple groups, the Kruskal-Wallis test was used with Dunn's post-hoc correction. If only two groups were compared and normally distributed, an unpaired t-test was used with Welch's correction. If this was non-parametric, a Mann-Whitney U test was conducted. Significance levels were taken as $p < 0.05$.

Chapter 3

Results

3.1 Differential antagonistic activity of β-AR antagonists at nanodomains

To accurately measure cAMP responses at specific subcellular compartments, as well as determine their magnitude and kinetics, a suite of targeted FRET reporters was utilised. The measurements were performed in NRVMs expressing the endogenous Epac based reporter (Epac-S^{H187} (cytosol)) and the sensors (AKAP-18δ CUTie (localised at the SERCA/PLB complex), AKAP-79 CUTie (localised at the sarcolemma), TnI CUTie (localised at the troponin complex on the myofilament)). This suite of sensors has been extensively validated in previous work from our group in terms of their localisations and usage to measure differential cAMP signalling in related subcellular compartments [82]. The architecture of these sensors and photophysical properties are previously described in **1.3.3** and **1.3.4**.

Representative images showing sensor localisation (presented in **Figure 3.1**).

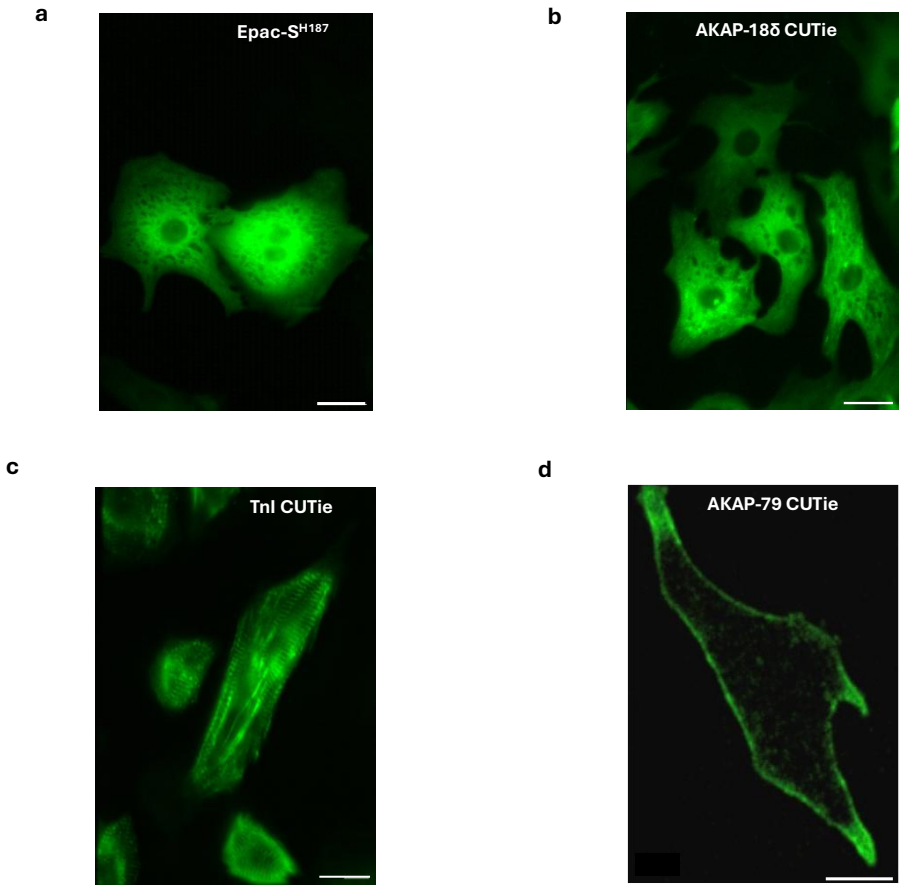


Figure 3.1: *cAMP signalling in nanodomains related to excitation-contraction coupling (ECC) and receptor internalisation. Representative images of neonatal rat ventricular myocytes (NRVMs) expressing the sensors: (a) Epac-SH187 (cytosol), (b) AKAP-18δ CUTie (SERCA/PLB), (c) TnI CUTie (myofilament), (d) AKAP-79 CUTie (plasmalemma, L-type Ca2+ channel). Scale bar: 20 μm.*

3.1.1 β-AR antagonists differentially inhibit ISO-stimulated cAMP across ECC nanodomains

First, the ability of carvedilol, bucindolol and metoprolol to inhibit β-AR mediated cAMP response elicited by isoproterenol was measured to determine the extent of their efficacy as antagonists and any compartment-selective effects. FRET responses in the following experiments were recorded when cells were

stimulated by co-administration of the respective β-antagonist (10 μM) and ISO (1 nM) followed by a saturating stimulus (25 μM FSK, 10 μM IBMX). Doses were selected to replicate previous investigations [9,41]. Administration was performed by bath application. In NRVMs expressing the Epac-S^{H187} sensor, the positive-control and non-selective β-agonist ISO elicited a mean FRET change of 30.31 ± 10.33% (n = 10) relative to the maximum response (**Figure 3.1.1a**).

Bucindolol, a β-blocker known to exhibit ISA, reduced the ISO-stimulated response, showing a mean FRET change of 12.71 ± 5.57% (n = 24) ($p<0.0001$) of the maximum response [111,112]. Carvedilol showed an even greater reduction in ISO-induced cAMP response, achieving a mean FRET change of 6.13 ± 4.25% (n = 28) of the maximum response ($p < 0.0001$). Metoprolol provided the largest reduction of ISO-induced cAMP, resulting in a mean FRET change of 2.20 ± 1.46% (n = 20) ($p < 0.0001$) (**Figure 3.1.1a-c**). Metoprolol was selected as a negative control as there currently exist no reports supporting it having ISA in addition to its approval for CHF and widespread clinical use [8,134,140,164,165]. While carvedilol achieved greater reduction of cAMP than bucindolol, there was no significant difference found when compared against metoprolol (mean difference = 3.93, 95% CI [-0.15, 8.02], p = 0.064). Nonetheless, all β-AR antagonists successfully produced a reduction of cAMP in the bulk cytosol.

Altogether, these findings are consistent with β-blockers functioning as antagonists and in the presence of catecholamines, in this case the synthetic catecholamine ISO.

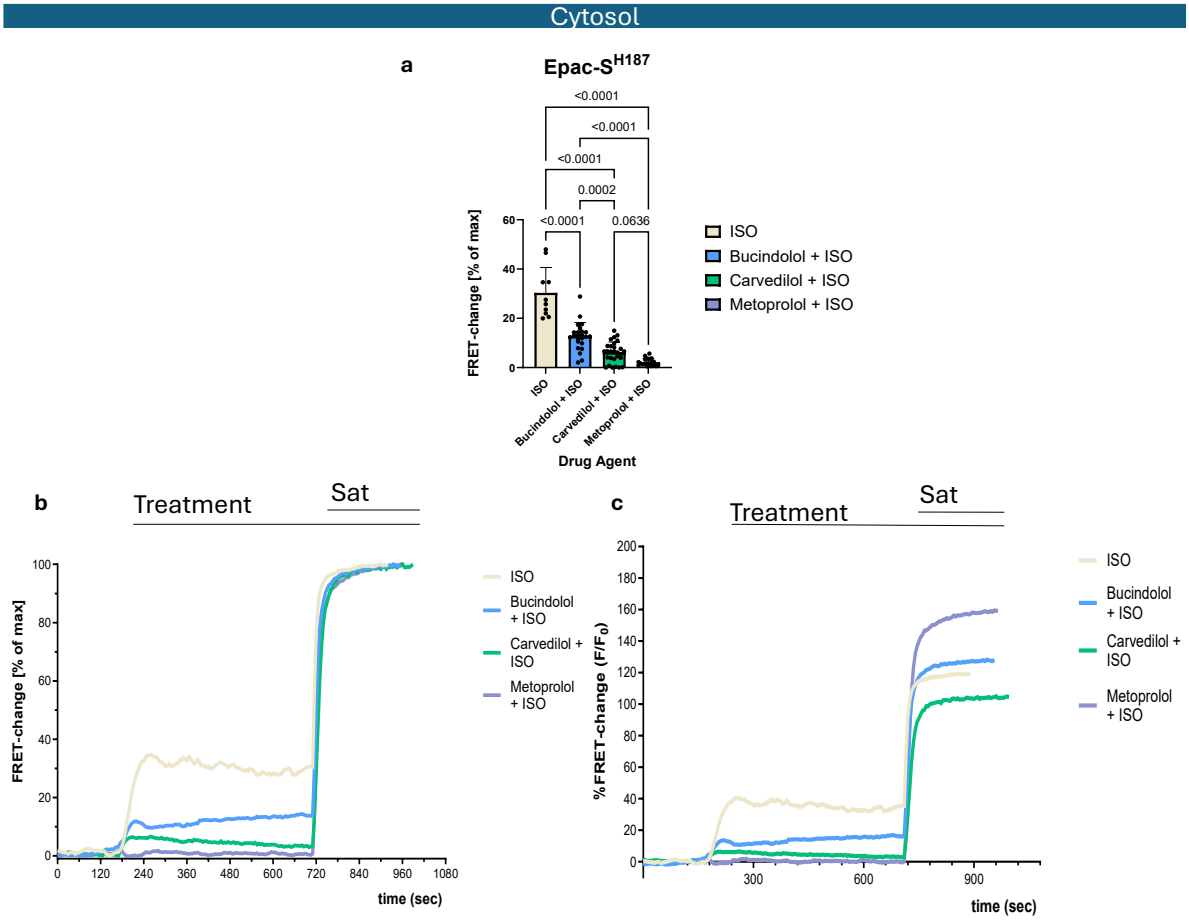


Figure 3.1.1: *Summary (a) and representative kinetics (b) and (c) of NRVM expressing Epac-SH187 in response to application of both 1 nM ISO and 10 μM drug (bucindolol, carvedilol and metoprolol). Data are expressed as either maximum FRET (%) change from saturating stimulus (25 μM FSK + 100 μM IBMX) (b) or % change from initial value (F/F0) (c). Each dot represents one individual cell from minimum three biological replicates. Error bars represent mean ± SD.*

Similarly, in NRVMs expressing AKAP-18δ CUTie, ISO elicited a positive mean FRET change of 23.88 ± 7.16% (n = 7) of the maximum response (**Figure 3.1.2a**). Notably, this result was significantly lower than in the cytosol. Application of

bucindolol + ISO resulted in a mean FRET change response (10.27 ± 5.42%, p < 0.0001) (n = 24). At this nanodomain, carvedilol almost completely abolished the FRET response elicited by ISO (3.08 ± 4.08%, p < 0.0001) (n = 20). Interestingly, this was in line with what was seen with metoprolol which yielded significant reduction in cAMP compared to ISO (2.14 ± 2.74%, p < 0.0001) (n = 18) but was like carvedilol (mean difference = 0.94, 95% CI [-3.07,4.95], p = 0.93) (**Figure 3.1.2a-c**). This may indicate that carvedilol's beta-blockade effect is more efficacious at the AKAP-18δ (SERCA/PLB) nanodomain, consistent with bucindolol, carvedilol and metoprolol being all lipophilic (**Table 2.2**) and potentially able to block internal receptors or may reflect tighter local regulation of this domain by PDEs. For example, this may occur through the hydrolytic activity of PDE3A1, which maintains basal cAMP at SERCA/PLB [73]. This will be revisited in a later experiment.

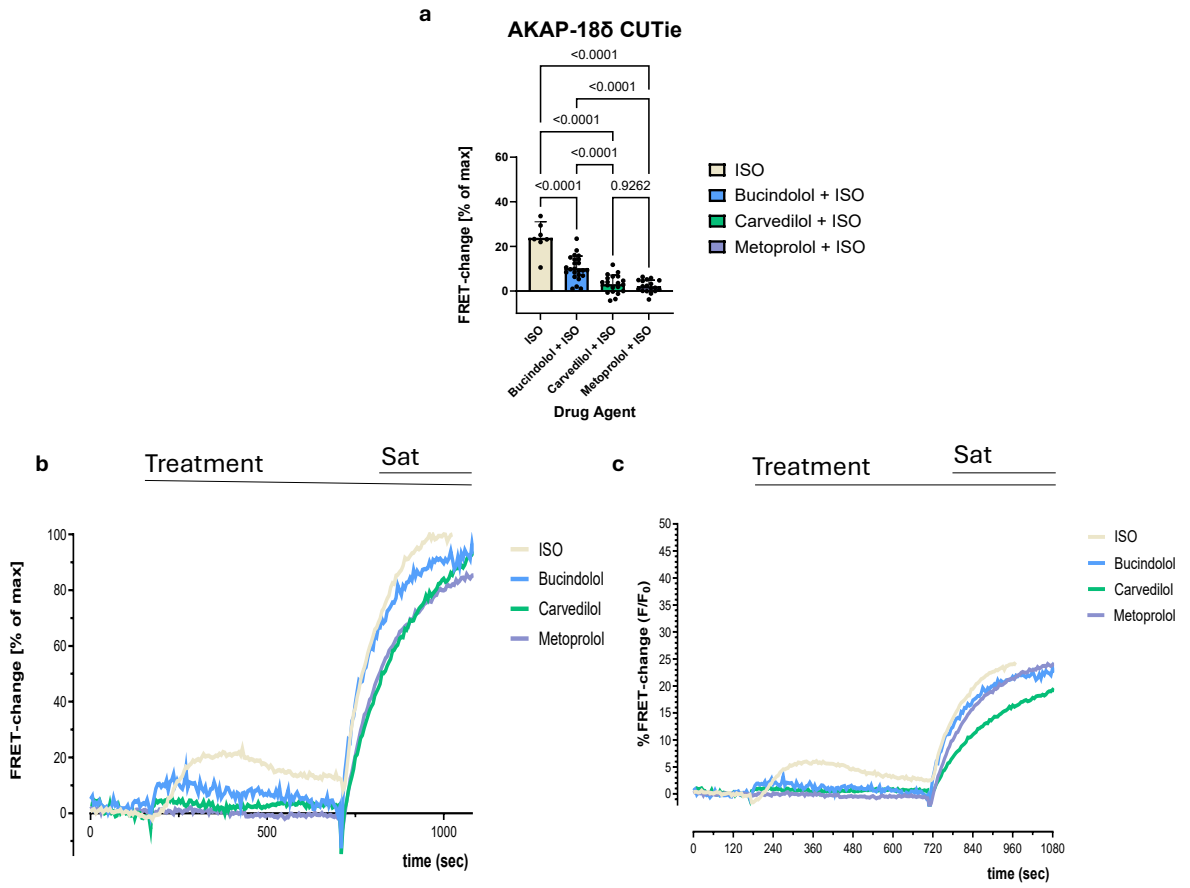


Figure 3.1.2: *Summary (a) and representative kinetics (b) and (c) of NRVM expressing AKAP-18δ CUTie in response to application of both 1 nM ISO and 10 μM drug (bucindolol, carvedilol and metoprolol). Data are expressed as either maximum FRET (%) change from saturating stimulus (25 μM FSK + 100 μM IBMX) (b) or % change from initial value (F/F0) (c). Each dot represents one individual cell from minimum three biological replicates. Error bars represent mean ± SD.*

In cells expressing AKAP-79 CUTie, a sarcolemmal nanodomain, ISO stimulated a mean response of cAMP similar to bulk cytosol and AKAP-18δ domain (28.12 ± 13.56%, n = 10) (**Figure 3.1.3**). In contrast, all β-AR antagonists similarly attenuated the cAMP response at this domain (**Figure 3.1.3**), suggesting a mechanism that achieves uniform inhibition at the receptor-proximal compartment, in contrast to the responses seen in more distal nanodomains

(**Figure 3.1.2, 3.1.4**). Bucindolol yielded a mean FRET-change of 5.07 ± 6.35% of the maximum compared to ISO (n = 29, p < 0.0001). This was no different from the effect of carvedilol or metoprolol which both had mean FRET changes of 1.21 (± 3.73%) and 3.14 (± 3.87%) respectively (**Figure 3.1.3a-c**).

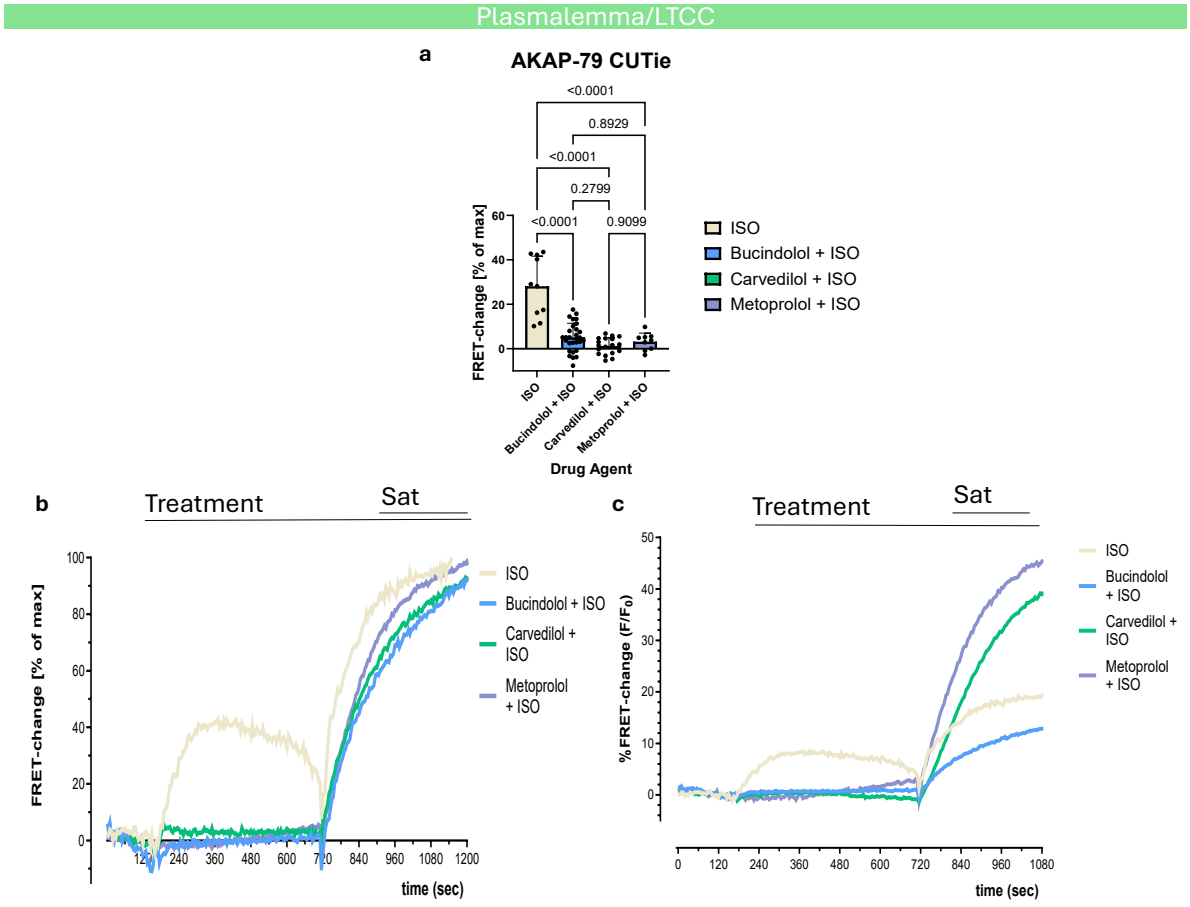


Figure 3.1.3: *Summary (a) and representative kinetics (b) and (c) of NRVM expressing AKAP-79 CUTie in response to application of both 1 nM ISO and 10 μM drug (bucindolol, carvedilol and metoprolol). Data are expressed as either maximum FRET (%) change from saturating stimulus (25 μM FSK + 100 μM IBMX) (b) or % change from initial value (F/F0) (c). Each dot represents one individual cell from minimum three biological replicates. Error bars represent mean ± SD.*

As expected, the full agonist ISO elicited a robust response (30.29 ± 8.21%, n = 5) in NRVMs expressing TnI CUTie (myofilament). In this compartment, carvedilol (21.53 ± 12.59%, n = 6, p = 0.35) or bucindolol (16.29 ± 9.77%, n = 7, p = 0.047) had a less pronounced inhibitory effect on ISO-driven cAMP than observed at other compartments. The reduced inhibitory activity at the myofilament is again suggestive of compartmentalisation, implying variation of β-AR antagonist activity between compartments. However, the traces for this set of experiments were noisier, and several cells failed to respond even to the saturating stimulus. These cells were excluded from the compiled data. Lastly, metoprolol once again significantly attenuated the ISO response (mean FRET change = 1.64 (± 2.51%), n = 9, p<0.0001). The results suggest that the compartment-specific inhibition pattern may arise from some residual agonist activity of certain agents such as bucindolol, a known ISA predominantly at the β1-AR [111,112]. To test whether such activity is present in this system, each β-blocker was next bath applied alone in the absence of ISO and the cAMP response elicited was measured at each ECC-related compartment.

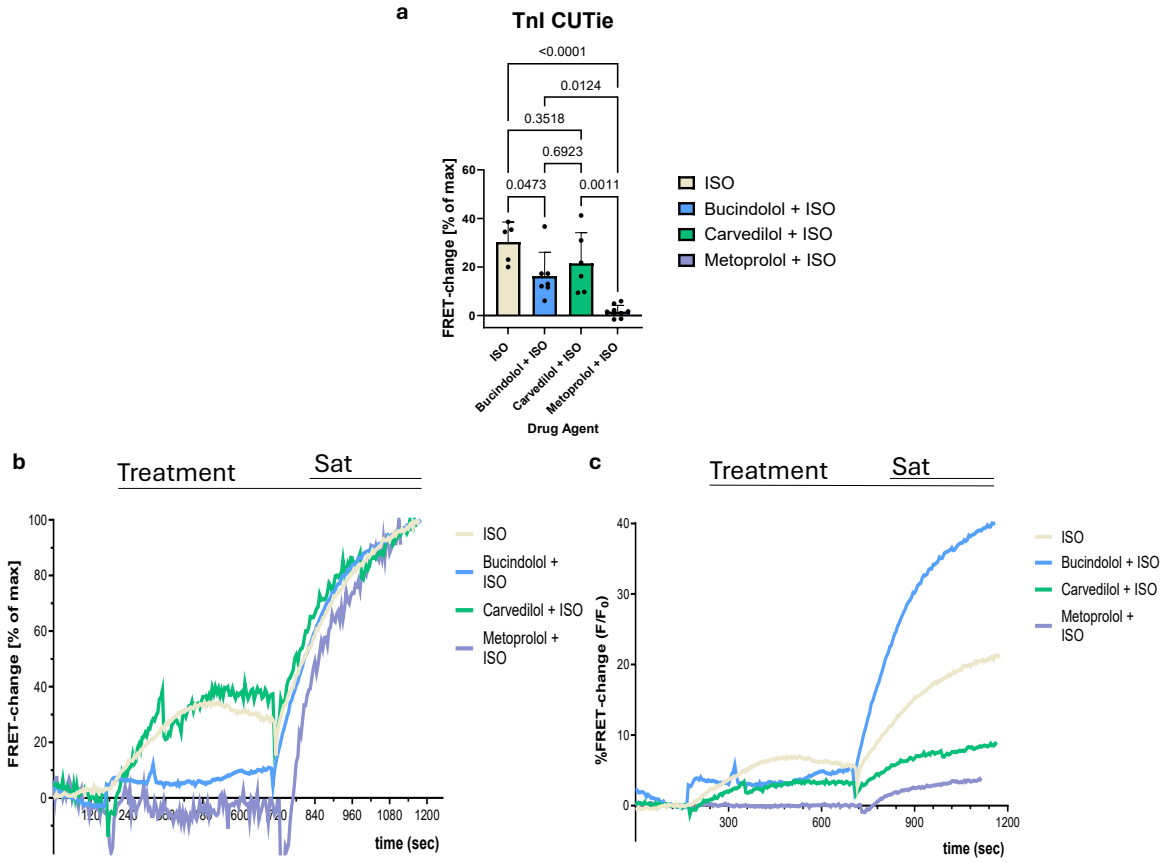


Figure 3.1.4: *Summary (a) and representative kinetics (b) and (c) of NRVM expressing TnI CUTie in response to application of both 1 nM ISO and 10 μM drug (bucindolol, carvedilol and metoprolol). Data are expressed as either maximum FRET (%) change from saturating stimulus (25 μM FSK + 100 μM IBMX) (b) or % change from initial value (F/F0) (c). Each dot represents one individual cell from minimum three biological replicates. Error bars represent mean ± SD.*

3.2 Carvedilol and bucindolol have partial agonist activity in cardiac myocytes

To determine if compartment-specific differences in the inhibitory effect of β-blockers may be due to residual ISA, first the effect of carvedilol and bucindolol alone on basal cAMP levels in the bulk cytosol was measured in NRVMs expressing Epac-S^{H187}. The resolution and dynamic range of this sensor allow

detection of the bulk effect, accounting for small changes in cAMP concentrations [86].

Bucindolol elicited a mean FRET change of 11.28 ± 2.56% (n = 13) of the maximum response, consistent with its classification as a compound exhibiting ISA (**Figure 3.2.1a-d**) [110–112]. An elevation of cAMP comparable to bucindolol ($p > 0.99$) was also recorded on application of carvedilol alone (10.84 ± 4.17%, n = 18), whereas metoprolol produced a negligible response (2.61 ± 1.18%, n = 19). These results indicate that both bucindolol (bucindolol vs ISO: mean difference = 19.03, 95% CI [14.08, 23.97], $p < 0.0001$) and carvedilol (carvedilol vs ISO: mean difference = 19.47, 95% CI [14.83, 24.10], $p < 0.0001$) have some partial agonistic activity at the β-AR, elevating cAMP to a lesser extent compared to the full agonist ISO (**Figure 3.2.1a-c,e**).

For bucindolol and metoprolol, the cAMP response to the antagonist alone was indistinguishable from that observed in the presence of ISO ($p = 0.79$ and $p = 0.96$ respectively) (**Figure 3.2.1d-f**) (**3.1.1**). Carvedilol produced a borderline higher rise of cAMP than during co-application with ISO ($p = 0.035$) (**3.1.1**).

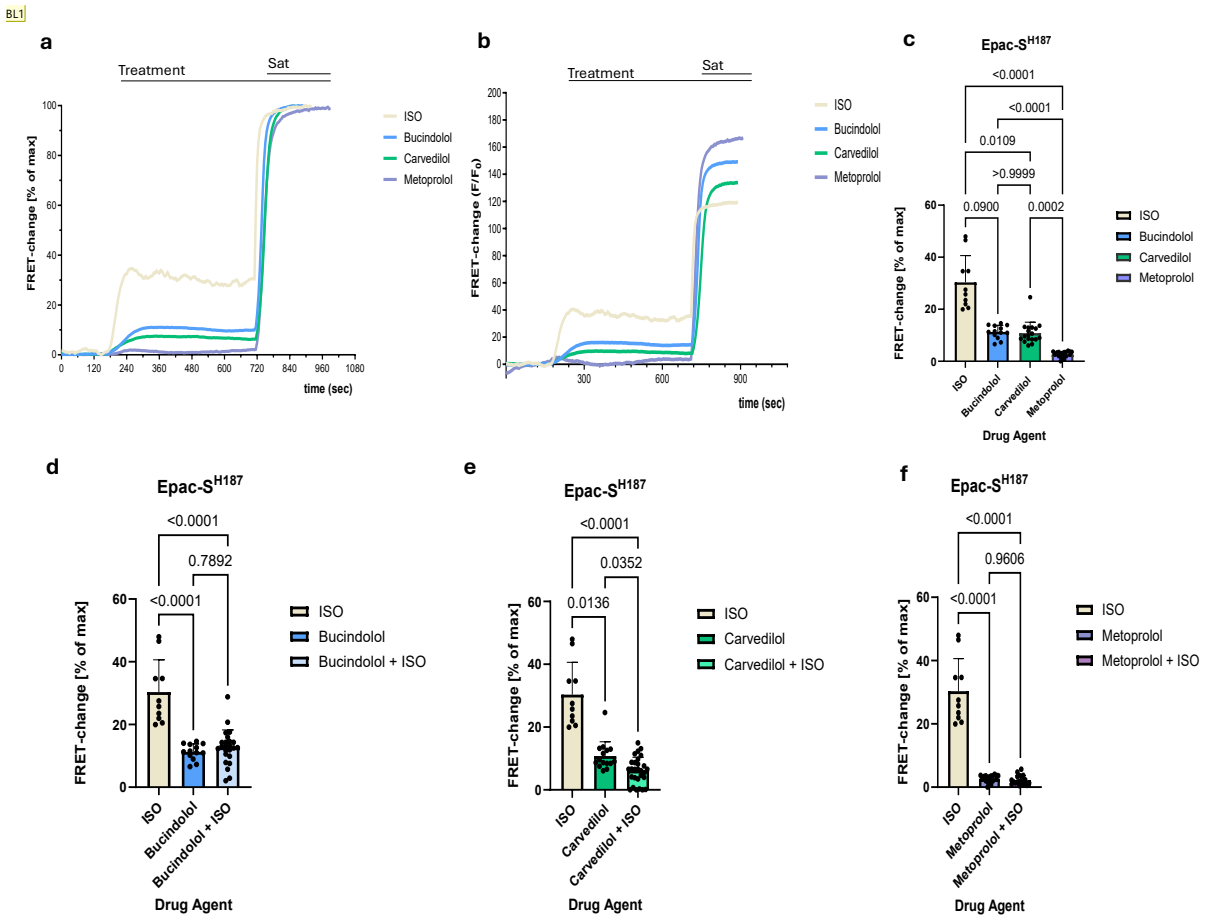


Figure 3.2.1: *Representative kinetics (a) and (b) and summary (c) of FRET change from neonatal rat ventricular myocytes (NRVM) expressing Epac-SH187 cAMP FRET reporter in response to bath application of 1 nM isoproterenol (ISO), 10 μM bucindolol, 10 μM carvedilol and 10 μM metoprolol. Summary comparison (d), (e) and (f) of NRVMs expressing Epac-SH187 upon application of solely 10 μM bucindolol, 10 μM carvedilol and 10 μM metoprolol against their co-application with 1 nM ISO. Data are expressed as either maximum FRET (%) change from saturating stimulus (25 μM FSK + 100 μM IBMX) (a), (c), (d), (e) and (f) or % change from initial value (F/F0) (b). Each dot represents one individual cell from minimum three biological replicates. Error bars represent mean ± SD.*

3.2.1 Partial agonist behaviour exhibited by carvedilol persists at lower concentrations

An argument against physiologically relevant partial agonist activity elicited by carvedilol could be the high concentration used in the experiments (10 μM). As aforementioned, a concentration of 10 μM carvedilol was selected to replicate

experiments previously performed by the Lefkowitz and Kostenis groups where partial agonist and β-arrestin biased activity was found [9,41]. For similar reasons, a concentration of 10 μM bucindolol was chosen given that the mean absolute maximum FRET change (F/F_0) of bucindolol was found to be comparable (18.00 ± 6.74%, n = 16) to carvedilol (16.05 ± 7.25%, n = 18) (**Figure 3.2.2a**).

In light of recent discourse (1.5.2), 10 μM has been criticised as an order of magnitude above the plasma concentrations carvedilol achieves clinically and G_s activity may not be present at lower concentrations [139]. Dose-response experiments and unpublished results performed by another student in our group using carvedilol have shown that it elicits a dose-dependent cAMP response. Low levels of cAMP persisted at lower concentrations (down to 0.1 μM) and were not limited at 10 μM (data not shown). Consequently, experiments were repeated with a lower concentration (1.5 μM) to approximate the effective myocardial concentration achieved at therapeutic doses (5-to-7-fold above its peak plasma concentration (~0.3 μM) clinically) [166–168].

Carvedilol (1.5 μM) produced a lower, albeit significant, mean FRET change of 5.03 (± 3.63%) of the maximum response (**Figure 3.2.2b**). These results confirm that carvedilol retains this property even at lower concentrations reflecting cardiac tissue accumulation.

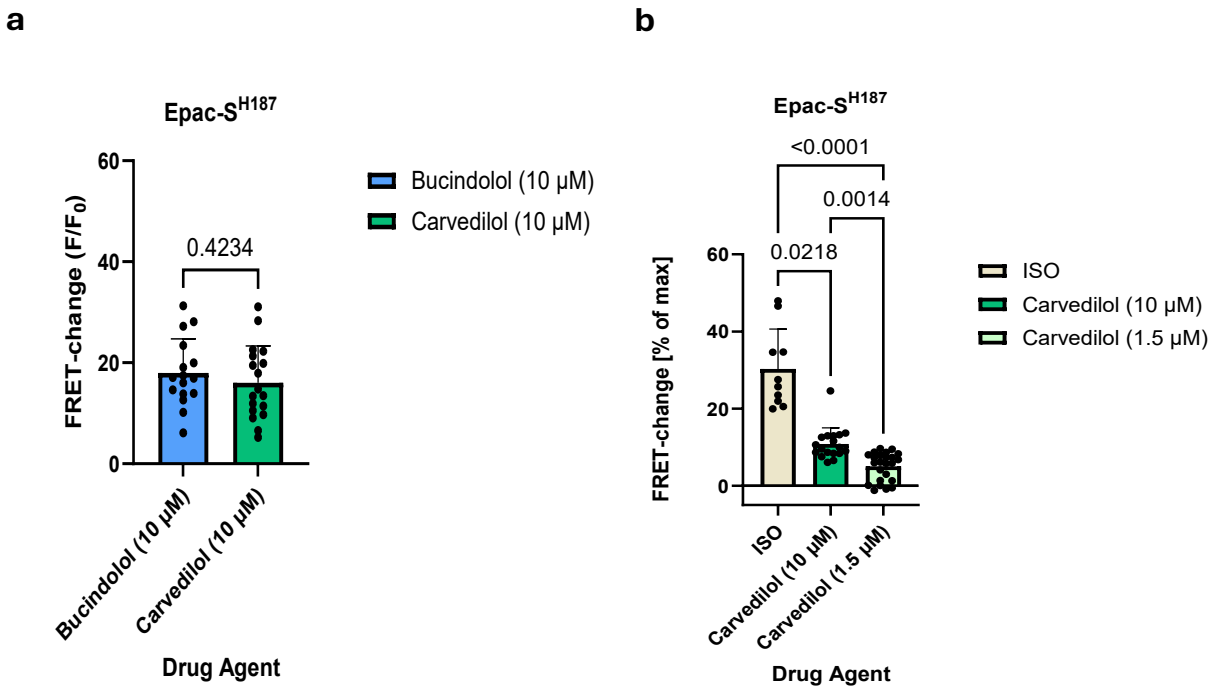


Figure 3.2.2: *Summary comparison (a) of NRVMs expressing Epac-SH187 upon application of 10 µM bucindolol or 10 µM carvedilol. Summary comparison (b) of NRVMs expressing Epac-SH187 upon application of 10 µM carvedilol and 1.5 µM carvedilol against 1 nM ISO. Data are expressed as either maximum FRET (%) change from saturating stimulus (25 µM FSK + 100 µM IBMX) (b) or % change from initial value (F/F0) (a). Each dot represents one individual cell from minimum three biological replicates. Error bars represent mean ± SD.*

3.2.2 Carvedilol and bucindolol elicit distinct, compartment-specific cAMP responses

Having established that carvedilol and bucindolol both exhibit ISA, their subcellular responses were investigated using targeted CUTie sensors (**Table 2.3**). ISO stimulated a full response in all compartments (**Figure 3.2.3a**) and metoprolol as expected, did not elicit a significant cAMP response in any compartment (**Figure 3.2.3d**). Notably, bucindolol produced robust cAMP responses in all compartments except the plasmalemma at the AKAP-79 nanodomain (mean

FRET change 3.78 ± 1.78%). Interestingly, the mean response of bucindolol at the myofilament was significantly higher than in all other compartments ($p < 0.05$). This indicates that there is a restricted pattern of cAMP signalling and that intrinsic sympathomimetic activity occurs in a compartmentalised manner (**Figure 3.2.3a-d**).

On the other hand, carvedilol produced comparably robust cAMP responses across most nanodomains but showed no cAMP elevation at the sarcoplasmic reticulum AKAP-18δ nanodomain (SERCA/PLB) (**Figure 3.2.3c**). A response at the AKAP-79 nanodomain, close to the LTCC ($Ca_v1.2$), was observed upon administration of carvedilol (16.54 ± 8.50%) (**Figure 3.2.3c**). Representative curves for results and their summary at each nanodomain can be found in the appendix (**Figures S1-S3**). This observation is consistent with reports by Benkel *et al.* that carvedilol induced cAMP occurs via β2-AR and that AKAP-79 is reported to co-localise with the β2-AR [9,70,109]. This will be revisited in later experiments using highly selective β-AR antagonists (**3.3**).

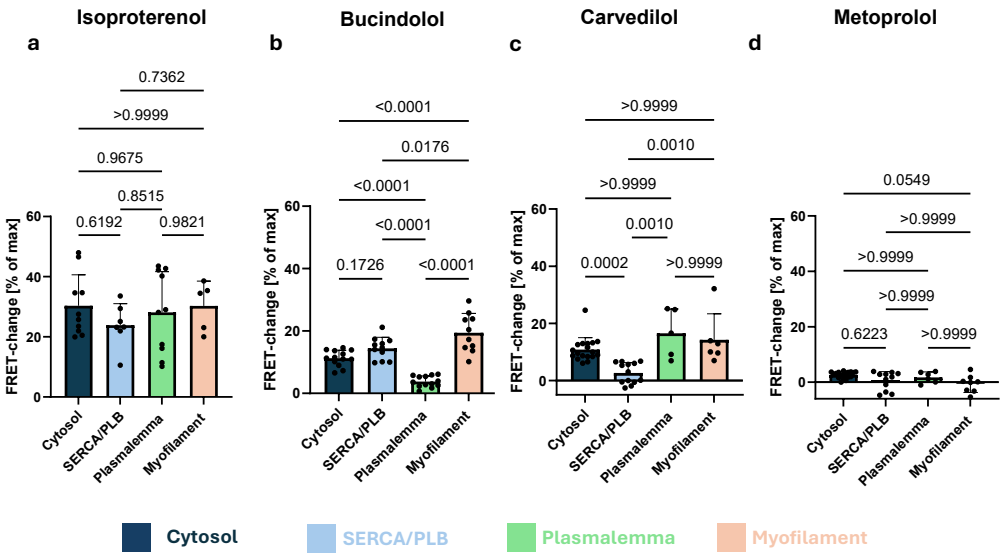


Figure 3.2.3: *Summary of FRET change in NRVM individually expressing Epac-SH187 (Cytosol), AKAP-18δ CUTie (SERCA/PLB), AKAP-79 CUTie (Plasmalemma) or TnI CUTie (Myofilament) cAMP FRET reporters in response to bath application of either (a) 1 nM isoproterenol, (b) 10 μM bucindolol, (c) 10 μM carvedilol, or (d) 10 μM metoprolol. Points represent maximum FRET change elicited by stimulus normalised to the maximum response elicited by a saturating stimulus (25 μM forskolin + 100 μM IBMX). Each dot represents one individual cell from minimum three biological replicates. Error bars represent mean ± SD.*

3.2.3 A nanodomain restricted interaction between carvedilol and ISO occurs at AKAP-79

Across ECC-related compartments tested thus far, the mean cAMP responses to each β-blocker (bucindolol, carvedilol and metoprolol) had no significant difference compared to co-application with ISO ($p > 0.05$) (**Figure 3.2.4**). This is consistent with the notion of residual activity after antagonism at the β-AR.

However, co-application of ISO and carvedilol reduced the response below that of carvedilol alone (mean difference = 15.33, 95% CI [4.70,25.94], $p = 0.0035$) (**Figure 3.2.4e**). While a definitive mechanistic explanation is beyond the scope

of these experiments, this is described in more detail in **section 4.2**. Given that this was the only significant pairwise reduction observed across all compartments, with a modest sample size in both experiments (n = 5-18), independent replication in larger cohorts will be required to confirm the effect and guide mechanistic interpretation.

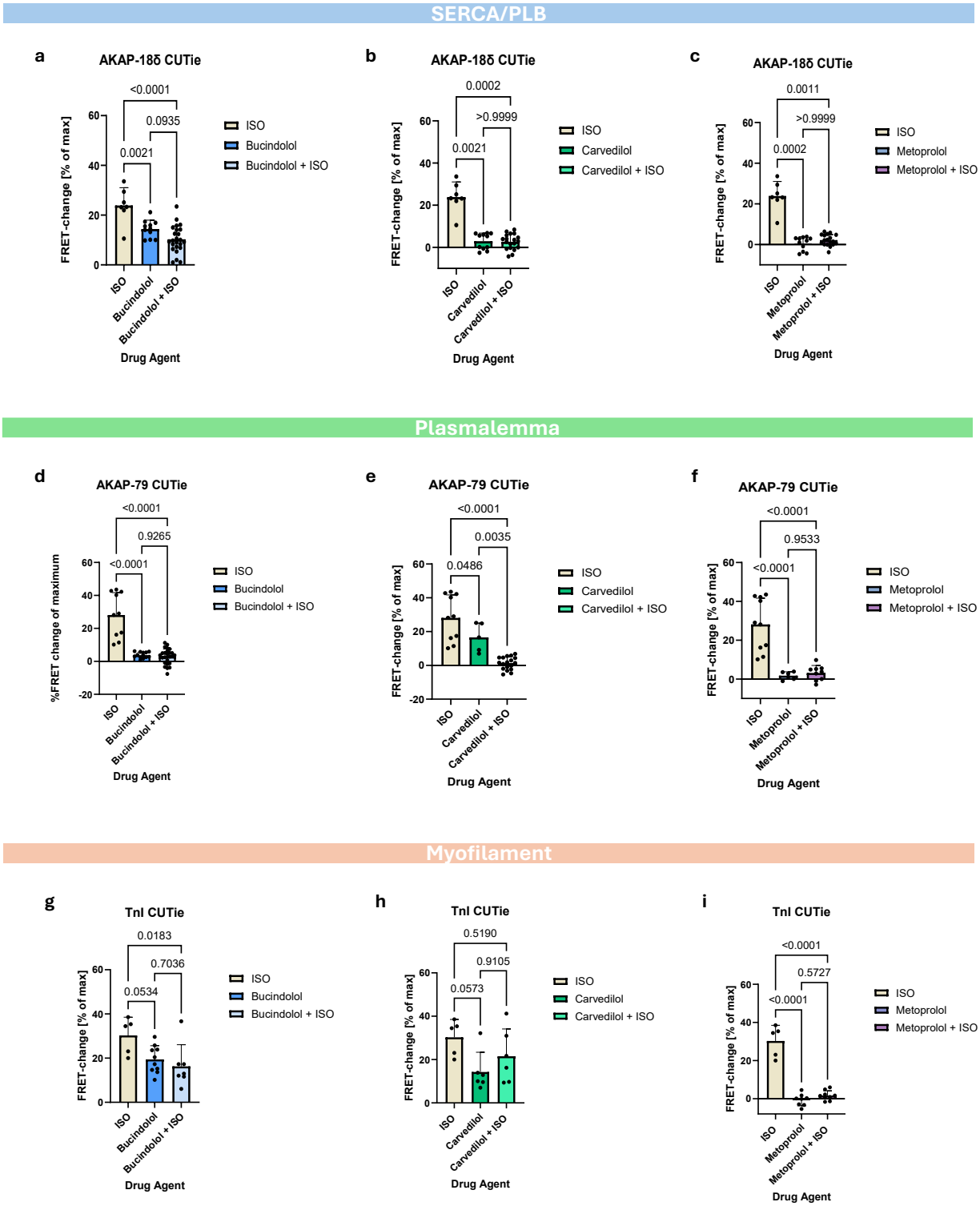


Figure 3.2.4: *Summary comparison (a), (b) and (c) of NRVMs expressing AKAP-18δ CUTie; (d), (e) and (f) of NRVMs expressing AKAP-79 CUTie; (g), (h) and (i) upon application of solely 10 µM bucindolol, 10 µM carvedilol and 10 µM metoprolol against their co-application with 1 nM ISO. Data are expressed as*

maximum FRET (%) change from saturating stimulus (25 μM FSK + 100 μM IBMX). Each dot represents one individual cell from minimum three biological replicates. Error bars represent mean ± SD.

3.2.4 ISA-exhibiting β-AR antagonists show distinct engagement kinetics

Beyond the maximum amplitude of the cAMP response, examination of response kinetics revealed further compound and compartment-specific behaviour (**Figure S4**). Upon bath application of a stimulus, the initial rate of cAMP accumulation was estimated from a linear fit to the first 20 seconds of the FRET response (**2.2.6**), restricted to antagonists previously shown to elicit a cAMP response at each nanodomain (**3.2.2**). A notable pattern emerged when an antagonist possessing ISA was co-applied with ISO: the rate of cAMP generation was generally slower than that observed with the antagonist alone. In the cytosol, this was seen with bucindolol with an initial $\Delta FRET.s^{-1}$ of 1.75 (±1.84) compared to 0.35 (± 0.33) when applied with ISO (mean rank difference = 12.79, p = 0.029). At the AKAP-79 nanodomain, this behaviour was also seen with carvedilol and carvedilol + ISO (mean rank difference = 14.45, p = 0.01). Contrastingly, no significant difference was found at the myofilament and SERCA/PLB domain suggesting that effect may be restricted to specific antagonist-compartment pairs (**Figure S4**). A detailed kinetic analysis of these responses is beyond the scope of the present work but is highlighted here as direction for future investigations.

3.3 Selective receptor antagonism identifies that partial agonist activity is β-AR specific

The compartment-specific carvedilol and bucindolol interaction observed at AKAP-18δ and AKAP-79 nanodomains suggested that there may be differential β1/β2 involvement of each ligand's partial agonism.

To determine the subtype contribution of cAMP generation, the β1 selective antagonist (CGP-20712A (CGP)) and β2 selective (ICI-118551 (ICI)) were used as described in **Chapter 2**. Bulk cytosolic measurements in NRVMs expressing Epac-S^{H187} suggested that bucindolol exhibits ISA through both β1 and β2 receptors, but predominantly via β1-AR (**Figure 3.3.1a,c**). Pretreatment with CGP partially attenuated the mean FRET change (7.27 ± 4.81%, n = 22) compared to untreated cells (mean difference = 4.01, 95% CI [0.49, 7.54], $p < 0.05$) and ICI treated cells (mean difference = -4.75, 95% CI [-8.91, -0.59], $p < 0.05$). No significant difference could be detected between ICI pretreatment and untreated responses (**Figure 3.3.1a,c**).

In contrast, the mean FRET changes of carvedilol in ICI treated cells (β2-AR blockade) significantly reduced the cAMP response (mean rank difference = 18.11, $p<0.0001$) whereas no difference was seen in CGP treated cells (**Figure 3.3.1**).

Together, these results demonstrate that carvedilol's ISA effect is primarily mediated by the β2-AR, in agreement with previous findings [9].

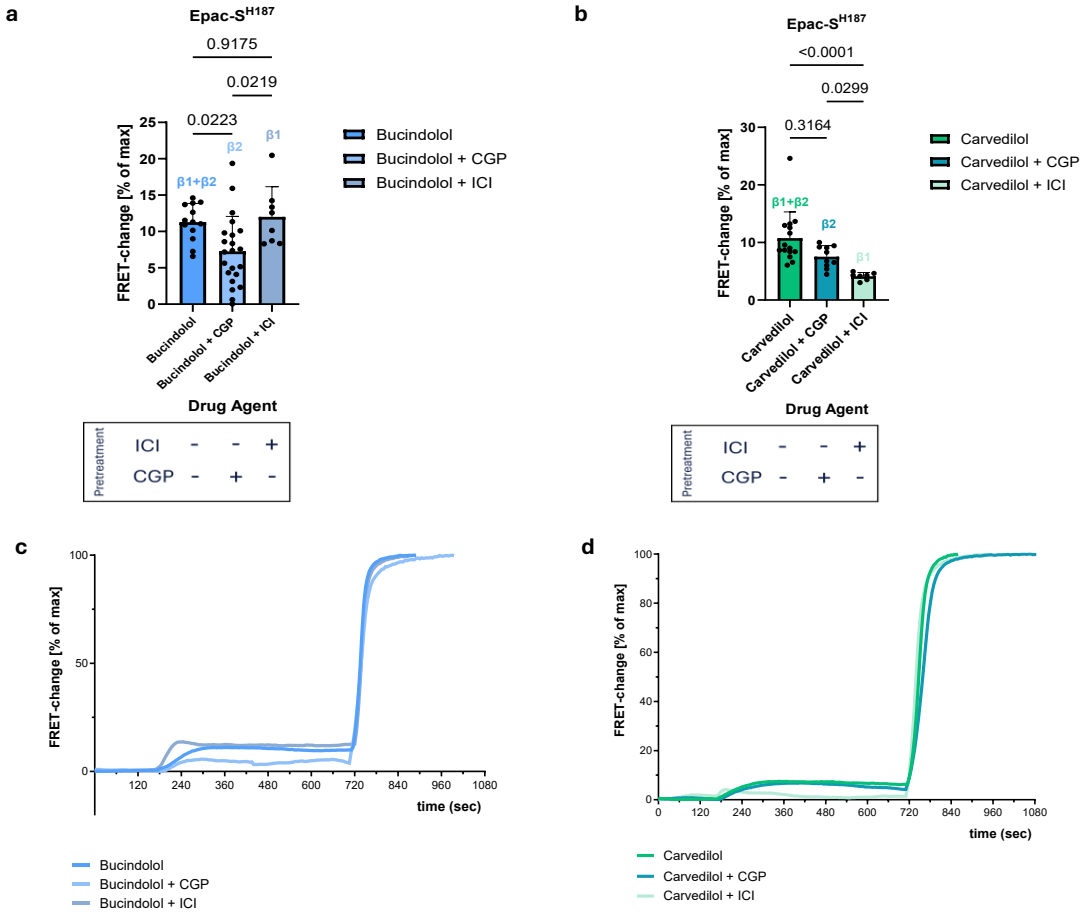


Figure 3.3.1: *Full summary comparisons (a) and (b) and representative kinetics (c) and (d) of FRET change in NRVM expressing Epac-SH187 in response to bath application of 10 μM bucindolol and carvedilol. Cells have been pretreated with either a β1-AR antagonist CGP-20712A (200 nM) or β2-AR antagonist ICI-118551 (200 nM) for at least 16 hours preceding imaging. Data are expressed as maximum FRET (%) change from saturating stimulus (25 μM FSK + 100 μM IBMX), (a-d). Each dot represents one individual cell from minimum three biological replicates. Error bars represent mean ± SD.*

3.3.1 β-AR subtype dependence is observed across ECC related nanodomains

The next aim was to determine whether β-AR subtype dependence identified in the cytosol is preserved at the nanodomain resolution. Thus, the same strategy was repeated with each drug in NRVMs expressing AKAP-18δ, AKAP-79 and TnI CUTie sensors.

At the AKAP-18δ nanodomain, the partial agonist activity of bucindolol persisted after both β1 and β2 blockade (**Figure 3.3.2a,c**). No significant difference between pairwise comparisons in the CGP and ICI groups were found (mean rank difference = 3.93, $p > 0.99$). Consistent with previous observations, carvedilol elicited a negligible cAMP response at this nanodomain in all treatment groups including ICI and CGP pretreated cells (**Figure 3.3.2b,d**).

In a similar vein, bucindolol did not yield a cAMP response at the AKAP-79 domain across the treatment groups (**Figure 3.3.3a,c**). Carvedilol produced a modest, albeit reduced, cAMP response (7.34 ± 3.90%, n = 13) in the CGP group compared to untreated (16.54 ± 8.50%, n = 5). After blockade of the β2-AR, a significant average FRET response of carvedilol could no longer be detected (2.04 ± 2.63%, n = 11). Thus, it can be speculated that the AKAP-79 nanodomain

associates with only a subpopulation of β2-AR that is accessible to carvedilol but not bucindolol.

In FRET experiments utilising TnI CUTie, bucindolol elicited a cAMP response that was significantly attenuated by β1-blockade with CGP (5.04 ± 8.20%, n = 13, p = 0.0025) but unaffected by β2-blockade with ICI (13.56 ± 12.57%, n = 7, p = 0.79) compared to the group without pretreatment (**Figure 3.3.4a-c**). This is consistent with the hypothesis that bucindolol's ISA is predominantly β1-mediated. Likewise, carvedilol produced a comparable initial response (13.86 ± 8.71%, n = 8) that was unaffected by CGP pretreatment (p = 0.99). This response was abolished by ICI (0.81 ± 1.01%, n = 5, p = 0.027), indicating that partial agonism at the myofilament by carvedilol is also β2-AR mediated (**Figure 3.3.4b-d**).

Collectively, these findings recapitulate results established in bulk cytosolic measurements (**3.3**). Representative curves and summaries can be found below (**Figure 3.3.2, 3.3.3 and 3.3.4**).

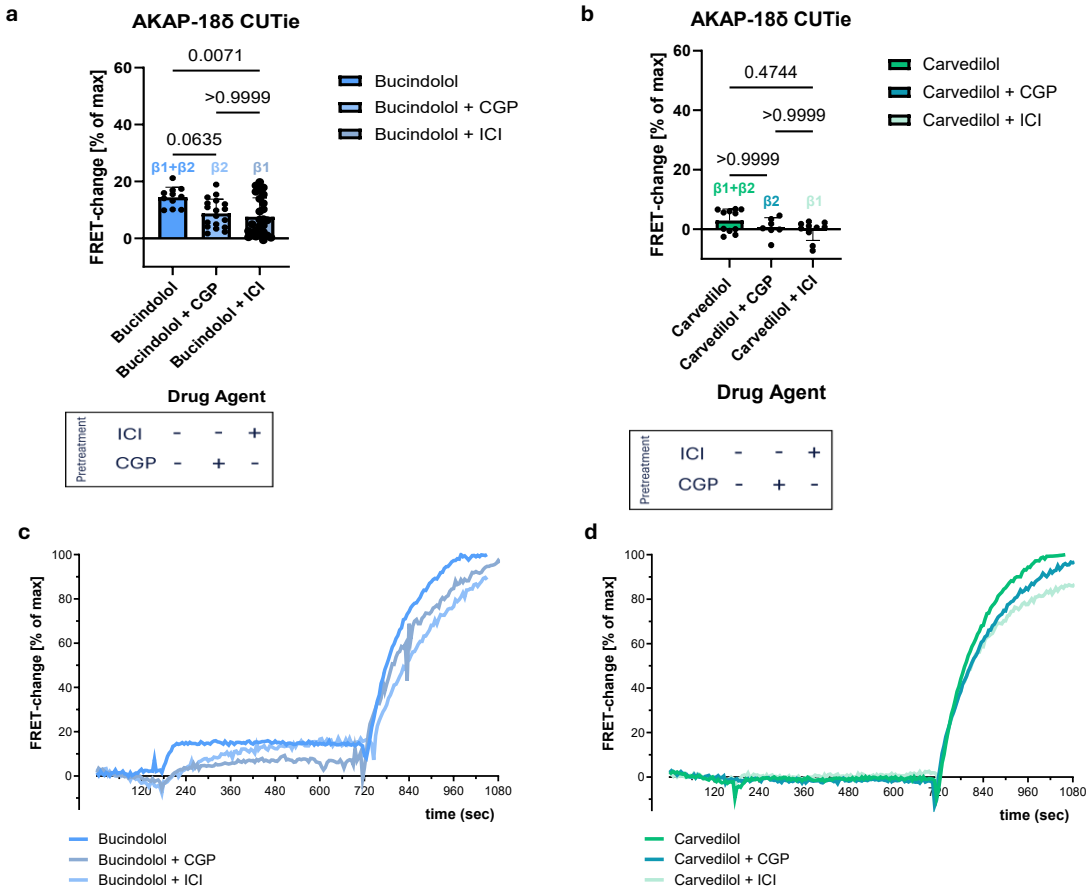


Figure 3.3.2: *Full summary comparisons (a) and (b) and representative kinetics (c) and (d) of FRET change in NRVM expressing AKAP-18δ CUTie, in response to bath application of 10 μM bucindolol and carvedilol. Cells have been pretreated with either a β1-AR antagonist CGP-20712A (200 nM) or β2-AR antagonist ICI-118551 (200 nM) for at least 16 hours preceding imaging. Full summary comparisons are shown (a) and (b). Data are expressed as maximum FRET (%) change from saturating stimulus (25 μM FSK + 100 μM IBMX), (a-d). Each dot represents one individual cell from minimum three biological replicates. Error bars represent mean ± SD.*

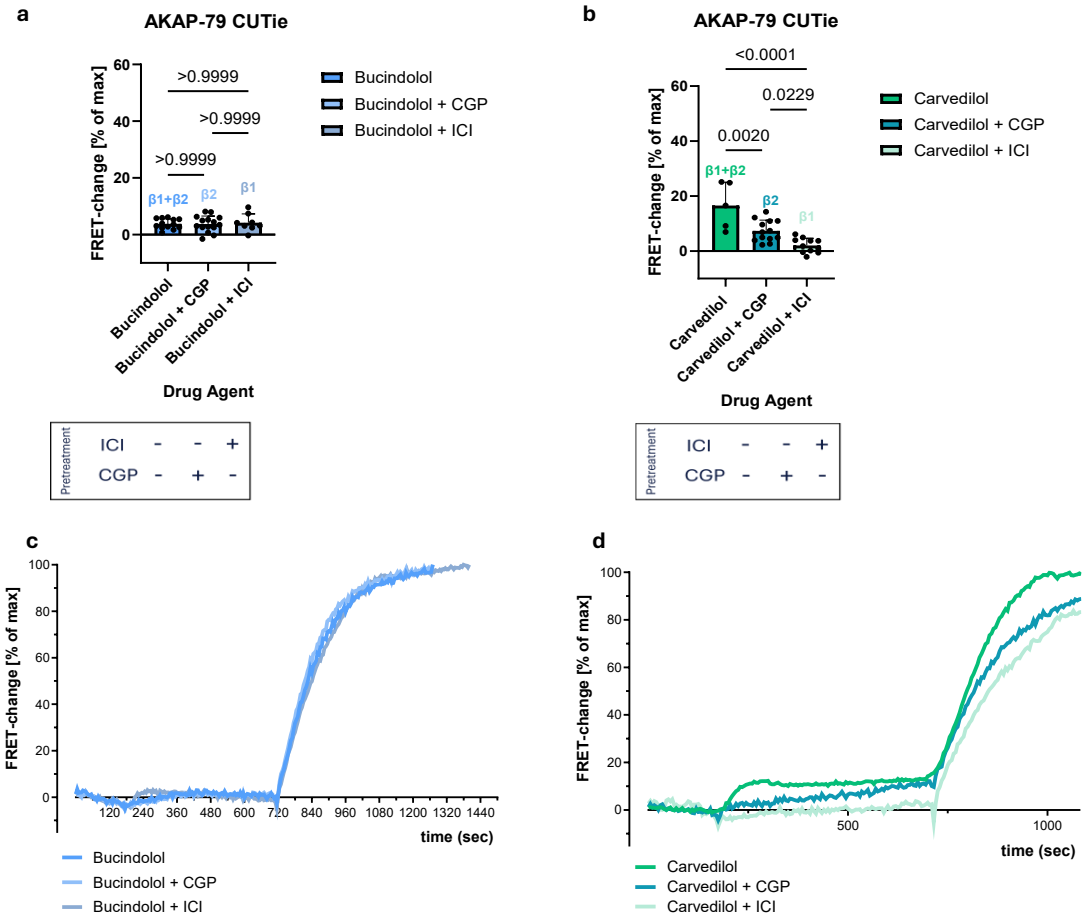


Figure 3.3.3: *Full summary comparisons (a) and (b) and representative kinetics (c) and (d) of FRET change in response to bath application of 10 μM bucindolol and carvedilol. Cells have been pretreated with either a β1-AR antagonist CGP-20712A (200 nM) or β2-AR antagonist ICI-118551 (200 nM) for at least 16 hours preceding imaging. Full summary comparisons are shown (a) and (b). Data are expressed as maximum FRET (%) change from saturating stimulus (25 μM FSK + 100 μM IBMX), (a-d). Each dot represents one individual cell from minimum three biological replicates. Error bars represent mean ± SD.*

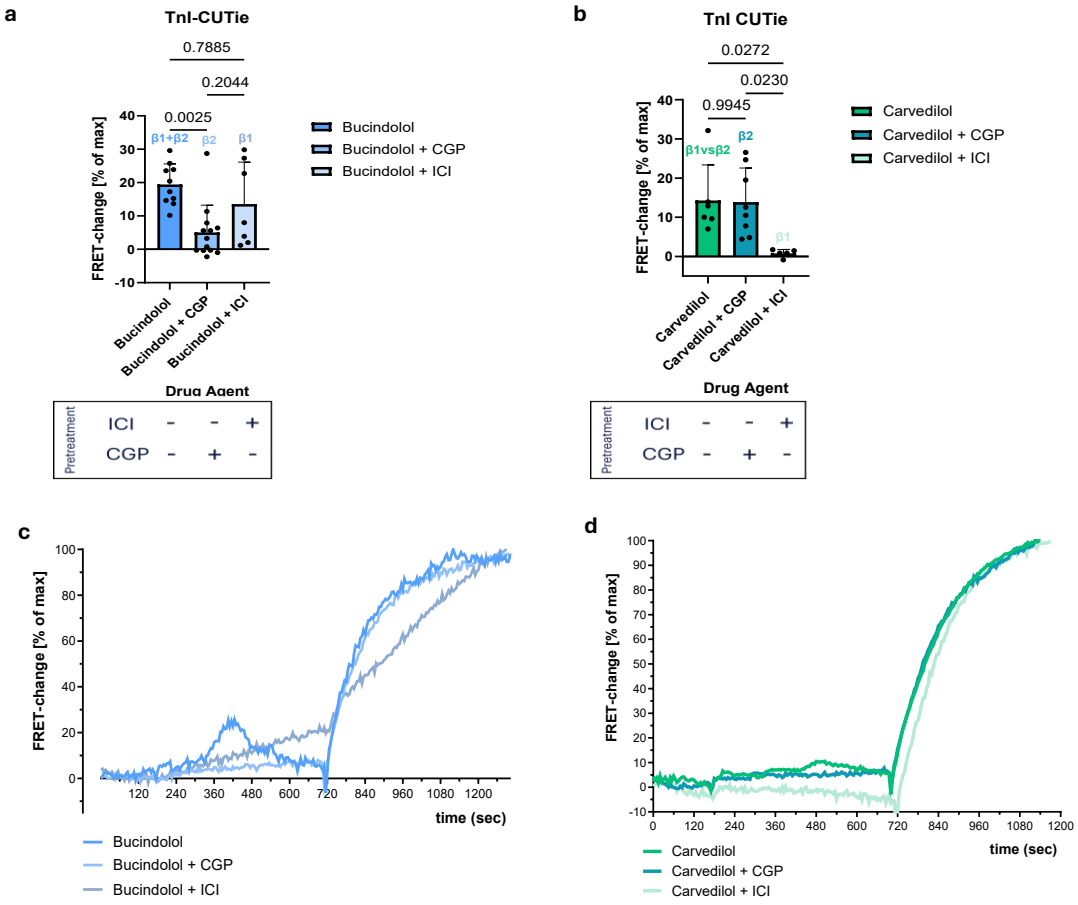


Figure 3.3.4: *Full summary comparisons (a) and (b) and representative kinetics (c) and (d) of FRET change in NRVM expressing TnI CUTie, in response to bath application of 10 μM bucindolol and carvedilol. Cells have been pretreated with either a β1-AR antagonist CGP-20712A (200 nM) or β2-AR antagonist ICI-118551 (200 nM) for at least 16 hours preceding imaging. Full summary comparisons are shown (a) and (b). Data are expressed as maximum FRET (%) change from saturating stimulus (25 μM FSK + 100 μM IBMX), (a-d). Each dot represents one individual cell from minimum three biological replicates. Error bars represent mean ± SD.*

3.4 The AKAP-18δ signalosome identifies a confined and distinct cAMP nanodomain at the SR

Having established that bucindolol, but not carvedilol, induces a cAMP response at the AKAP-18δ nanodomain, an observation that could provide an explanation for their differing outcomes in the clinic [6,124,141]. We next asked whether the different response elicited by these two drugs resulted from a specific regulation at the AKAP-18δ signalling complex or whether similar differences could be detected more generally at the SR membrane.

In experiments addressing this, the cAMP signal detected by the AKAP-18δ CUTie sensor was compared with the signal detected by a FRET reporter targeted generally to the SR membrane. This sensor is based on the EpacH90 reporter (hereafter ER-cyto-H90), and was generated and validated by Dr Miguel Lobo (previous DPhil student) [82,169]. ER-cyto-H90 is localised at the SR and facing the cytosol, functioning as a proxy for cAMP signalling generally at the SR (**Figure 3.4.1a**). Conversely, the AKAP-18δ signalosome is coupled functionally to SERCA/PLB and specific PDEs (**1.2.3**). The same series of experiments as outlined in **3.1** and **3.2** were therefore replicated with this ER-cyto-H90.

3.4.1 β-blocker antagonism at the SR-facing cAMP pool is attenuated

As described in 3.1.1, 10 μM of bucindolol, carvedilol and metoprolol were co-applied with 1 nM ISO in NRVMs expressing ER-cyto-H90 (**Figure 3.4.1a**). ISO alone induced a robust mean FRET change of 25.56 ± 17.47% (n = 6) of the maximum change. Co-application with carvedilol (12.43 ± 2.66%, n = 13) and bucindolol (13.23 ± 5.06%, n = 8) produced a modest, non-significant reduction of cAMP ($p > 0.05$) (**Figure 3.4.1b-d**). This behaviour suggests an attenuated β-blocker response at the SR-facing cytosol relative to that observed in the bulk cytosol (**3.1.1**), where similar concentrations of carvedilol for example, produced significant inhibition of cAMP. Given the small n and response variability, a definitive conclusion may require additional cells. Application of metoprolol + ISO abolished ISO-mediated cAMP production (2.13 ± 1.87%, n = 8, $p < 0.0001$), confirming that this pool remains accessible to the effects of β-blockade (**Figure 3.4.1b-d**).

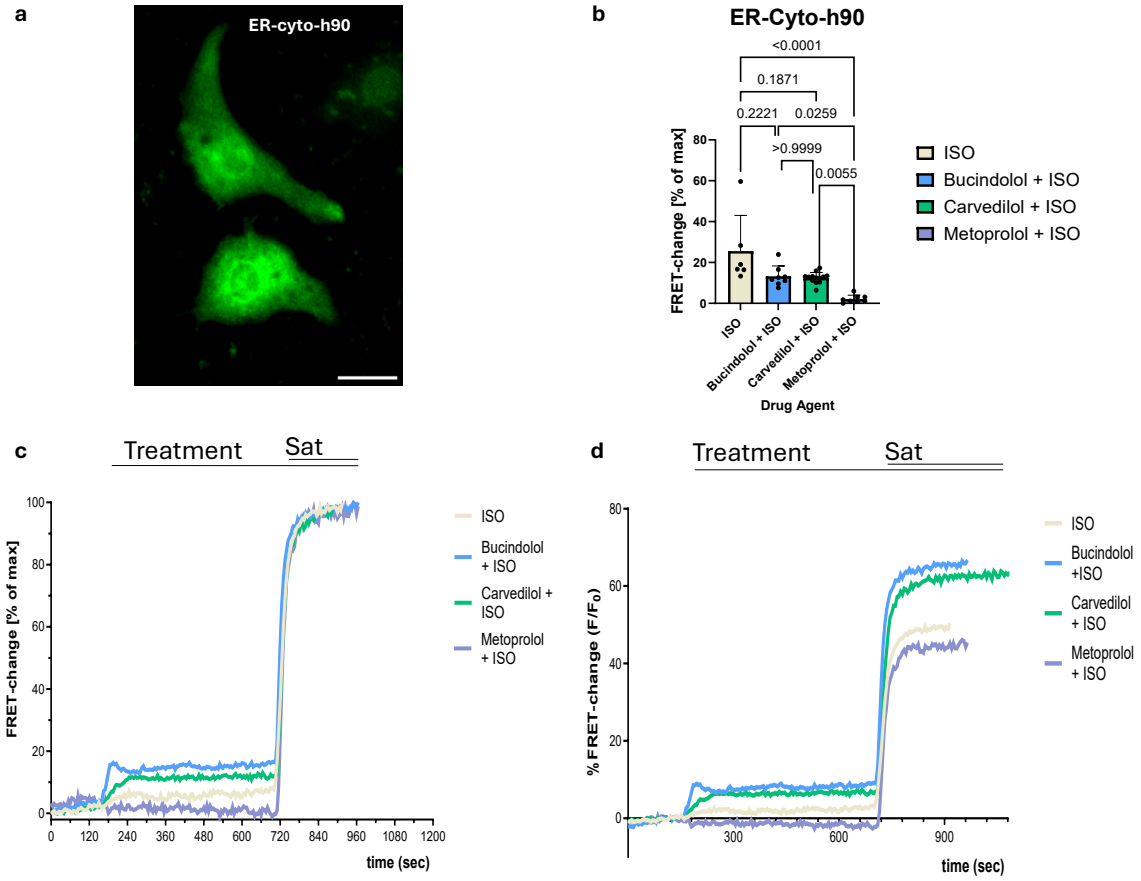


Figure 3.4.1: *Representative image (a) of neonatal rat ventricular myocytes (NRVMs) expressing the ER-cyto-H90. Scale bar: 20 µm. Summary (b) and representative kinetics (c) and (d) of NRVM expressing ER-cyto-H90 in response to application of both 1 nM ISO and 10 µM drug (bucindolol, carvedilol and metoprolol). Data are expressed as either maximum FRET (%) change from saturating stimulus (25 µM FSK + 100 µM IBMX) (c) or % change from initial value (F/F0) (d). Each dot represents one individual cell from minimum three biological replicates. Error bars represent mean ± SD.*

3.4.2 Carvedilol elicits a measurable cAMP response at the SR membrane

To investigate whether any ISA activity elicited by a β-blocker could be detected at the SR membrane, the same experiments conducted in 3.2.2 were repeated in NRVMs expressing ER-cyto-H90 (**Figure 3.4.2**). Together, bucindolol (12.46 ± 3.51%, n = 7) and carvedilol (10.33 ± 4.01%, n = 10) produced a comparably

significant but lower cAMP response than ISO alone (**Figure 3.4.2a**). No effective cAMP response could be detected with metoprolol (1.83 ± 1.83%, n = 14, p < 0.0001) (**Figure 3.4.2**). Direct comparative analysis of carvedilol's response at the AKAP-18δ signalosome against the ER-cyto-H90 response confirms this significant difference (p = 0.0002) (**Figure 3.4.2b**).

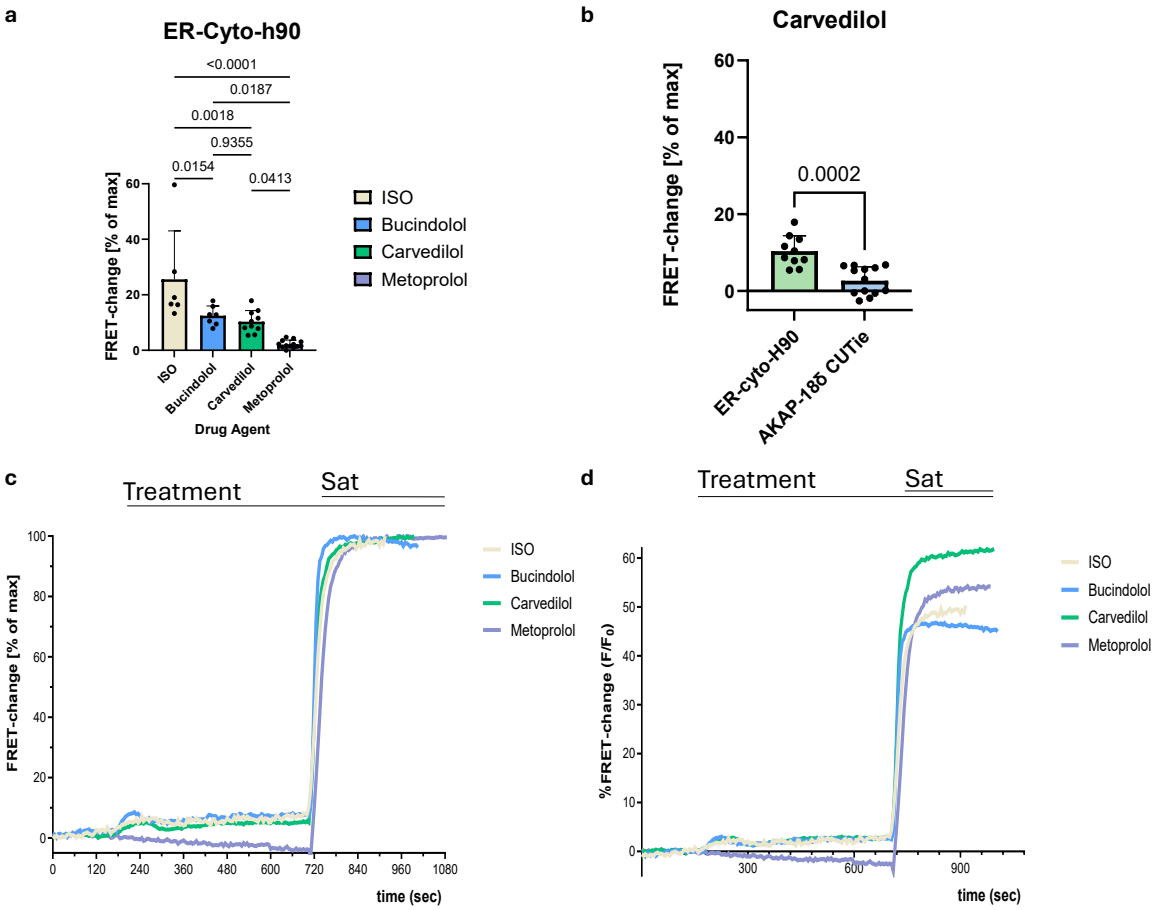


Figure 3.4.2: *Representative kinetics (c) and (d) and summary (a) of NRVM expressing ER-cyto-H90 in response to application of both 1 nM ISO and 10 μM drug (bucindolol, carvedilol and metoprolol). Summary comparison (b) of carvedilol responses in NRVMs expressing ER-cyto-H90 against AKAP-18δ CUTie. Data are expressed as either maximum FRET (%) change from saturating stimulus (25 μM FSK + 100 μM IBMX) (c) or % change from initial value (F/F0) (d). Each dot represents one individual cell from minimum three biological replicates. Error bars represent mean ± SD.*

3.5 Preliminary findings for a Golgi associated cAMP pool in cardiac myocytes

As outlined in **section 1.4.3**, β-AR signalling can originate via intracellular receptors though the functional significance remains poorly understood. Despite evidence identifying β1-ARs present at the Golgi apparatus, the contribution of these receptors to cAMP compartmentalisation remains largely unexplored [39,118,170,171]. This is pertinent especially when considering the physicochemical and membrane permeant properties of both carvedilol and bucindolol (**Table 2.2**).

GalT CUTie is a FRET reporter developed within the laboratory and has previously been characterised and validated in HEK293T cells. However, it has not been previously tested in primary cardiomyocytes. To assess whether GalT CUTie retains its Golgi targeting in primary cardiomyocytes, NRVMs were transfected with GalT CUTie (**2.2.3**) and imaged by confocal microscopy. Characteristic perinuclear distribution of the Golgi apparatus, co-localised with the Golgi marker (Golgi matrix protein 130 (GM130)), was identified on immunofluorescence which indicated correct subcellular targeting (**Figure 3.5.1**).

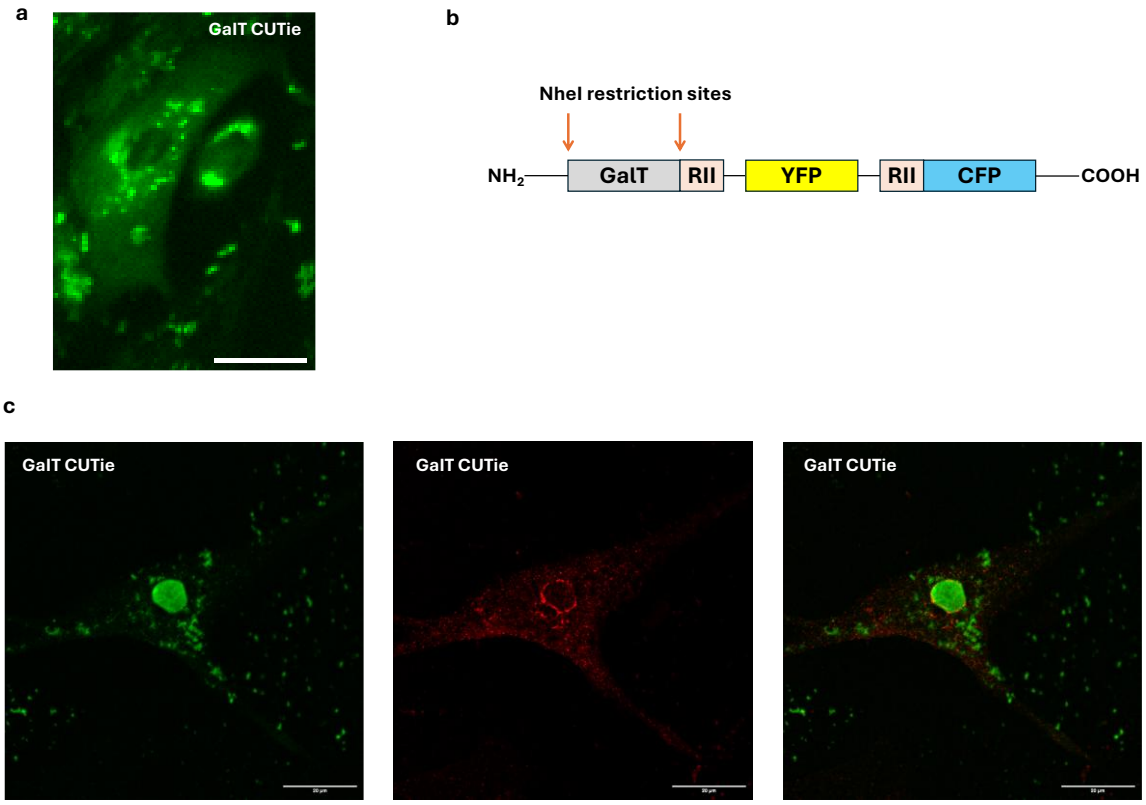


Figure 3.5.1: *Characterisation of GalT CUTie sensor. (a) Representative image of neonatal rat ventricular myocytes (NRVMs) expressing GalT CUTie, a Golgi-targeted FRET sensor. (b) GalT CUTie was generated in-house by another lab member using β-1.4-Galactosyltransferase (GalT), a commonly used trans-Golgi marker. GalT was subcloned from pCMV-GalT-mCherry, a gift from Shinya Tsukiji (Addgene plasmid #214271) and inserted between two NheI restriction sites in AKAP-18δ CUTie. (c) Representative images of immunofluorescence staining showing Golgi localisation of GalT CUTie. GalT CUTie fluorescence is shown in green, GM130/GOLGA2 immunostaining marking is shown in red. Scale bar: 20 μm.*

3.5.1 Bucindolol and carvedilol elicit divergent cAMP responses at the Golgi

The GalT sensor exhibited a weak baseline fluorescence signal and necessitated the use of higher excitation intensities to obtain a detectable FRET change. Consequently, recordings were highly prone to photo-bleaching and associated baseline drift which limited the effective duration for stable acquisition.

Therefore, given the preliminary scope of this section and the above limitations, evaluation at this compartment was prioritised for compounds established in this work to elicit a cAMP response (**3.2 and 3.4**). Metoprolol, whose behaviour is consistent with competitive antagonism, was not evaluated. Thus, bath application of ISO, bucindolol and carvedilol was conducted in NRVMs expressing GalT CUTie.

ISO elicited a robust mean cAMP response (18.43 ± 8.55%, n = 9), whilst bucindolol produced a comparable signal increase (14.86 ± 6.52%, n = 5) (**Figure 3.5.2a-c**). On the other hand, carvedilol did not produce a significant FRET change (2.23 ± 4.14%, n = 8). As a non-selective partial agonist (**3.3.1**) and lipophilic compound (**Table 2.2**), bucindolol would be expected to engage the Golgi-resident β1-AR pool [118]. The absence of a detectable response by carvedilol, characterised as a predominantly β2-AR partial agonist (**3.3.1**), is supported by evidence that β2-ARs have not been reported at the Golgi apparatus.

To summarise, these preliminary observations suggest that there is a Golgi-associated cAMP pool that is generated in a ligand-specific manner. Owing to the small sample size and technical limitations of the sensor, a more complete analysis that investigates the antagonistic activity of ligands at this nanodomain is a priority for future studies and is considered further in **section 4.4**.

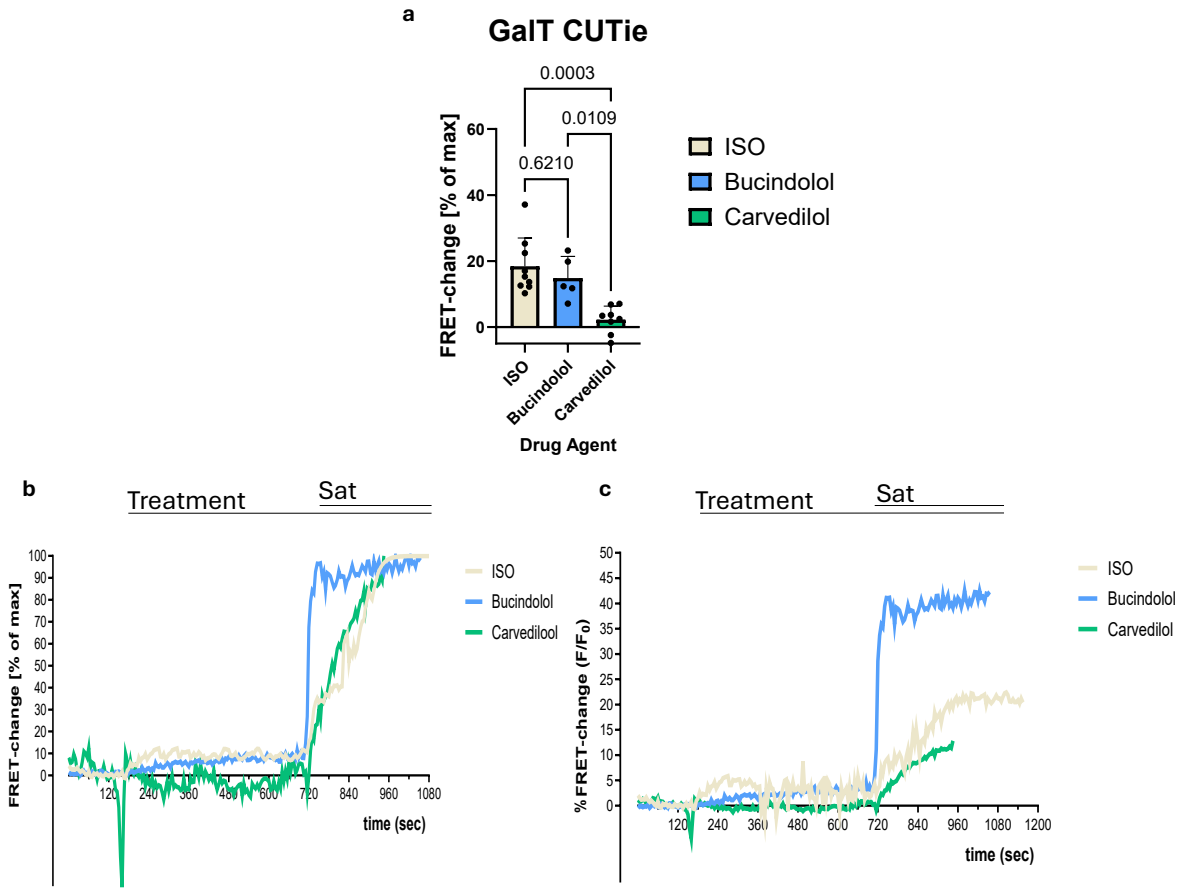


Figure 3.5.2: *Representative kinetics (c) and (d) and summary (a) of NRVM expressing GalT CUTie in response to application of both 1 nM ISO and 10 μM drug (bucindolol and carvedilol). Data are expressed as either maximum FRET (%) change from saturating stimulus (25 μM FSK + 100 μM IBMX) (b) or % change from initial value (F/F0) (c). Each dot represents one individual cell from minimum three biological replicates. Error bars represent mean ± SD.*

Chapter 4

Discussion

4.1 Classification and pharmacology of carvedilol and bucindolol

Collectively, our results demonstrate that the effects of β-blockers are shaped not only by receptor affinity but also by the specific nanodomain engaged. This compartmentalised model may underlie the divergent clinical profiles of individual agents, particularly carvedilol's unique survival benefit in CHF [6].

This framework is particularly pertinent when considering the pharmacology of carvedilol and bucindolol, where there have been controversies in their classifications with no consensus. Both compounds have been variously described as neutral or inverse antagonists and as partial agonists, with carvedilol further characterised as a β-arrestin-biased ligand [9,41,111,112,140].

As outlined in **section 1.5.2**, the Lefkowitz group proposed carvedilol as a β-arrestin-biased ligand at the β2-AR [41]. Interestingly, the group also found that carvedilol displayed inverse agonist activity at G_s-dependent AC [41]. However, this interpretation is complicated by subsequent proximity ligation assays and

fluorescence-based imaging, which support the possibility that carvedilol can also activate G-proteins through receptor engagement [9,172]. Studies assessing ISA using rat and human myocardial preparations reported a net negative inotropic effect for carvedilol, albeit weaker than that of metoprolol [111,140]. Nevertheless, the effect of carvedilol on cAMP production remains unclear. Across the literature, reports have recorded increases, decreases or no effect on downstream levels of cAMP (**Table 4.1**). There is also inconsistency on which β-AR subtype carvedilol engages: studies have reported exclusively β1, exclusively β2, or dual engagement [9,38,145,172,173].

Similarly, bucindolol functions as a well-matched pharmacological counterpart to carvedilol, being another third-generation β-blocker [174]. Although contemporarily classified as possessing ISA, early evidence for bucindolol's partial agonist activity was itself inconsistent (**Table 4.1**). Early studies in cardiac tissue explants reported a net negative inotropic effect for bucindolol [111]. A similar profile emerged in studies of β1-AR polymorphism variants: both bucindolol and carvedilol exerted inverse agonist activity in β1-Arg389 hearts [175,176]. This raises the possibility that polymorphisms in the β-AR itself contribute to the heterogeneous clinical responses reported across the β-blocker class. In contrast, the majority of studies investigating cAMP broadly show that bucindolol raises

cAMP via β1-AR [40,112,177]. However, a very early study in reserpinised adult rats (in which reserpine depleted endogenous catecholamine stores) demonstrated that bucindolol induced β2-associated vasodilatory actions and increased heart rate [178]. The observations are in line with our results in NRVMs, showing that bucindolol exhibits non-selective ISA, acting predominantly at the β1-AR (**3.3**). Nevertheless, older studies on ventricular tissue report bucindolol to have little to no effect on cAMP or AC (**Table 4.1**) [140,179].

In studies focussing on biased signalling, carvedilol has always been shown to increase ERK1/2 phosphorylation, though whether this reflects β-arrestin bias is unresolved [9,172,177,180]. More recent reports have suggested that ERK1/2 phosphorylation may instead occur through G-protein-dependent and β-arrestin-independent mechanisms [9,172]. On the other hand, the signalling bias of bucindolol has been less extensively characterised. Available evidence suggests it is a biased ligand, stabilising a distinct β1-AR conformation and promoting MAPK activation in a G-protein-independent manner [177,181].

Table 4.1: *Summary of previous experiments assessing ISA in carvedilol and bucindolol. N/A = not available.*

Reference	**Model**	**Drug**	**cAMP effect**	**Contractility**/HR
Marwood and Stokes (1986) [178]	Reserpinised adult rats	Bucindolol	Increased (β2-stimulation)	Increased HR

Hershberger *et al.* (1990) [179]	Human ventricular tissue	Bucindolol	No effect on AC	None
Bristow *et al.* (1992) [137]	Failing human ventricular tissue	Carvedilol	No effect on AC	N/A
Willette *et al.* (1998) [110]	Pitched rat (in vivo)	Bucindolol	N/A	Increased HR
		Carvedilol	No effect	No effect
Maack *et al.* (2000) [111]	Human ventricular papillary muscle strips	Bucindolol	N/A	Negative inotropic effect in 5/8 explants, positive in 3/8
		Carvedilol	N/A	Negative inotropic effect in 6/7 explants, positive in 1/7
Brixius *et al.* (2001) [140]	Human ventricular tissue	Bucindolol	No effect	N/A
		Carvedilol	No effect	Negative
Andreka *et al.* (2002) [112]	Myocardial strips from rat and humans	Bucindolol	Increased	N/A
		Carvedilol	No effect	N/A
Yao *et al.* (2002) [182]	Adult guinea pig ventricular myocytes	Carvedilol	Increased	N/A
Baker *et al.* (2003a) [173]	CHO overexpressing β1-AR	Carvedilol	Increased	N/A
Baker *et al.* (2003b) [145]	CHO overexpressing β2-AR	Carvedilol	Increased	N/A
Maack *et al.* (2003) [183]	Human ventricular muscle strip	Bucindolol	N/A	Significantly increased inotropy
		Bucindolol	Increased	N/A

Galandrin and Bouvier (2006) [40]	HEK-293 stably expressing β1	Carvedilol	Increased	N/A
	HEK-293 stably expressing β2	Bucindolol	No effect	N/A
		Carvedilol	No effect	N/A
Liggett *et al.* (2006) [175]	Healthy and failing human ventricular tissue with polymorphisms	Bucindolol	N/A	Inverse agonist in Arg-389 hearts
		Carvedilol	N/A	No effect
Wisler *et al.* (2007) [41]	HEK-293 overexpressing β2-AR	Carvedilol	Decrease	N/A
Rochais *et al.* (2007) [176]	Transgenic primary rat cardiomyocyte	Carvedilol	Reduced	Inverse agonist effects in Arg-389 and Gly-389 hearts
Galandrin *et al.* (2008) [177]	HEK-293 stably expressing β1	Bucindolol	Increase	N/A
Shen *et al.* (2019) [172]	HEK-293 stably expressing β2	Carvedilol	Increased	N/A
Benkel *et al.* (2022) [9]	HEK-293 overexpressing β2-AR	Carvedilol	Increased	N/A
	Adult mouse ventricular myocytes		Increased	Heart rate increased

Ultimately, bucindolol remains the most classically characterised partial agonist from the β-blocker family. However, limited evidence characterising bucindolol as a biased agonist suggests it should not be treated purely as a partial agonist. In

this work, shared behaviour of both carvedilol and bucindolol may therefore reflect common consequences of residual agonist activity, whereas ligand-specific differences may reflect distinct receptor conformations and downstream engagement.

Nevertheless, the evidence base is not without criticism. One limitation in the literature is heterogeneous study design and experimental models. Heterologous cell lines (HEK-293, CHO etc.) and tissue-based studies do not accurately represent the endogenous cardiomyocyte environment, including receptor stoichiometry, scaffold organisation and cellular architecture. Importantly, however, the inconsistency in the literature is not solely due to the use of non-cardiomyocyte models since conflicting results have been reported in the same cell line [171,184]. This suggests the discrepancies instead stem from a combination of other factors, one being assay sensitivity. For example, several studies measured cAMP and ISA-related effects in whole-cell lysates using radioligand assays, over extended time courses in the presence of PDE inhibitor IBMX [111,112,140]. This does not reflect the physiological environment as accurately as our experiments in intact NRVMs. In the limited studies that do measure cAMP in primary myocytes also using FRET, carvedilol has been

reported to elevate cAMP [9,182]. Furthermore, experimental systems such as overexpression of β-ARs and arrestins can affect signalling behaviour.

In neonatal rat cardiomyocytes, both bucindolol and carvedilol elevated bulk cytosolic cAMP above baseline, consistent with partial-agonist activity at the β-AR (**Figure 3.1.1**). For bucindolol this behaviour is expected, given its established classification as an ISA-containing β-blocker. For carvedilol, the finding is the more consequential of the two, reproducing a low-level G_s signal consistent with previous reports [9]. This supports interpreting carvedilol as a low-efficacy partial agonist rather than a purely β-arrestin-biased ligand. It may also reflect the sensitivity of live-cell FRET to small cAMP changes that other approaches miss (**Table 4.1**).

4.2 Compartmentalisation of cAMP by β-adrenergic antagonists

Evidence for compartmentalised cAMP signalling has been derived almost exclusively from full agonists at the β-AR. Early functional studies showed that ISO stimulated lower levels of cAMP than forskolin (FSK), yet produced greater levels of protein phosphorylation and stronger effects on contractility [185]. Similarly, ISO and FSK were found to differ in their effects on Ca^{2+} transients and myocyte shortening [186]. More recent studies using CUTie sensors (**1.3.4**)

targeted at ECC-related nanodomains confirmed that agonist-induced cAMP differs in both amplitude and kinetics, with the TnI site exhibiting a smaller and more delayed signal than AKAP-18δ or AKAP-79 [82].

This work extended the compartmentalisation principle to β-AR antagonists, revealing that both antagonistic and partial agonist activity vary across subcellular compartments (**Figure 3.1.1-3.1.4**). The pattern of antagonism was not uniform. At the AKAP-18δ signalosome, carvedilol fully suppressed ISO-stimulated cAMP levels comparably to metoprolol (**Figure 3.1.2**). This near-complete attenuation may reflect differences in hydrolytic activity of local PDEs to maintain a low basal cAMP at the SERCA/PLB microdomain [53,61]. Contrastingly, the weaker effect of bucindolol at AKAP-18δ and carvedilol at the myofilament suggests that each drug's ISA may partially offset its antagonism in a compartment-specific manner. All three ligands also produced statistically equivalent levels of inhibition at the AKAP-79 signalosome (**Figure 3.1.3**). Collectively, these findings show that the antagonistic effects also reflect downstream changes in compartmentalisation.

When applied in the absence of ISO, carvedilol and bucindolol displayed opposing patterns of ISA (**Figure 3.2.3**). Bucindolol elevated cAMP at the AKAP-18δ signalosome and the myofilament yet failed to produce a detectable response at

the plasmalemmal AKAP-79 domain. As bucindolol's ISA is predominantly β1-mediated (**3.3**), it may be unable to generate sufficient cAMP at a nanodomain preferentially associated with the β2-AR [109]. Alternatively, bucindolol may act as a biased ligand in this domain, promoting a conformational shift that favours desensitisation and internalisation at AKAP-79 [181]. Conversely, carvedilol produced a cAMP response at AKAP-79 and the myofilament, but no detectable signal was seen at AKAP-18δ. The response at the AKAP-79 signalosome is consistent with reports that carvedilol exerts ISA at the β2-AR, while the response we observed at the myofilament may indicate a minor contribution from β1-ARs (**Figure 3.3.1**). However, this does not explain why there is no response at SERCA/PLB [9,40,172]. One possibility is that diffusion limitation, as described by the sink model (**1.2.4**), imposes a higher threshold for cAMP detection at AKAP-18δ that carvedilol's weak partial agonist signal cannot overcome. However, this explanation is difficult to reconcile with the observation that bucindolol generates a comparable bulk cytosolic cAMP response (**Figure 3.2.2**) at the same nanodomain as carvedilol. Further dose-response analyses would help resolve whether the absence reflects a sensitivity threshold.

We then sought to elucidate if the AKAP-18δ signalosome is subject to distinct local regulation. The cAMP responses were compared with ER-cyto-H90, a

reporter localised at the SR but facing the cytosol and uncoupled from SERCA/PLB (**3.4**). Carvedilol generated a robust cAMP response comparable to bucindolol here, and akin to the response elicited in the bulk cytosol, suggesting that the AKAP-18δ signalosome is more tightly regulated and shielded from the cAMP elicited by carvedilol. This insulation is physiologically consistent: PKA-mediated phosphorylation of PLB directly governs SR calcium reuptake and aberrant phosphorylation of PLB can drive SR overload. This can lead to impaired diastole, spontaneous calcium release and arrhythmias due to delayed afterdepolarisations (DADs) [187]. A local PDE pool at AKAP-18δ would therefore protect diastolic calcium handling from weak or non-specific cAMP elevations. The exclusion of carvedilol's ISA from this domain may in part contribute to its favourable clinical profile relative to bucindolol.

Unexpectedly, carvedilol applied alone generated a clear cAMP signal at the AKAP-79 nanodomain, yet no signal was detected when it was co-applied with ISO (**Figure 3.1.3**). While a mechanistic explanation cannot be offered from the data currently available, several possibilities can be considered. One possibility is that the co-presence of both ligands at the β2-AR also promotes a receptor conformation that favours β-arrestin recruitment or internalisation at this nanodomain. Alternatively, ISO may drive the β2-AR toward a fully active G_s-

coupled state, and competitive displacement by carvedilol may replace this with a less productive conformation, yielding net lower cAMP than carvedilol alone. This is consistent with a concept known as protean agonism, whereby a ligand can act as a partial agonist in a quiescent system but as an inverse agonist in a constitutively active one [188]. Nonetheless, no existing records show that carvedilol is a protean agonist, so further studies would be needed to substantiate this.

One framework for reconciling these compartment-specific patterns is "cell-based" functional selectivity, as described by Kenakin (2007) [188]. In cell-based functional selectivity, the "strength of signal" from a partial agonist is filtered by the local coupling environment, such that ISA may only be detected at nanodomains where receptor densities and PDEs permit it. In contrast, biased agonism (a type of receptor-based functional selectivity) occurs when a ligand stabilises a conformation that produces a qualitatively different output (**1.1.4**). Both mechanisms are likely to operate in parallel across cardiac nanodomains.

The compartment-specific patterns described above extend beyond cAMP amplitude to temporal kinetics. Preliminary analysis of cAMP accumulation kinetics revealed that when ISA-associated antagonists were co-applied with ISO, the initial rate of cAMP generation was broadly slower than when the antagonist

was applied alone (**Figure S4**). This kinetic delay is consistent with a state of hemi-equilibrium, in which the agonist response develops before the pre-bound antagonist has fully dissociated from the receptor [189,190]. Additionally, the difference in kinetics may be due to rate of hydrolysis by PDEs, as small elevations of cAMP by ISA may be sufficient to initiate PKA-mediated phosphorylation of local PDE isoforms before ISO-driven cAMP can accumulate [191]. Distinguishing between these mechanisms would require direct measurement of antagonist association and dissociation rate constants, alongside sequential application protocols that separate receptor-level from downstream contributions to the observed kinetic delay. A novel label-free kinetics approach, in which antagonist dissociation rate constants were derived from the degree of antagonist E_{max} depression under hemi-equilibrium conditions, could be adapted to our CUTie experiments [190]. Such an analysis would determine whether the compartment-specific kinetic differences reflect differential antagonist residence times or downstream variation in signalosome-level regulation.

4.3 β1 and β2-AR contributions to compartment-specific cAMP

Carvedilol is a non-selective β-blocker; however, reports suggest that it exhibits higher affinity for β2-ARs than β1-ARs (**Table 2.1**). Studies investigating ISA,

though inconsistent, attribute carvedilol's cAMP generation to act through the β2-AR (**Table 4.1**). Likewise, bucindolol is a non-selective β-blocker, but with comparable affinities for both receptors (**Table 2.1**). Notably, both bucindolol and carvedilol have greater affinities for both β-ARs than metoprolol, which is classified as a β1-selective agent [151]. At the 10 μM concentration used, both receptors are expected to be near-saturated, so compartment-specific ISA patterns likely reflect β-AR subtype differences rather than occupancy. Understanding which receptor subtype drives each compartment's signal is clinically relevant, as β1- and β2-ARs, despite both coupling to G_s and activating AC, produce distinct physiological outcomes: β1-AR stimulation is the primary driver of inotropy and lusitropy, whereas β2-AR activation contributes predominantly to chronotropy [192].

Carvedilol's selectivity to the β2-AR is one possible explanation for the distinct compartmentalised cAMP signatures seen. At the plasmalemma, AKAP-79 organises a subsarcolemmal signalosome that scaffolds PKA and the Ca^{2+} dependent phosphatase calcineurin at $Ca_v1.2$, where PKA anchoring is required for β-adrenergic regulation of L-type calcium current [69,72,106]. Moreover, substantial evidence supports its close association with the β2-AR [109]. Consistent with this, carvedilol stimulates a PKA-dependent increase in LTCC

conductance in hippocampal neurons [172]. However, this cAMP pool would not explain how carvedilol has negative inotropic effects (**Table 4.1**). In rodent myocytes, cAMP degradation within this nanodomain is mediated predominantly by PDE4B and PDE4D, consistent with the tight regulation observed at AKAP-79 (**Figure 3.1.3**) [193]. However, our results upon selective β2-AR blockade show that a weak cAMP signal persists with carvedilol at the cytosol, suggesting partial involvement from the β1-AR (**Figure 3.3.1**). Indeed, weak β1-AR signalling may partly account for carvedilol's cAMP response at the myofilament (**Figure 3.2.3**). Furthermore, it remains unclear why β1-AR stimulation fails to generate a detectable cAMP signal at AKAP-79, given that β1-ARs are also present in T-tubular membrane fractions and co-precipitate with AKAP-79 [108]. Investigations using a plasma membrane-targeted sensor could clarify whether there is functional heterogeneity in cAMP production across the sarcolemma. Overall, carvedilol exerts partial agonist activity preferentially at the β2-AR. This may partly explain why its ISA was characterised inconsistently in earlier tissue studies, where β1-ARs predominate [112,137,183].

Conversely, bucindolol's partial agonist activity acts predominantly through the β1-AR (**Figure 3.3.1**). The β1-AR is known to stimulate a broadly distributed cAMP signal that reaches cytoplasmic targets including the sarcoplasmic

reticulum and myofilament, whereas the β2-AR produces comparatively little phosphorylation at these sites [103,194,195]. Our data confirm that β1-AR-dependent cAMP is excluded from the AKAP-79 nanodomain (**Figure 3.3.3**). Nevertheless, bucindolol also binds the β2-AR, raising the question of why no ISA is detected at the β2-associated AKAP-79 nanodomain. One possibility is that only a functional subset of β2-ARs associates with the AKAP-79 signalosome, and bucindolol may not engage this population. Alternatively, bucindolol may occupy the β2-AR without stabilising a conformation that productively couples to G_s. Structural studies of the β-ARs support this possibility: crystallographic data show that carvedilol and bucindolol share identical core contacts in the orthosteric pocket and both possess bulky aromatic extensions that engage extracellular loop 2 (EL2) through distinct bonding [181]. Notably, EL2 engagement is a shared feature of certain characterised biased agonists at the β1-AR and these distinct contacts may transmit different conformational changes to potentially determine which nanodomains a ligand can access [181]. Nonetheless, structural analyses largely find that agonists bind with an overall similar complex architecture with only local conformational differences [196]. Moreover, crystallography only captures a single low-energy state and does not capture the dynamic conformational ensembles that may produce nanodomain-selective

signalling in living cells. This underscores the need for complementary approaches such as NMR spectroscopy or molecular dynamics simulations [197].

High-resolution FRET imaging in adult rat ventricular myocytes has demonstrated that β1-AR stimulation produces a broadly distributed cAMP signal across both T-tubular and crest regions, whereas β2-AR stimulation generates a signal largely confined to the T-tubules [105]. Our results challenge this view on both fronts. We show that β2-AR-driven cAMP is confined to discrete nanodomains, specifically the domain associated with AKAP-79. Furthermore, β1-AR-dependent cAMP is not simply a diffuse global signal but engages distinct subcellular compartments differentially, driving cAMP generation at internal targets such as the SR and myofilament while failing to produce a detectable response at AKAP-79. It should be noted that these comparisons must be interpreted with caution as NRVMs lack a well-developed T-tubule network and the spatial distribution of β-AR subtypes may differ relative to an adult system [198]. It remains to be determined whether the nanodomain selective patterns we describe are preserved in mature T-tubular architecture.

4.4 The emerging role of intracellular receptors

A further dimension of spatial signalling complexity is the emerging evidence for functional β-AR pools at intracellular membranes (**1.4.3**). These have been found at the Golgi, SR and even early endosomes [118–120]. Important pharmacological considerations arise from this, as carvedilol, bucindolol and metoprolol are all membrane-permeable and therefore may activate intracellular receptor pools (**Table 2.2**).

As carvedilol, bucindolol and metoprolol are all membrane-permeable, any partial agonist activity could engage intracellular as well as plasmalemmal β-ARs. In cardiomyocytes, a pre-existing pool of β1-ARs (but not β2-ARs) has been described that does not undergo internalisation, resides at the Golgi apparatus and signals canonically via G_s [117]. Notably, the hydrophilic antagonist sotalol could not access this pool, whereas lipophilic drugs diffuse freely across the membrane to reach it. Using a Golgi-targeted light-activated adenylyl cyclase, another recent study demonstrated that physiological levels of cAMP generated at the trans-Golgi selectively control phosphorylation of PLB without affecting TnI or RyR2 [170]. In contrast, selective activation of plasma β1-ARs produced the opposite phosphorylation pattern. It remains unclear if Golgi-resident β1-ARs

have functions distinct from those of plasma β1-ARs, or if there is influence from β2-ARs, which have been identified in endosomes [119].

A limitation of optogenetic approaches is that expression of a bacterial photoactivable adenylyl cyclase (bPAC) generates cAMP directly and bypasses receptor activation [170]. As a result, such systems isolate a single cAMP source rather than capturing the parallel multi-compartmental signalling that occurs when a ligand engages β-ARs at the plasma membrane. To address this, we generated a CUTie sensor (GalT CUTie) targeted to the trans-Golgi (**Figure 3.5.1**), which reports endogenous cAMP generated at the precise location while preserving physiological receptor signalling through the endogenous receptor-AC axis. Given the physical adjacency of the Golgi and SR membranes, we next asked whether Golgi-derived cAMP contributes to the pools detected at the AKAP-18δ signalosome and SR-facing cytosol [199]. This may help explain the divergent findings seen when utilising AKAP-18δ CUTie against ER-cyto-H90 sensors (**Figure 3.2.1, 3.4.1**). Our preliminary analysis showed that bucindolol stimulates a detectable cAMP response at the Golgi, whereas carvedilol did not show clear partial agonist activity, despite a similar physicochemical profile (**Figure 3.5.2**). The absence of signal at the AKAP-18δ nanodomain may therefore indicate an inability of carvedilol to activate β1-ARs at the Golgi sufficiently to

drive phosphorylation of PLB. Alternatively, as carvedilol appears to exert ISA primarily through β2-ARs, the lack of Golgi response may also reflect limited evidence of β2-AR localisation in this compartment.

For a ligand to access intracellular receptors, it must either possess sufficient lipophilicity to cross the membrane by passive diffusion or be actively transported. Endogenous catecholamines such as epinephrine and norepinephrine are membrane-impermeant and require the organic cation transporter 3 (OCT3) to reach intracellular β1-ARs [39,120]. Genetic ablation of OCT3 was found to significantly attenuate catecholamine-induced PLB phosphorylation, confirming that this transporter plays a role in mediating cardiac lusitropy [120]. In line with this, high throughput in silico analyses have identified carvedilol as capable of inhibiting OCT3 [200]. Given that carvedilol also partitions in the cell membrane, it is possible that its inhibition of OCT3 directly limits its transport to β1-ARs [201]. It is unknown if bucindolol shares this property; however, its structural similarity and lipophilic properties to carvedilol suggest this is plausible [180]. The OCT3 pathway is therefore likely to be more relevant to endogenous catecholamine signalling than to carvedilol.

Our data on the Golgi, though preliminary, illustrates that the spatial pharmacology of these drugs extends beyond the plasma membrane. If the Golgi

β1-AR pool selectively controls PLB phosphorylation and diastolic relaxation, clinical consequences of ISA may also depend on which intracellular compartment it reaches.

4.5 Clinical and therapeutic implications

Traditionally, ISA has been associated with worse outcomes and prognosis (**1.5.1**). In the BEST trial, bucindolol failed to show a significant survival benefit, and earlier agents like xamoterol worsened clinical outcomes [131,141]. Yet this interpretation treats ISA as a binary property and cannot explain why carvedilol, which we confirm possesses ISA, is among the most effective β-blockers in heart failure [6,125]. The nanodomain-specific ISA patterns described in this work offer a new perspective that functional effects depend on the subcellular compartments a signal reaches.

The inability of carvedilol to generate a cAMP signal at the AKAP-18δ signalosome may partly explain its superior clinical profile. In cardiomyocytes, SERCA2a actively transports Ca^{2+} into the SR during diastole, driving a concentration gradient for Ca^{2+} efflux needed for systole [203]. Classically, PKA-mediated phosphorylation of PLB relieves its inhibition on SERCA to restore depressed Ca^{2+} reuptake in failing myocytes [203]. While PLB phosphorylation is traditionally considered beneficial for systolic function, sustained activation in

heart failure may be counterproductive. Sustained SERCA activity, as the most ATP-consuming pump in the cardiomyocyte, compounds the energy deficit of the failing heart [204]. In line with this, a phase 2b trial on AAV1/SERCA2a gene therapy found no evidence of improved outcomes in HFrEF patients [205]. This may be compounded by potential hyperphosphorylation of RyR2 in HF, further promoting diastolic calcium leak from the SR and exacerbating the already reduced SR Ca^{2+} content [206]. Thus, the tight regulation of AKAP-18δ and the absence of carvedilol's ISA at this signalosome may help preserve the energetic balance of the failing myocardium, while still enhancing the signal at AKAP-79 and TnI domains. Interestingly, studies have shown carvedilol to shift substrate utilisation from fatty acid to glucose oxidation increasing energetic efficiency [207,208]. Conversely, our findings may also explain bucindolol's lack of favourable outcomes in CHF [5]. Nonetheless, these interpretations must be weighed alongside carvedilol's many ancillary properties, including α-adrenoceptor blockade [135,136].

Both bucindolol and carvedilol also generate cAMP at the myofilament, where PKA-mediated phosphorylation of TnI reduces myofilament calcium sensitivity and accelerates Ca^{2+} dissociation from troponin C [209]. ISA at this compartment could therefore enhance lusitropy through a mechanism that is independent of,

and energetically less costly than, increased SERCA activity at the SR. Importantly, this myofilament ISA is not accompanied by cAMP elevation at AKAP-18δ, meaning that carvedilol can promote relaxation without driving SR calcium overload or store-overload-induced calcium release (SOICR), both of which cause DADs. Consistent with this, carvedilol has been shown to suppress SOICR and stress-induced arrhythmogenesis [172]. These observations align with the COPERNICUS trial, in which carvedilol significantly reduced arrhythmic admissions and sudden death [124].

At the population level, genetic polymorphisms in the β1-AR may modulate these nanodomain-specific effects. The Arg389 variant, which is the most common β1-AR allele, displays a two-fold greater inverse agonist response to carvedilol compared to the wild-type variant Gly389 [176]. A similar genotype-dependent difference has been reported for bucindolol [175]. If the Arg389 variant alters coupling efficiency at specific nanodomains, the spatial ISA profile of a given drug could itself be genotype-dependent, adding a further factor to the pharmacological complexity described here. Complementary studies using CRISPR-engineered receptor variants (e.g. Arg389Gly β1-AR) could test whether nanodomain-specific ISA patterns are genotype-dependent.

Lastly, our findings indicate the importance of semantic precision. The term "ISA" currently used in pharmacology describes β-blockers with partial agonist activity. This definition does not consider clinically relevant heterogeneity, as two drugs possessing ISA may generate different cAMP pools across cardiac nanodomains. A more informative classification may involve characterising drugs by the subcellular nanodomains activated. Such a framework may aid in predicting clinical outcomes and inform the design of next-generation β-blockers to exploit nanodomain selectivity.

4.6 Limitations and future directions

The findings presented in this thesis (**Chapter 3**) provide evidence that β-AR blockers produce ligand-specific spatial patterns of cAMP signalling. However, several methodological and interpretive limitations must be acknowledged, and further targeted experiments would strengthen the conclusions drawn.

A primary limitation is the use of NRVMs, which, as aforementioned, lack the mature T-tubule network present in adult cardiomyocytes. This may result in spatially different AKAP-scaffolded signalosomes and altered cAMP signalling [198]. Other differences include β1/β2-AR expression levels and calcium homeostasis [210,211]. Nonetheless, NRVMs have been widely used in previous studies of cAMP compartmentalisation and facilitate key comparisons [9,82].

Replication of key findings in adult rat ventricular cardiomyocytes, human iPSC-derived cardiomyocytes or human adult cardiac myocytes would be an important next step to confirm translational relevance.

A further limitation concerns the coverage of FRET-based sensors used. CUTie sensors report cAMP only at the nanodomains to which they are targeted, whereas Epac-S^{H187} was used in the cytosol due to its greater sensitivity [82,86]. Consequently, absolute FRET magnitudes are not directly comparable between the cytosolic and nanodomain-targeted sensors, though relative differences between drug conditions within each sensor remain interpretable. Differences in biosensor sensitivity and dynamic range may influence detection of smaller changes in cAMP (**Table 2.4**). Although our ratiometric approach minimises this influence, higher or lower expression levels across replicates may alter signal amplitude and kinetics. This notwithstanding, it should be noted that previous work has demonstrated that targeted CUTie expression did not significantly alter FRET change and kinetics [82].

Sensor variability in baseline FRET noise posed a further practical constraint, particularly for the TnI and GalT CUTie sensors, where a substantial proportion of cells had to be excluded due to excessive noise. This reduced the number of viable recordings and may have introduced selection bias towards cells with more

favourable expression levels or morphology. Moreover, other nanodomains showing evidence of β-AR modulation, such as the endosomal and mitochondrial compartments, remain uncharacterised in this present study [119,212]. Overexpression of CUTie sensors may also alter the stoichiometry of local PDE/PKA complexes, potentially affecting the measured signal.

A related consideration can be made regarding the statistical treatment of FRET datasets presented. Data points each represent a single cell and observations were unevenly distributed between sensors and conditions. Thus, conditions sampled at higher cell numbers and replicates may return highly significant p-values despite a relatively modest effect size. On the other hand, datasets with fewer acquired cells or isolations require a larger effect to reach the same threshold. Statistical significance is not weighted equally in the datasets presented here and caution should be given when comparing p-values between sensors. Moreover, FRET amplitudes recorded using a single coverslip were heterogenous and the usage of different coverslips introduces variance in sensor expression and cell maturity. This means that significant differences in a group may only arise from a responsive subpopulation of cells. Consequently, an apparently nanodomain-specific response could reflect signal-to-noise between sensors and statistically significant cAMP elevation may still fall below a biologically significant threshold.

Overall, it should be recognised that confirmation of results through adequately powered biological replication and further measurement of downstream substrate phosphorylation may be required.

While we demonstrate the presence of distinct SR and trans-Golgi cAMP pools, experiments isolating the individual contributions of the β1- and β2-AR subtypes have not been undertaken. Further work should be done to determine if there is β-AR selectivity, or if these intracellular pools are accessible to blockade, particularly at the Golgi where only β1-ARs have been identified [118]. Our clinical interpretations drawn from cAMP data alone (**4.5**) are inferential, necessitating biochemistry studies measuring downstream phosphorylation of key substrates (PLB, TnI, RyR2) in response to each drug.

The AKAP-79 nanodomain remains incompletely characterised. Only carvedilol and not bucindolol generated detectable cAMP at this site, and the possibility that β2-AR association with the scaffold may influence the readout of our CUTie sensor cannot be excluded. Therefore, it is imperative that other plasma membrane/sub-sarcolemmal pools of cAMP are tested. Parallel studies in the group are investigating additional plasma membrane nanodomains to determine whether the cAMP patterns observed at AKAP-79 generalise across the sarcolemma or reflect a feature unique to this signalosome.

Several pharmacological limitations should also be considered. Selective antagonists (CGP-20712A and ICI-118551) were used to isolate β-AR subtype contributions, but at the concentrations used, residual cross-reactivity with the non-target subtype cannot be excluded. Additionally, all experiments were conducted acutely, whereas the clinical action of β-blockers in heart failure develops over weeks and involves chronic adaptations in receptor density and scaffold composition that our experimental design cannot capture. Furthermore, this study examined only bucindolol as an agent with established ISA. Extending the analysis to different ISA agents such as xamoterol and pindolol could test whether the observed nanodomain-specific cAMP patterns are a general property of partial agonism.

Heterologous expression of individual β-AR subtypes in CHO cells, which lack endogenous adrenoceptors, would allow ISA to be studied at defined receptor populations without the cross-reactivity limitations of subtype-selective antagonists as described [213]. This system would also test whether β2-AR association with the AKAP-79 signalosome influences CUTie sensor activity independently of cAMP. In preliminary experiments, we confirmed by FRET that CHO cells lack endogenous β-AR expression and successfully introduced exogenous β2-AR expression in these cells. However, owing to protocol

optimisation limitations within the 10-month timeframe of this project, these experiments did not extend to carvedilol or bucindolol (**Figure S5**).

Finally, the present work examines only G_s-mediated cAMP generation, yet physiological β-AR signalling is tonically opposed by G_i-coupled muscarinic M2 receptors. Incorporating parasympathomimetic stimulation (e.g. carbachol) in future experiments would test whether G_i-mediated cAMP degradation is itself spatially organised across nanodomains.

Chapter 5

Conclusions

This thesis extended the established concept of cAMP compartmentalisation by examining how β-adrenoceptor antagonists shape the subcellular organisation of cAMP signalling. Using FRET-based nanodomain sensors in cardiac myocytes, we demonstrated that cAMP generation by β-blockers associated with ISA activity is both ligand- and receptor subtype-specific. Compartmentalisation of cAMP is not a fixed property of the cell but exists in a dynamic state that varies with the ligand involved, extending the principles of biased agonism and functional selectivity. Consistent with previous studies, we established that both

carvedilol and bucindolol are partial agonists and globally elevate cAMP in cardiomyocytes. To summarise the novel findings reported in this thesis:

- Bucindolol, carvedilol and metoprolol successfully suppressed ISO-stimulated cAMP, although the degree of suppression varies by compartment. These differences indicate that the antagonistic efficacy of a β-blocker itself is affected by compartmentalisation, where local PDE composition, scaffold organisation and receptor proximity may all contribute to differential effects.
- Carvedilol and bucindolol exhibit intrinsic sympathomimetic activity of different extents in different compartments in the cardiomyocyte. Of particular interest is the AKAP-18δ signalosome, which appears tightly regulated and shielded from carvedilol-associated ISA activity, with potential clinical relevance.
- The compartment-specific differences detected on application of different β-blockers are not fully attributable to β-AR subtype selectivity. Selective antagonism establishes that carvedilol's ISA is predominantly β2-AR-mediated and bucindolol's predominantly β1-AR-mediated, although a weaker residual cAMP signal persisted after subtype-selective blockade, indicating a contribution from the non-target subtype.

- Preliminary experiments identify a Golgi-associated cAMP pool that is accessible to bucindolol but not carvedilol. This supports an emerging role for intracellular receptors in shaping the cAMP response.

Together, these findings establish that ISA is not a binary property but a spatially resolved phenomenon whose functional consequences depend on the nanodomain at which it acts. It should be emphasised, however, that this work characterises where these compartment-specific effects arise rather than resolving the precise molecular mechanisms that produce them, which remain to be defined.

Beyond these mechanistic insights, the findings carry implications for drug development, which has canonically been guided by principles such as receptor selectivity. Given that GPCRs are the target of a substantial proportion of licensed therapeutics, the recognition that a single ligand may determine where its second messenger is generated establishes subcellular location as an additional factor that could be exploited to generate cAMP in compartments coupled with beneficial effects, while sparing those linked to adverse effects. Characterising β-blockers, and more broadly other GPCR ligands, by their nanodomain signalling profile may further refine their clinical use and guide the design of the next generation of therapeutics.

A

Appendix

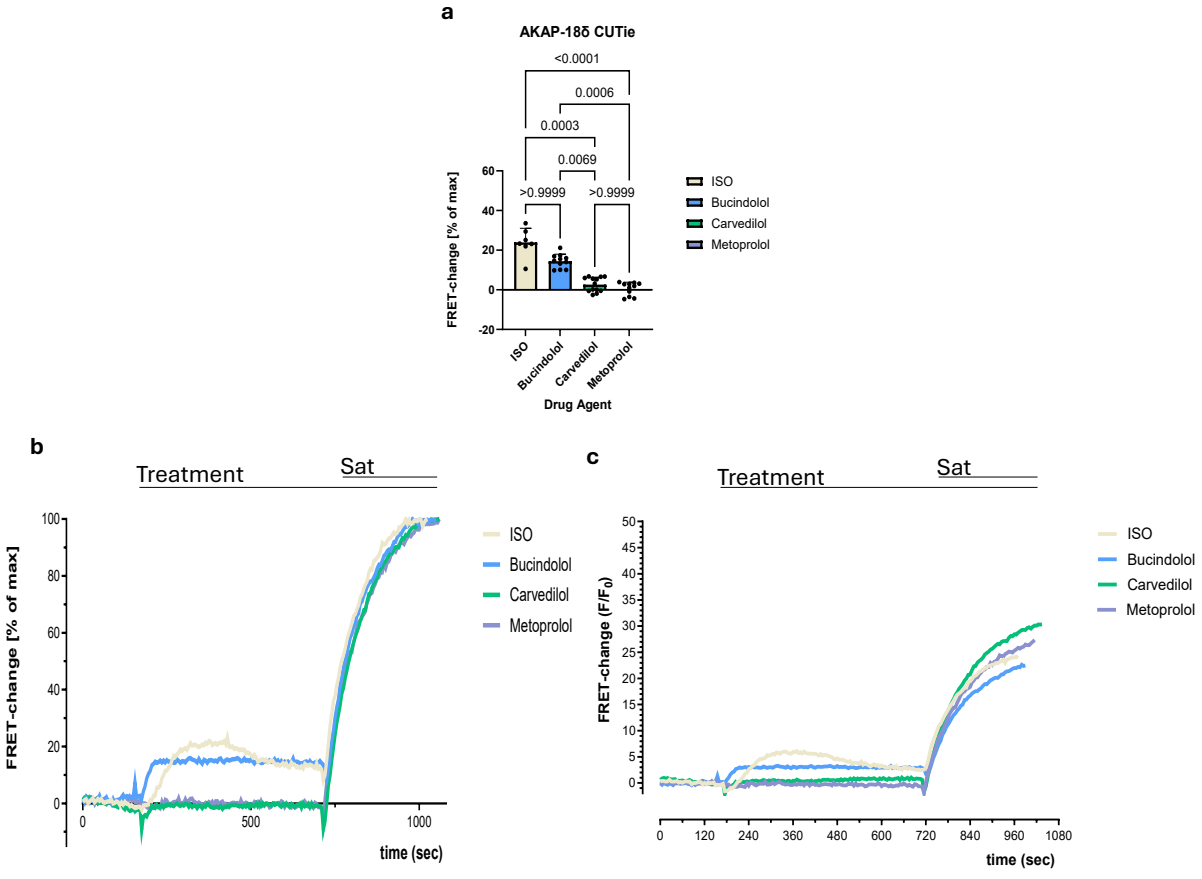


Figure S1: *Representative kinetics (b) and (c) and summary (a) of FRET change from neonatal rat ventricular myocytes (NRVM) expressing AKAP-18δ cAMP FRET reporter in response to bath application of 1 nM isoproterenol (ISO), 10 μM bucindolol, 10 μM carvedilol and 10 μM metoprolol. Each*

dot represents one individual cell from minimum three biological replicates. Error bars represent mean ± SD.

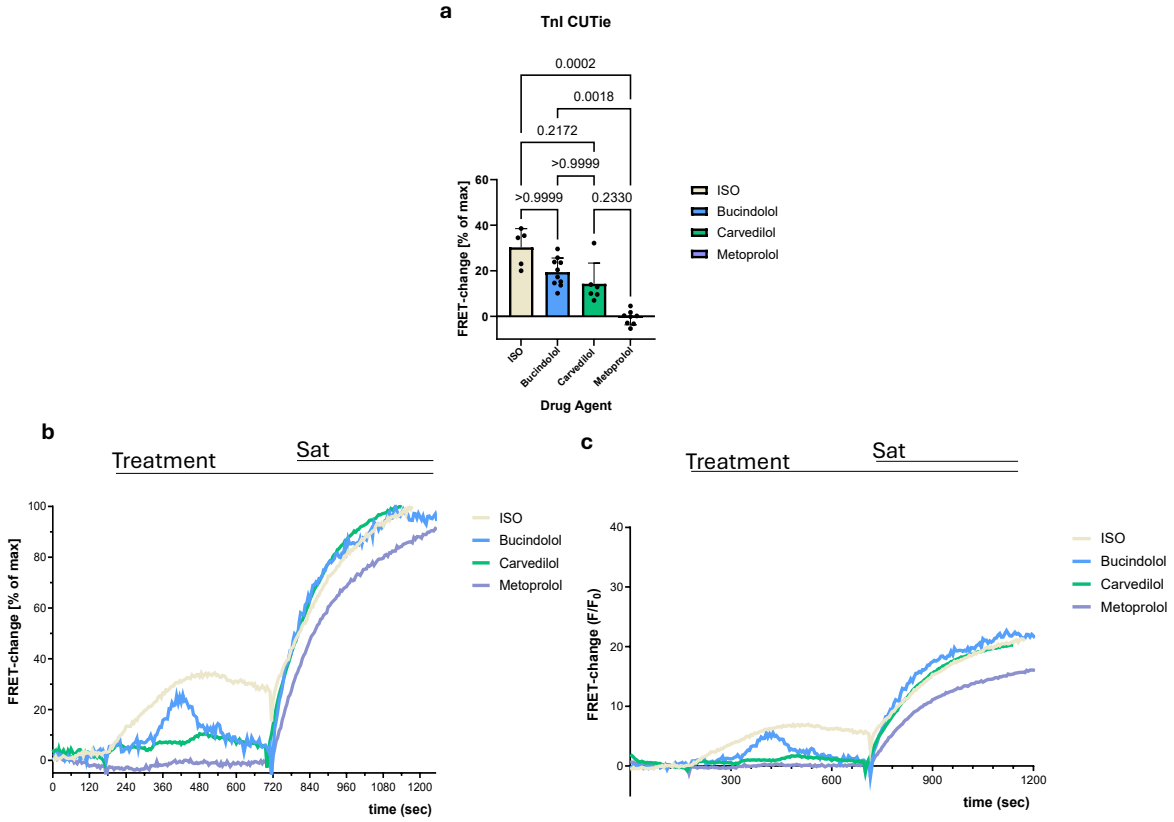


Figure S2: *Representative kinetics (b) and (c) and summary (a) of FRET change from neonatal rat ventricular myocytes (NRVM) expressing TnI cAMP FRET reporter in response to bath application of 1 nM isoproterenol (ISO), 10 μM bucindolol, 10 μM carvedilol and 10 μM metoprolol. Each dot represents one individual cell from minimum three biological replicates. Error bars represent mean ± SD.*

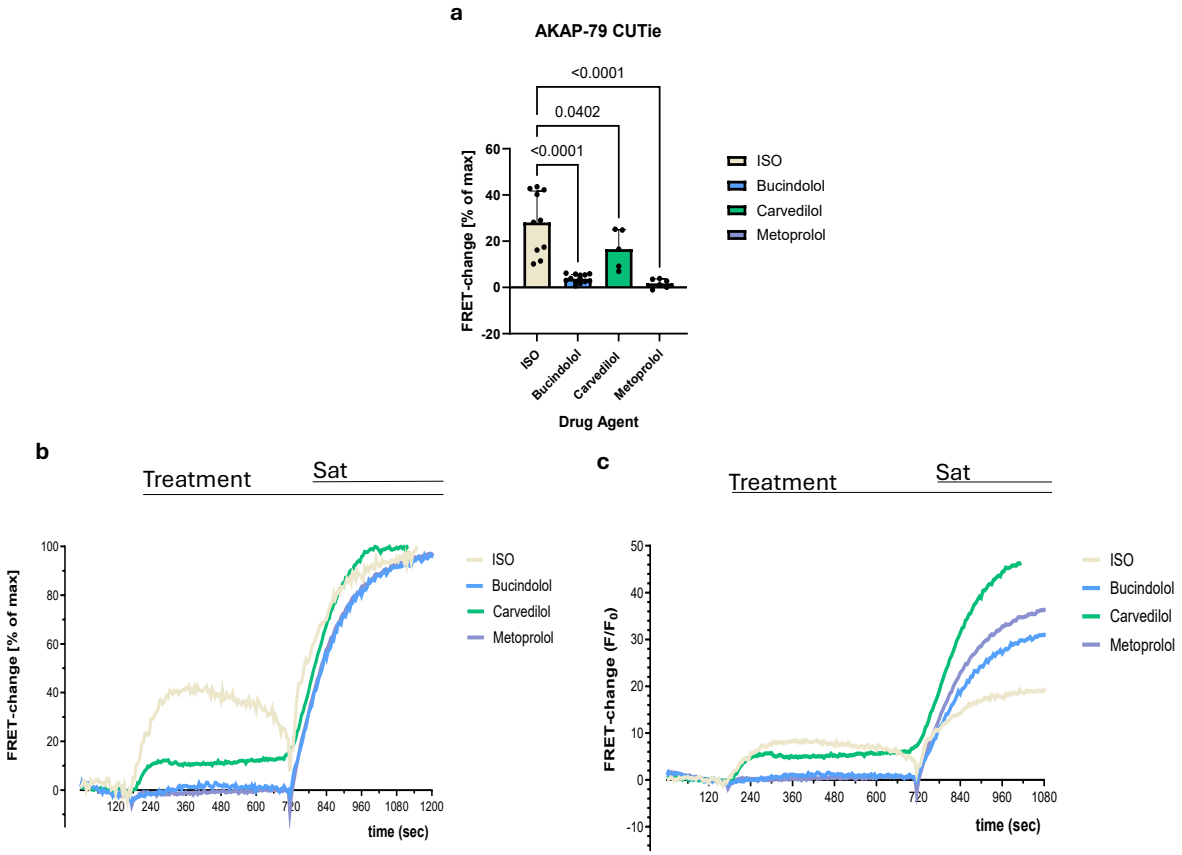


Figure S3: *Representative kinetics (b) and (c) and summary (a) of FRET change from neonatal rat ventricular myocytes (NRVM) expressing AKAP-79 cAMP FRET reporter in response to bath application of 1 nM isoproterenol (ISO), 10 μM bucindolol, 10 μM carvedilol and 10 μM metoprolol. Each dot represents one individual cell from minimum three biological replicates. Error bars represent mean ± SD.*

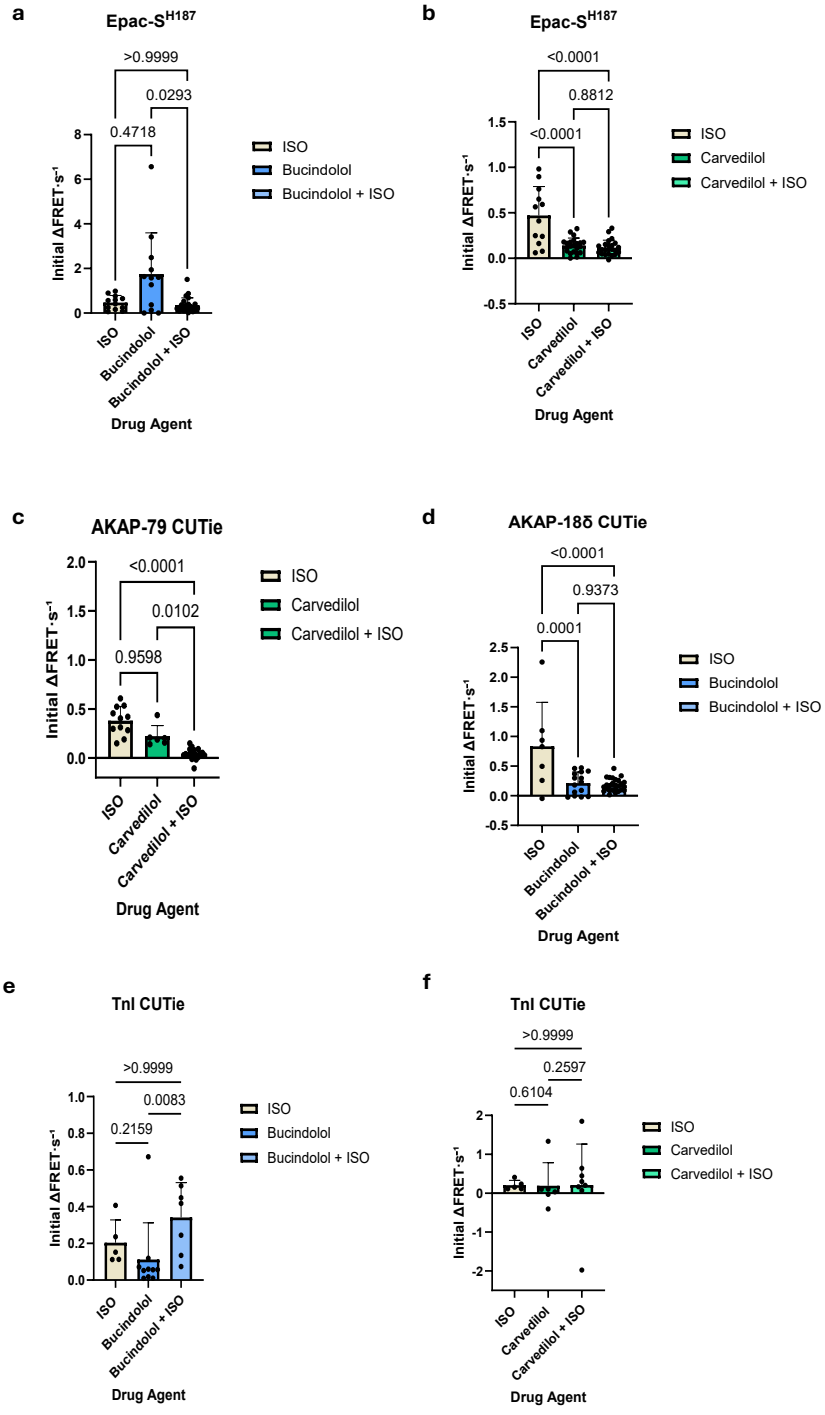


Figure S4: *Summary (a-f) of initial response kinetics for ligands in compartments where a measurable response was observed following stimulation. Initial FRET kinetics were calculated as the linear slope of the response during the first 20s after stimulation of ligand. Each point represents an individual cell and error bars represent mean ± SD.*

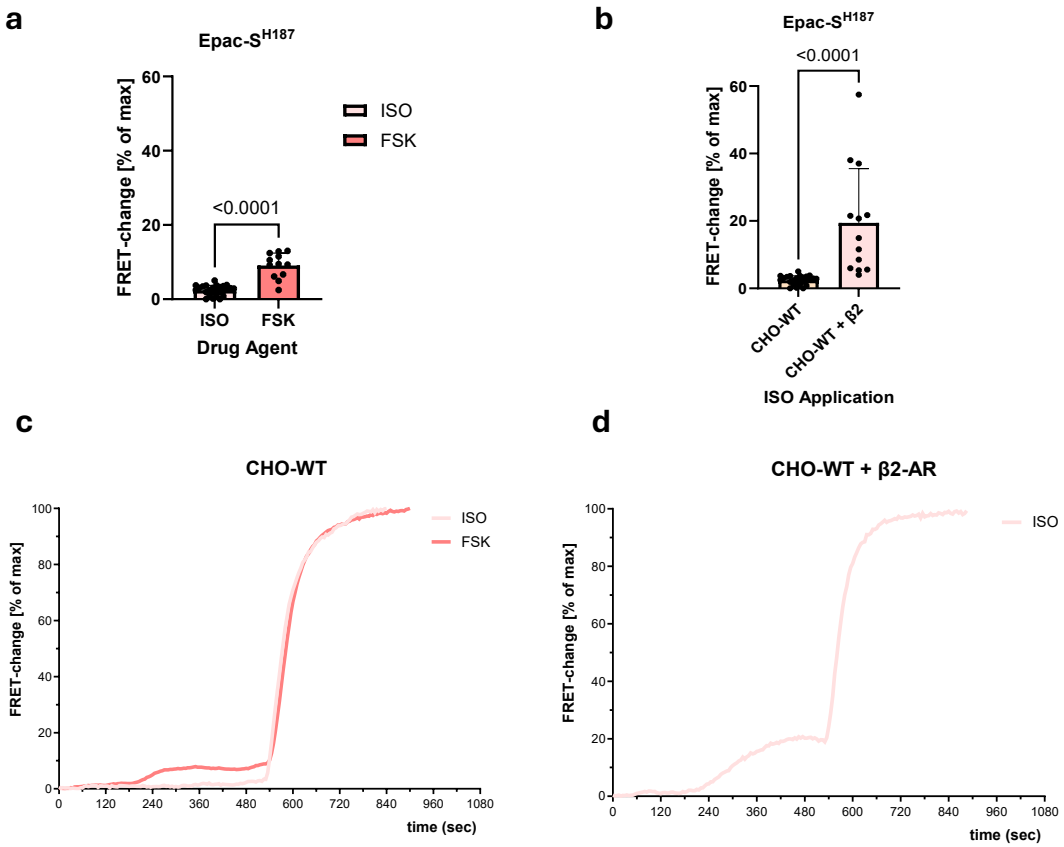


Figure S5: *Validation of CHO-WT cells. Summary (a) of FRET change in CHO-WT upon application of 1 nM ISO and 100 nM forskolin (FSK), a direct activator of adenylyl cyclase. Summary (b) of FRET change in CHO-WT and CHO-WT expressing transiently transfected β2-AR upon application of 1 nM ISO. Representative kinetics (c) of CHO-WT upon application of 1 nM ISO and 100 nM forskolin. Representative kinetics (d) of CHO-WT expressing transiently transfected β2-AR upon application of 1 nM ISO. Each dot represents one individual cell from minimum three biological replicates. Error bars represent mean ± SD.*

Bibliography

[1] Lorente JS, Sokolov AV, Ferguson G, Schiöth HB, Hauser AS, Gloriam DE. GPCR drug discovery: new agents, targets and indications. Nat Rev Drug Discov 2025;24:458–79. https://doi.org/10.1038/s41573-025-01139-y.

[2] Caroli J, Andreassen SN, Lorente JS, Xiao B, Pándy-Szekeres G, Gloriam DE. An online GPCR drug discovery resource. Npj Drug Discov 2025;2:17. https://doi.org/10.1038/s44386-025-00010-9.

[3] Valente V, Laborante R, Abdin A, Becher PM, Lainscak M, Polovina M, et al. The Global Epidemiology of Heart Failure: A Comprehensive and Contemporary Review. Eur J Heart Fail 2026:xuag121. https://doi.org/10.1093/ejhf/xuag121.

[4] Schwinger RH, Böhm M, Erdmann E. The effect of xamoterol in failing human myocardium. Eur Heart J 1990;11:323–7. https://doi.org/10.1093/oxfordjournals.eurheartj.a059705.

[5] The Beta-Blocker Evaluation of Survival Trial Investigators. A Trial of the Beta-Blocker Bucindolol in Patients with Advanced Chronic Heart Failure. N Engl J Med 2001;344:1659–67. https://doi.org/10.1056/NEJM200105313442202.

[6] Poole-Wilson PA, Swedberg K, Cleland JGF, Di Lenarda A, Hanrath P, Komajda M, et al. Comparison of carvedilol and metoprolol on clinical outcomes in patients with chronic heart failure in the Carvedilol Or Metoprolol European Trial (COMET): randomised controlled trial. Lancet 2003;362:7–13. https://doi.org/10.1016/S0140-6736(03)13800-7.

[7] The Cardiac Insufficiency Bisoprolol Study II (CIBIS-II): a randomised trial. Lancet 1999;353:9–13.

[8] Hjalmarson Å, Goldstein S, Fagerberg B, Wedel H, Waagstein F, Kjekshus J, et al. Effects of Controlled-Release Metoprolol on Total Mortality, Hospitalizations, and Well-being in Patients With Heart Failure: The Metoprolol CR/XL Randomized Intervention Trial in Congestive Heart Failure (MERIT-HF). JAMA 2000;283:1295. https://doi.org/10.1001/jama.283.10.1295.

[9] Benkel T, Zimmermann M, Zeiner J, Bravo S, Merten N, Lim VJY, et al. How Carvedilol activates β2-adrenoceptors. Nat Commun 2022;13:7109. https://doi.org/10.1038/s41467-022-34765-w.

[10] Rosenbaum DM, Rasmussen SGF, Kobilka BK. The structure and function of G-protein-coupled receptors. Nature 2009;459:356–63. https://doi.org/10.1038/nature08144.

[11] Alexander SP, Christopoulos A, Davenport AP, Kelly E, Marrion NV, Peters JA, et al. THE CONCISE GUIDE TO PHARMACOLOGY 2017/18: G protein-coupled receptors. Br J Pharmacol 2017;174. https://doi.org/10.1111/bph.13878.

[12] Wootten D, Christopoulos A, Marti-Solano M, Babu MM, Sexton PM. Mechanisms of signalling and biased agonism in G protein-coupled receptors. Nat Rev Mol Cell Biol 2018;19:638–53. https://doi.org/10.1038/s41580-018-0049-3.

[13] Scholz N, Langenhan T, Schöneberg T. Revisiting the classification of adhesion GPCRs. Ann N Y Acad Sci 2019;1456:80–95. https://doi.org/10.1111/nyas.14192.

[14] Fredriksson R, Lagerström MC, Lundin L-G, Schiöth HB. The G-Protein-Coupled Receptors in the Human Genome Form Five Main Families. Phylogenetic Analysis, Paralogon Groups, and Fingerprints. Mol Pharmacol 2003;63:1256–72. https://doi.org/10.1124/mol.63.6.1256.

[15] Liu S, Anderson PJ, Rajagopal S, Lefkowitz RJ, Rockman HA. G Protein-Coupled Receptors: A Century of Research and Discovery. Circ Res 2024;135:174–97. https://doi.org/10.1161/CIRCRESAHA.124.323067.

[16] Zhang M, Chen T, Lu X, Lan X, Chen Z, Lu S. G protein-coupled receptors (GPCRs): advances in structures, mechanisms and drug discovery. Signal Transduct Target Ther 2024;9:88. https://doi.org/10.1038/s41392-024-01803-6.

[17] Herrera LPT, Andreassen SN, Caroli J, Rodríguez-Espigares I, Kermani AA, Keserű GM, et al. GPCRdb in 2025: adding odorant receptors, data mapper, structure similarity search and models of physiological ligand complexes. Nucleic Acids Res 2025;53:D425–35. https://doi.org/10.1093/nar/gkae1065.

[18] Jiang H, Galtes D, Wang J, Rockman HA. G protein-coupled receptor signaling: transducers and effectors. Am J Physiol-Cell Physiol 2022;323:C731–48. https://doi.org/10.1152/ajpcell.00210.2022.

[19] Ahmad R, Lahuna O, Sidibe A, Daulat A, Zhang Q, Luka M, et al. GPR50-Ctail cleavage and nuclear translocation: a new signal transduction mode for G protein-coupled receptors. Cell Mol Life Sci 2020;77:5189–205. https://doi.org/10.1007/s00018-019-03440-7.

[20] Cox AD, Der CJ. Ras history: The saga continues. Small GTPases 2010;1:2–27. https://doi.org/10.4161/sgtp.1.1.12178.

[21] Liu Y, Wang X, Dong D, Guo L, Dong X, Leng J, et al. Research Advances in Heterotrimeric G-Protein α Subunits and Uncanonical G-Protein Coupled Receptors in Plants. Int J Mol Sci 2021;22:8678. https://doi.org/10.3390/ijms22168678.

[22] Milligan G, Kostenis E. Heterotrimeric G-proteins: a short history. Br J Pharmacol 2006;147. https://doi.org/10.1038/sj.bjp.0706405.

[23] Boron WF, Boulpaep EL, editors. Medical physiology. Third edition. Philadelphia, PA: Elsevier; 2017.

[24] Hauser AS, Avet C, Normand C, Mancini A, Inoue A, Bouvier M, et al. Common coupling map advances GPCR-G protein selectivity. eLife 2022;11:e74107. https://doi.org/10.7554/eLife.74107.

[25] Alberts B, Johnson A, Lewis J, Raff M, Roberts K, Walter P. Signaling through G-Protein-Linked Cell-Surface Receptors. Mol. Biol. Cell 4th Ed., Garland Science; 2002.

[26] Gurevich VV, Gurevich EV. GPCR Signaling Regulation: The Role of GRKs and Arrestins. Front Pharmacol 2019;10. https://doi.org/10.3389/fphar.2019.00125.

[27] Kohout TA, Lefkowitz RJ. Regulation of G Protein-Coupled Receptor Kinases and Arrestins During Receptor Desensitization. Mol Pharmacol 2003;63:9–18. https://doi.org/10.1124/mol.63.1.9.

[28] Smith JS, Pack TF. Noncanonical interactions of G proteins and β-arrestins: from competitors to companions. FEBS J 2021;288:2550–61. https://doi.org/10.1111/febs.15749.

[29] Lefkowitz RJ, Shenoy SK. Transduction of Receptor Signals by β-Arrestins. Science 2005;308:512–7. https://doi.org/10.1126/science.1109237.

[30] Kühn H. Light-regulated binding of rhodopsin kinase and other proteins to cattle photoreceptor membranes. Biochemistry 1978;17:4389–95. https://doi.org/10.1021/bi00614a006.

[31] Tian X, Kang DS, Benovic JL. β-Arrestins and G Protein-Coupled Receptor Trafficking. In: Gurevich VV, editor. Arrestins - Pharmacol. Ther. Potential, Berlin, Heidelberg: Springer; 2014, p. 173–86. https://doi.org/10.1007/978-3-642-41199-1_9.

[32] Shenoy SK, Drake MT, Nelson CD, Houtz DA, Xiao K, Madabushi S, et al. β-Arrestin-dependent, G Protein-independent ERK1/2 Activation by the β2 Adrenergic Receptor. J Biol Chem 2006;281:1261–73. https://doi.org/10.1074/jbc.M506576200.

[33] Madhu MK, Murarka RK. Mechanistic Basis for GPCR Phosphorylation-Dependent Allosteric Signaling Specificity of β-Arrestin 1 and 2. J Chem Inf Model 2025;65:11173–86. https://doi.org/10.1021/acs.jcim.5c01078.

[34] Goodman OB, Krupnick JG, Santini F, Gurevich VV, Penn RB, Gagnon AW, et al. Beta-arrestin acts as a clathrin adaptor in endocytosis of the beta2-adrenergic receptor. Nature 1996;383:447–50. https://doi.org/10.1038/383447a0.

[35] Thomsen ARB, Plouffe B, Cahill TJ, Shukla AK, Tarrasch JT, Dosey AM, et al. GPCR-G Protein-β-Arrestin Super-Complex Mediates Sustained G Protein Signaling. Cell 2016;166:907–19. https://doi.org/10.1016/j.cell.2016.07.004.

[36] Calebiro D, Nikolaev VO, Gagliani MC, Filippis T de, Dees C, Tacchetti C, et al. Persistent cAMP-Signals Triggered by Internalized G-Protein–Coupled Receptors. PLOS Biol 2009;7:e1000172. https://doi.org/10.1371/journal.pbio.1000172.

[37] Nguyen AH, Lefkowitz RJ. Signaling at the endosome: cryo-EM structure of a GPCR-G protein-beta-arrestin megacomplex. FEBS J 2021;288:2562–9. https://doi.org/10.1111/febs.15773.

[38] Shukla AK, Westfield GH, Xiao K, Reis RI, Huang L-Y, Tripathi-Shukla P, et al. Visualization of arrestin recruitment by a G-protein-coupled receptor. Nature 2014;512:218–22. https://doi.org/10.1038/nature13430.

[39] Irannejad R, Pessino V, Mika D, Huang B, Wedegaertner PB, Conti M, et al. Functional selectivity of GPCR-directed drug action through location bias. Nat Chem Biol 2017;13:799–806. https://doi.org/10.1038/nchembio.2389.

[40] Galandrin S, Bouvier M. Distinct signaling profiles of beta1 and beta2 adrenergic receptor ligands toward adenylyl cyclase and mitogen-activated protein kinase reveals the pluridimensionality of efficacy. Mol Pharmacol 2006;70:1575–84. https://doi.org/10.1124/mol.106.026716.

[41] Wisler JW, DeWire SM, Whalen EJ, Violin JD, Drake MT, Ahn S, et al. A unique mechanism of β-blocker action: Carvedilol stimulates β-arrestin signaling. Proc Natl Acad Sci 2007;104:16657–62. https://doi.org/10.1073/pnas.0707936104.

[42] Reiter E, Ahn S, Shukla AK, Lefkowitz RJ. Molecular Mechanism of β-Arrestin-Biased Agonism at Seven-Transmembrane Receptors. Annu Rev Pharmacol Toxicol 2012;52:179–97. https://doi.org/10.1146/annurev.pharmtox.010909.105800.

[43] Ahn D, Ham D, Chung KY. The conformational transition during G protein–coupled receptor (GPCR) and G protein interaction. Curr Opin Struct Biol 2021;69:117–23. https://doi.org/10.1016/j.sbi.2021.03.013.

[44] McDonald PH, Chow C-W, Miller WE, Laporte SA, Field ME, Lin F-T, et al. β-Arrestin 2: A Receptor-Regulated MAPK Scaffold for the Activation of JNK3. Science 2000;290:1574–7. https://doi.org/10.1126/science.290.5496.1574.

[45] Pakharukova N, Masoudi A, Pani B, Staus DP, Lefkowitz RJ. Allosteric activation of proto-oncogene kinase Src by GPCR–beta-arrestin complexes. J Biol Chem 2020;295:16773–84. https://doi.org/10.1074/jbc.RA120.015400.

[46] Azzi M, Charest PG, Angers S, Rousseau G, Kohout T, Bouvier M, et al. Beta-arrestin-mediated activation of MAPK by inverse agonists reveals distinct active conformations for G protein-coupled receptors. Proc Natl Acad Sci U S A 2003;100:11406–11. https://doi.org/10.1073/pnas.1936664100.

[47] Ma Y, Patterson B, Zhu L. Biased signaling in GPCRs: Structural insights and implications for drug development. Pharmacol Ther 2025;266:108786. https://doi.org/10.1016/j.pharmthera.2024.108786.

[48] Sutherland EW, Rall TW. Fractionation and characterization of a cyclic adenine ribonucleotide formed by tissue particles. J Biol Chem 1958;232:1077–91.

[49] Ostrom KF, LaVigne JE, Brust TF, Seifert R, Dessauer CW, Watts VJ, et al. Physiological roles of mammalian transmembrane adenylyl cyclase isoforms. Physiol Rev 2022;102:815–57. https://doi.org/10.1152/physrev.00013.2021.

[50] Ludwig M-G, Seuwen K. Characterization of the human adenylyl cyclase gene family: cDNA, gene structure, and tissue distribution of the nine isoforms. J Recept Signal Transduct Res 2002;22:79–110. https://doi.org/10.1081/rrs-120014589.

[51] Sassone-Corsi P. The Cyclic AMP Pathway. Cold Spring Harb Perspect Biol 2012;4:a011148. https://doi.org/10.1101/cshperspect.a011148.

[52] Sherstnev I, Judina A, Luciani GB, Ghigo A, Hirsch E, Gorelik J. Role of PDE4 Family in Cardiomyocyte Physiology and Heart Failure. Cells 2025;14. https://doi.org/10.3390/cells14060460.

[53] Mongillo M, McSorley T, Evellin S, Sood A, Lissandron V, Terrin A, et al. Fluorescence resonance energy transfer-based analysis of cAMP dynamics in live neonatal rat cardiac myocytes reveals distinct functions of

compartmentalized phosphodiesterases. Circ Res 2004;95:67–75. https://doi.org/10.1161/01.RES.0000134629.84732.11.

[54] Rochais F, Abi-Gerges A, Horner K, Lefebvre F, Cooper DMF, Conti M, et al. A specific pattern of phosphodiesterases controls the cAMP signals generated by different Gs-coupled receptors in adult rat ventricular myocytes. Circ Res 2006;98:1081–8. https://doi.org/10.1161/01.RES.0000218493.09370.8e.

[55] Zaccolo M, Movsesian MA. cAMP and cGMP Signaling Cross-Talk. Circ Res 2007;100:1569–78. https://doi.org/10.1161/CIRCRESAHA.106.144501.

[56] Brand T, Schindler R. New kids on the block: The Popeye domain containing (POPDC) protein family acting as a novel class of cAMP effector proteins in striated muscle. Cell Signal 2017;40:156–65. https://doi.org/10.1016/j.cellsig.2017.09.015.

[57] Froese A, Breher SS, Waldeyer C, Schindler RFR, Nikolaev VO, Rinné S, et al. Popeye domain containing proteins are essential for stress-mediated modulation of cardiac pacemaking in mice. J Clin Invest 2012;122:1119–30. https://doi.org/10.1172/JCI59410.

[58] Zhang X, Zhu F, Xiao Z, Wang H. The role of A-kinase anchoring proteins in cardiovascular diseases and recent advances. Front Cell Dev Biol 2025;13. https://doi.org/10.3389/fcell.2025.1611583.

[59] Colombe A-S, Pidoux G. Cardiac cAMP-PKA Signaling Compartmentalization in Myocardial Infarction. Cells 2021;10:922. https://doi.org/10.3390/cells10040922.

[60] Zhang Y, Wang WE, Zhang X, Li Y, Chen B, Liu C, et al. Cardiomyocyte PKA Ablation Enhances Basal Contractility While Eliminates Cardiac β-Adrenergic Response Without Adverse Effects on the Heart. Circ Res 2019;124:1760–77. https://doi.org/10.1161/CIRCRESAHA.118.313417.

[61] Zaccolo M, Zerio A, Lobo MJ. Subcellular Organization of the cAMP Signaling Pathway. Pharmacol Rev 2021;73:278–309. https://doi.org/10.1124/pharmrev.120.000086.

[62] Kawasaki H, Springett GM, Mochizuki N, Toki S, Nakaya M, Matsuda M, et al. A family of cAMP-binding proteins that directly activate Rap1. Science 1998;282:2275–9. https://doi.org/10.1126/science.282.5397.2275.

[63] Ruiz-Hurtado G, Morel E, Domínguez-Rodríguez A, Llach A, Lezoualc'h F, Benitah J-P, et al. Epac in cardiac calcium signaling. J Mol Cell Cardiol 2013;58:162–71. https://doi.org/10.1016/j.yjmcc.2012.11.021.

[64] Redden JM, Dodge-Kafka KL. AKAP Phosphatase Complexes in the Heart: J Cardiovasc Pharmacol 2011;58:354–62. https://doi.org/10.1097/FJC.0b013e31821e5649.

[65] Kar P, Barak P, Zerio A, Lin Y-P, Parekh AJ, Watts VJ, et al. AKAP79 Orchestrates a Cyclic AMP Signalosome Adjacent to Orai1 Ca(2+) Channels. Funct Oxf Engl 2021;2:zqab036. https://doi.org/10.1093/function/zqab036.

[66] Scott JD, Santana LF. A-Kinase Anchoring Proteins: Getting to the Heart of the Matter. Circulation 2010;121:1264–71. https://doi.org/10.1161/CIRCULATIONAHA.109.896357.

[67] Scott JD, Dessauer CW, Taskén K. Creating Order from Chaos: Cellular Regulation by Kinase Anchoring. Annu Rev Pharmacol Toxicol 2013;53:187–210. https://doi.org/10.1146/annurev-pharmtox-011112-140204.

[68] Mauban J, O'Donnell M, Warrier S, Manni S, Bond M. AKAP-scaffolding proteins and regulation of cardiac physiology. Physiol Bethesda Md 2009;24:78–87. https://doi.org/10.1152/physiol.00041.2008.

[69] Kritzer MD, Li J, Dodge-Kafka K, Kapiloff MS. AKAPs: The architectural underpinnings of local cAMP signaling. J Mol Cell Cardiol 2012;52:351–8. https://doi.org/10.1016/j.yjmcc.2011.05.002.

[70] Musheshe N, Lobo MJ, Schmidt M, Zaccolo M. Targeting FRET-Based Reporters for cAMP and PKA Activity Using AKAP79. Sensors 2018;18. https://doi.org/10.3390/s18072164.

[71] Carlson CR, Aronsen JM, Bergan-Dahl A, Moutty MC, Lunde M, Lunde PK, et al. AKAP18δ Anchors and Regulates CaMKII Activity at Phospholamban-SERCA2 and RYR. Circ Res 2022;130:27–44. https://doi.org/10.1161/CIRCRESAHA.120.317976.

[72] Chen M-H, Malbon CC. G-protein-coupled receptor-associated A-kinase anchoring proteins AKAP5 and AKAP12: differential trafficking and distribution. Cell Signal 2009;21:136–42. https://doi.org/10.1016/j.cellsig.2008.09.019.

[73] Zaccolo M, Kovanich D. Nanodomain cAMP signaling in cardiac pathophysiology: potential for developing targeted therapeutic interventions. Physiol Rev 2025;105:541–91. https://doi.org/10.1152/physrev.00013.2024.

[74] Zaccolo M, Pozzan T. Discrete Microdomains with High Concentration of cAMP in Stimulated Rat Neonatal Cardiac Myocytes. Science 2002;295:1711–5. https://doi.org/10.1126/science.1069982.

[75] Yadav R, Zaccolo M. GPCR signaling via cAMP nanodomains. Biochem J 2025;482:519–33. https://doi.org/10.1042/BCJ20253088.

[76] Beavo JA, Brunton LL. Cyclic nucleotide research — still expanding after half a century. Nat Rev Mol Cell Biol 2002;3:710–7. https://doi.org/10.1038/nrm911.

[77] Koschinski A, Zaccolo M. Activation of PKA in cell requires higher concentration of cAMP than in vitro: implications for compartmentalization of cAMP signalling. Sci Rep 2017;7:14090. https://doi.org/10.1038/s41598-017-13021-y.

[78] Lohse C, Bock A, Maiellaro I, Hannawacker A, Schad LR, Lohse MJ, et al. Experimental and mathematical analysis of cAMP nanodomains. PloS One 2017;12:e0174856. https://doi.org/10.1371/journal.pone.0174856.

[79] Zaccolo M, De Giorgi F, Cho CY, Feng L, Knapp T, Negulescu PA, et al. A genetically encoded, fluorescent indicator for cyclic AMP in living cells. Nat Cell Biol 2000;2:25–9. https://doi.org/10.1038/71345.

[80] Demby A, Zaccolo M. Investigating G-protein coupled receptor signalling with light-emitting biosensors. Front Physiol 2024;14. https://doi.org/10.3389/fphys.2023.1310197.

[81] Sun Y, Rombola C, Jyothikumar V, Periasamy A. Förster resonance energy transfer microscopy and spectroscopy for localizing protein-protein interactions in living cells. Cytom Part J Int Soc Anal Cytol 2013;83:780–93. https://doi.org/10.1002/cyto.a.22321.

[82] Surdo NC, Berrera M, Koschinski A, Brescia M, Machado MR, Carr C, et al. FRET biosensor uncovers cAMP nano-domains at β-adrenergic targets that dictate precise tuning of cardiac contractility. Nat Commun 2017;8:15031. https://doi.org/10.1038/ncomms15031.

[83] Adams SR, Harootunian AT, Buechler YJ, Taylor SS, Tsien RY. Fluorescence ratio imaging of cyclic AMP in single cells. Nature 1991;349:694–7. https://doi.org/10.1038/349694a0.

[84] Jiang JY, Falcone JL, Curci S, Hofer AM. Interrogating cyclic AMP signaling using optical approaches. Cell Calcium 2017;64:47–56. https://doi.org/10.1016/j.ceca.2017.02.010.

[85] Nikolaev VO, Bünemann M, Hein L, Hannawacker A, Lohse MJ. Novel Single Chain cAMP Sensors for Receptor-induced Signal Propagation * ♦. J Biol Chem 2004;279:37215–8. https://doi.org/10.1074/jbc.C400302200.

[86] Klarenbeek J, Goedhart J, van Batenburg A, Groenewald D, Jalink K. Fourth-Generation Epac-Based FRET Sensors for cAMP Feature Exceptional Brightness, Photostability and Dynamic Range: Characterization of Dedicated Sensors for FLIM, for Ratiometry and with

High Affinity. PLoS ONE 2015;10:e0122513. https://doi.org/10.1371/journal.pone.0122513.

[87] Ponsioen B, Zhao J, Riedl J, Zwartkruis F, van der Krogt G, Zaccolo M, et al. Detecting cAMP-induced Epac activation by fluorescence resonance energy transfer: Epac as a novel cAMP indicator. EMBO Rep 2004;5:1176–80. https://doi.org/10.1038/sj.embor.7400290.

[88] Schleicher K, Zaccolo M. Using cAMP Sensors to Study Cardiac Nanodomains. J Cardiovasc Dev Dis 2018;5. https://doi.org/10.3390/jcdd5010017.

[89] Goedhart J, von Stetten D, Noirclerc-Savoye M, Lelimousin M, Joosen L, Hink MA, et al. Structure-guided evolution of cyan fluorescent proteins towards a quantum yield of 93%. Nat Commun 2012;3:751. https://doi.org/10.1038/ncomms1738.

[90] Chao Y-C, Surdo NC, Pantano S, Zaccolo M. Imaging cAMP nanodomains in the heart. Biochem Soc Trans 2019;47:1383–92. https://doi.org/10.1042/BST20190245.

[91] Klein F, Abreu C, Pantano S. How to Make the CUTiest Sensor in Three Simple Steps for Computational Pedestrians. Methods Mol Biol 2022;2483:255–64. https://doi.org/10.1007/978-1-0716-2245-2_16.

[92] Kaumann AJ, Preitner F, Sarsero D, Molenaar P, Revelli J-P, Giacobino JP. (−)-CGP 12177 Causes Cardiostimulation and Binds to Cardiac Putative β4-Adrenoceptors in Both Wild-Type and β3-Adrenoceptor Knockout Mice. Mol Pharmacol 1998;53:670–5. https://doi.org/10.1124/mol.53.4.670.

[93] Madamanchi A. Beta-adrenergic receptor signaling in cardiac function and heart failure. McGill J Med MJM Int Forum Adv Med Sci Stud 2007;10:99–104.

[94] Xu X, Kaindl J, Clark MJ, Hübner H, Hirata K, Sunahara RK, et al. Binding pathway determines norepinephrine selectivity for the human β1AR over β2AR. Cell Res 2021;31:569–79. https://doi.org/10.1038/s41422-020-00424-2.

[95] Xiao R-P, Zhu W, Zheng M, Cao C, Zhang Y, Lakatta EG, et al. Subtype-specific α1- and β-adrenoceptor signaling in the heart. Trends Pharmacol Sci 2006;27:330–7. https://doi.org/10.1016/j.tips.2006.04.009.

[96] Wang W, Zhu W, Wang S, Yang D, Crow MT, Xiao R-P, et al. Sustained β1-Adrenergic Stimulation Modulates Cardiac Contractility by Ca2+/Calmodulin Kinase Signaling Pathway. Circ Res 2004;95:798–806. https://doi.org/10.1161/01.RES.0000145361.50017.aa.

[97] Liu Y, Shao Q, Cheng H-J, Li T, Zhang X, Callahan MF, et al. Chronic Ca2+/Calmodulin-Dependent Protein Kinase II Inhibition Rescues Advanced Heart Failure. J Pharmacol Exp Ther 2021;377:316–25. https://doi.org/10.1124/jpet.120.000361.

[98] Xiang YK. Compartmentalization of β-Adrenergic Signals in Cardiomyocytes. Circ Res 2011;109:231–44. https://doi.org/10.1161/CIRCRESAHA.110.231340.

[99] Rybin VO, Xu X, Lisanti MP, Steinberg SF. Differential targeting of beta -adrenergic receptor subtypes and adenylyl cyclase to cardiomyocyte caveolae. A mechanism to functionally regulate the cAMP signaling pathway. J Biol Chem 2000;275:41447–57. https://doi.org/10.1074/jbc.M006951200.

[100] Macdougall DA, Agarwal SR, Stopford EA, Chu H, Collins JA, Longster AL, et al. Caveolae compartmentalise β2-adrenoceptor signals by curtailing cAMP production and maintaining phosphatase activity in the sarcoplasmic reticulum of the adult ventricular myocyte. J Mol Cell Cardiol 2012;52:388–400. https://doi.org/10.1016/j.yjmcc.2011.06.014.

[101] Liu R, Ramani B, Soto D, De Arcangelis V, Xiang Y. Agonist dose-dependent phosphorylation by protein kinase A and G protein-coupled receptor kinase regulates beta2 adrenoceptor coupling to G(i) proteins in cardiomyocytes. J Biol Chem 2009;284:32279–87. https://doi.org/10.1074/jbc.M109.021428.

[102] Wang Y, De Arcangelis V, Gao X, Ramani B, Jung Y, Xiang Y. Norepinephrine- and epinephrine-induced distinct beta2-adrenoceptor signaling is dictated by GRK2 phosphorylation in cardiomyocytes. J Biol Chem 2008;283:1799–807. https://doi.org/10.1074/jbc.M705747200.

[103] Xiao RP, Cheng H, Zhou YY, Kuschel M, Lakatta EG. Recent advances in cardiac beta(2)-adrenergic signal transduction. Circ Res 1999;85:1092–100. https://doi.org/10.1161/01.res.85.11.1092.

[104] Zhu W, Petrashevskaya N, Ren S, Zhao A, Chakir K, Gao E, et al. Gi-biased β2AR signaling links GRK2 upregulation to heart failure. Circ Res 2012;110:265–74. https://doi.org/10.1161/CIRCRESAHA.111.253260.

[105] Nikolaev VO, Bünemann M, Schmitteckert E, Lohse MJ, Engelhardt S. Cyclic AMP imaging in adult cardiac myocytes reveals far-reaching beta1-adrenergic but locally confined beta2-adrenergic receptor-mediated signaling. Circ Res 2006;99:1084–91. https://doi.org/10.1161/01.RES.0000250046.69918.d5.

[106] Nichols CB, Rossow CF, Navedo MF, Westenbroek RE, Catterall WA, Santana LF, et al. Sympathetic stimulation of adult cardiomyocytes requires association of AKAP5 with a sub-population of L-type calcium channels. Circ Res 2010;107:10.1161/CIRCRESAHA.109.216127. https://doi.org/10.1161/CIRCRESAHA.109.216127.

[107] Folkmanaite M, Zaccolo M. Regulation of cardiac function by cAMP nanodomains. Biosci Rep 2023;43. https://doi.org/10.1042/BSR20220953.

[108] Li X, Nooh MM, Bahouth SW. Role of AKAP79/150 Protein in β1-Adrenergic Receptor Trafficking and Signaling in Mammalian Cells *. J Biol Chem 2013;288:33797–812. https://doi.org/10.1074/jbc.M113.470559.

[109] Fraser ID, Cong M, Kim J, Rollins EN, Daaka Y, Lefkowitz RJ, et al. Assembly of an A kinase-anchoring protein-beta(2)-adrenergic receptor complex facilitates receptor phosphorylation and signaling. Curr Biol CB 2000;10:409–12. https://doi.org/10.1016/s0960-9822(00)00419-x.

[110] Willette RN, Mitchell MP, Ohlstein EH, Lukas MA, Ruffolo RR. Evaluation of intrinsic sympathomimetic activity of bucindolol and carvedilol in rat heart. Pharmacology 1998;56:30–6. https://doi.org/10.1159/000028179.

[111] Maack C, Cremers B, Flesch M, Höper A, Südkamp M, Böhm M. Different intrinsic activities of bucindolol, carvedilol and metoprolol in human failing myocardium. Br J Pharmacol 2000;130:1131–9. https://doi.org/10.1038/sj.bjp.0703400.

[112] Andreka P, Aiyar N, Olson LC, Wei JQ, Turner MS, Webster KA, et al. Bucindolol Displays Intrinsic Sympathomimetic Activity in Human Myocardium. Circulation 2002;105:2429–34. https://doi.org/10.1161/01.CIR.0000016050.79810.18.

[113] Liggett SB. β-Adrenergic receptors in the failing heart: the good, the bad, and the unknown. J Clin Invest 2001;107:947–8. https://doi.org/10.1172/JCI12774.

[114] Nikolaev VO, Moshkov A, Lyon AR, Miragoli M, Novak P, Paur H, et al. β2-Adrenergic Receptor Redistribution in Heart Failure Changes cAMP Compartmentation. Science 2010;327:1653–7. https://doi.org/10.1126/science.1185988.

[115] Kwan Z, Paulose Nadappuram B, Leung MM, Mohagaonkar S, Li A, Amaradasa KS, et al. Microtubule-Mediated Regulation of β2AR Translation and Function in Failing Hearts. Circ Res 2023;133:944–58. https://doi.org/10.1161/CIRCRESAHA.123.323174.

[116] Heilbrunn SM, Shah P, Bristow MR, Valantine HA, Ginsburg R, Fowler MB. Increased beta-receptor density and improved hemodynamic response to catecholamine stimulation during long-term metoprolol therapy in heart failure from dilated cardiomyopathy. Circulation 1989;79:483–90. https://doi.org/10.1161/01.cir.79.3.483.

[117] Nash CA, Wei W, Irannejad R, Smrcka AV. Golgi localized β1-adrenergic receptors stimulate Golgi PI4P hydrolysis by PLCε to regulate cardiac hypertrophy. eLife 2019;8:e48167. https://doi.org/10.7554/eLife.48167.

[118] Nash CA, Wei W, Irannejad R, Smrcka AV. Golgi localized β1-adrenergic receptors stimulate Golgi PI4P hydrolysis by PLCε to regulate cardiac hypertrophy. eLife n.d.;8:e48167. https://doi.org/10.7554/eLife.48167.

[119] Irannejad R, Tomshine JC, Tomshine JR, Chevalier M, Mahoney JP, Steyaert J, et al. Conformational biosensors reveal GPCR signalling from endosomes. Nature 2013;495:534–8. https://doi.org/10.1038/nature12000.

[120] Wang Y, Shi Q, Li M, Zhao M, Reddy Gopireddy R, Teoh J-P, et al. Intracellular β1-Adrenergic Receptors and Organic Cation Transporter 3 Mediate Phospholamban Phosphorylation to Enhance Cardiac Contractility. Circ Res 2021;128:246–61. https://doi.org/10.1161/CIRCRESAHA.120.317452.

[121] Chen X, Slättengren T, de Lange ECM, Smith DE, Hammarlund-Udenaes M. Revisiting atenolol as a low passive permeability marker. Fluids Barriers CNS 2017;14:30. https://doi.org/10.1186/s12987-017-0078-x.

[122] Reiter MJ. Cardiovascular drug class specificity: beta-blockers. Prog Cardiovasc Dis 2004;47:11–33. https://doi.org/10.1016/j.pcad.2004.04.004.

[123] Oliver E, Mayor Jr F, D'Ocon P. Beta-blockers: Historical Perspective and Mechanisms of Action. Rev Esp Cardiol Engl Ed 2019;72:853–62. https://doi.org/10.1016/j.rec.2019.04.006.

[124] Packer M, Coats AJS, Fowler MB, Katus HA, Krum H, Mohacsi P, et al. Effect of Carvedilol on Survival in Severe Chronic Heart Failure. N Engl J Med 2001;344:1651–8. https://doi.org/10.1056/NEJM200105313442201.

[125] MERIT-HF Study Group. Effect of metoprolol CR/XL in chronic heart failure: Metoprolol CR/XL Randomised Intervention Trial in-Congestive Heart Failure (MERIT-HF). The Lancet 1999;353:2001–7. https://doi.org/10.1016/S0140-6736(99)04440-2.

[126] Khilnani G, Khilnani AK. Inverse agonism and its therapeutic significance. Indian J Pharmacol 2011;43:492–501. https://doi.org/10.4103/0253-7613.84947.

[127] Erickson CE, Gul R, Blessing CP, Nguyen J, Liu T, Pulakat L, et al. The β-blocker Nebivolol Is a GRK/β-arrestin Biased Agonist. PLoS ONE 2013;8:e71980. https://doi.org/10.1371/journal.pone.0071980.

[128] Kim I-M, Tilley DG, Chen J, Salazar NC, Whalen EJ, Violin JD, et al. Beta-blockers alprenolol and carvedilol stimulate beta-arrestin-mediated EGFR transactivation. Proc Natl Acad Sci U S A 2008;105:14555–60. https://doi.org/10.1073/pnas.0804745105.

[129] Wang J, Hanada K, Staus DP, Makara MA, Dahal GR, Chen Q, et al. Gαi is required for carvedilol-induced β1 adrenergic receptor β-arrestin biased signaling. Nat Commun 2017;8:1706. https://doi.org/10.1038/s41467-017-01855-z.

[130] Noma T, Lemaire A, Prasad SVN, Barki-Harrington L, Tilley DG, Chen J, et al. β-Arrestin–mediated β_1-adrenergic receptor transactivation of the EGFR confers cardioprotection. J Clin Invest 2007;117:2445–58. https://doi.org/10.1172/JCI31901.

[131] Ikram H, Crozier IG. Xamoterol in severe heart failure. The Lancet 1990;336:517–8. https://doi.org/10.1016/0140-6736(90)92078-V.

[132] Ray S, Saboo B, Roy D, Prasad Sinha D, Kahali D, Kanti Das M, et al. The Beta-blocker chronicle: From past principles to present practice – Implications for the Indian subcontinent. Indian Heart J 2025;77:471–9. https://doi.org/10.1016/j.ihj.2025.10.006.

[133] Packer M, Carver JR, Rodeheffer RJ, Ivanhoe RJ, DiBianco R, Zeldis SM, et al. Effect of Oral Milrinone on Mortality in Severe Chronic Heart Failure. N Engl J Med 1991;325:1468–75. https://doi.org/10.1056/NEJM199111213252103.

[134] Ishikura F, Takano Y, Ueyama T. Acute effects of beta-blocker with intrinsic sympathomimetic activity on stress-induced cardiac dysfunction in rats. J Cardiol 2012;60:470–4. https://doi.org/10.1016/j.jjcc.2012.07.004.

[135] Naccarelli GV, Lukas MA. Carvedilol's antiarrhythmic properties: Therapeutic implications in patients with left ventricular dysfunction. Clin Cardiol 2006;28:165–73. https://doi.org/10.1002/clc.4960280403.

[136] Yue TL, Cheng HY, Lysko PG, McKenna PJ, Feuerstein R, Gu JL, et al. Carvedilol, a new vasodilator and beta adrenoceptor antagonist, is an antioxidant and free radical scavenger. J Pharmacol Exp Ther 1992;263:92–8.

[137] Bristow MR, Larrabee P, Minobe W, Roden R, Skerl L, Klein J, et al. Receptor Pharmacology of Carvedilol in the Human Heart. J Cardiovasc Pharmacol 1992;19:S68.

[138] Woo AYH, Xiao R. β-Adrenergic receptor subtype signaling in heart: From bench to bedside. Acta Pharmacol Sin 2012;33:335–41. https://doi.org/10.1038/aps.2011.201.

[139] Lefkowitz RJ, Rockman HA, Shim PJ, Liu S, Ahn S, Pani B, et al. How carvedilol does not activate β2-adrenoceptors. Nat Commun 2023;14:7866. https://doi.org/10.1038/s41467-023-42848-5.

[140] Brixius K, Bundkirchen A, Bölck B, Mehlhorn U, Schwinger RHG. Nebivolol, bucindolol, metoprolol and carvedilol are devoid of intrinsic sympathomimetic activity in human myocardium. Br J Pharmacol 2001;133:1330–8. https://doi.org/10.1038/sj.bjp.0704188.

[141] null null. A Trial of the Beta-Blocker Bucindolol in Patients with Advanced Chronic Heart Failure. N Engl J Med 2001;344:1659–67. https://doi.org/10.1056/NEJM200105313442202.

[142] Pani B, Ahn S, Rambarat PK, Vege S, Kahsai AW, Liu A, et al. Unique Positive Cooperativity Between the β-Arrestin–Biased β-Blocker Carvedilol and a Small Molecule Positive Allosteric Modulator of the β2-Adrenergic Receptor. Mol Pharmacol 2021;100:513–25. https://doi.org/10.1124/molpharm.121.000363.

[143] Morgan T. Clinical pharmacokinetics and pharmacodynamics of carvedilol. Clin Pharmacokinet 1994;26:335–46. https://doi.org/10.2165/00003088-199426050-00002.

[144] Baker JG. The selectivity of β -adrenoceptor antagonists at the human β 1, β 2 and β 3 adrenoceptors. Br J Pharmacol 2005;144:317–22. https://doi.org/10.1038/sj.bjp.0706048.

[145] Baker JG, Hall IP, Hill SJ. Agonist and Inverse Agonist Actions of β-Blockers at the Human β2-Adrenoceptor Provide Evidence for Agonist-Directed Signaling. Mol Pharmacol 2003;64:1357–69. https://doi.org/10.1124/mol.64.6.1357.

[146] Baker JG, Hall IP, Hill SJ. Influence of agonist efficacy and receptor phosphorylation on antagonist affinity measurements: differences between second messenger and reporter gene responses. Mol Pharmacol 2003;64:679–88. https://doi.org/10.1124/mol.64.3.679.

[147] Kostenis E, Gomeza J, Miess-Tanneberg E, Blum NK, Benkel T, Chevigné A, et al. Reply to: How carvedilol does not activate β2-adrenoceptors. Nat Commun 2023;14:7867. https://doi.org/10.1038/s41467-023-42849-4.

[148] Bilski AJ, Halliday SE, Fitzgerald JD, Wale JL. The pharmacology of a beta 2-selective adrenoceptor antagonist (ICI 118,551). J Cardiovasc

Pharmacol 1983;5:430–7. https://doi.org/10.1097/00005344-198305000-00013.

[149] Dooley DJ, Bittiger H, Reymann NC. CGP 20712 A: a useful tool for quantitating beta 1- and beta 2-adrenoceptors. Eur J Pharmacol 1986;130:137–9. https://doi.org/10.1016/0014-2999(86)90193-7.

[150] Sato Y, Kurose H, Isogaya M, Nagao T. Molecular characterization of pharmacological properties of T-0509 for β-adrenoceptors. Eur J Pharmacol 1996;315:363–7. https://doi.org/10.1016/S0014-2999(96)00648-6.

[151] Baker JG. The selectivity of β-adrenoceptor agonists at human β1-, β2- and β3-adrenoceptors. Br J Pharmacol 2010;160:1048–61. https://doi.org/10.1111/j.1476-5381.2010.00754.x.

[152] Candelore MR, Deng L, Tota L, Guan XM, Amend A, Liu Y, et al. Potent and selective human beta(3)-adrenergic receptor antagonists. J Pharmacol Exp Ther 1999;290:649–55.

[153] Watts SW, Fink GD, Silver PJ, Cushing DJ. Interaction of the beta adrenergic receptor antagonist bucindolol with serotonergic receptors. J Cardiovasc Pharmacol 2000;35:29–36. https://doi.org/10.1097/00005344-200001000-00004.

[154] Louis SN, Nero TL, Iakovidis D, Jackman GP, Louis WJ. LK 204-545, a highly selective beta1-adrenoceptor antagonist at human beta-adrenoceptors. Eur J Pharmacol 1999;367:431–5. https://doi.org/10.1016/s0014-2999(99)00019-9.

[155] Sato T, Baker J, Warne T, Brown GA, Leslie AGW, Congreve M, et al. Pharmacological Analysis and Structure Determination of 7-Methylcyanopindolol-Bound β1-Adrenergic Receptor. Mol Pharmacol 2015;88:1024–34. https://doi.org/10.1124/mol.115.101030.

[156] Wildman SA, Crippen GM. Prediction of Physicochemical Parameters by Atomic Contributions. J Chem Inf Comput Sci 1999;39:868–73. https://doi.org/10.1021/ci990307l.

[157] Ertl P, Rohde B, Selzer P. Fast calculation of molecular polar surface area as a sum of fragment-based contributions and its application to the prediction of drug transport properties. J Med Chem 2000;43:3714–7. https://doi.org/10.1021/jm000942e.

[158] Daina A, Michielin O, Zoete V. SwissADME: a free web tool to evaluate pharmacokinetics, drug-likeness and medicinal chemistry friendliness of small molecules. Sci Rep 2017;7:42717. https://doi.org/10.1038/srep42717.

[159] Kim S, Chen J, Cheng T, Gindulyte A, He J, He S, et al. PubChem 2025 update. Nucleic Acids Res 2025;53:D1516–25. https://doi.org/10.1093/nar/gkae1059.

[160] M A, M Y, T M, A K, K A, F N, et al. ORP9-PH domain-based fluorescent reporters for visualizing phosphatidylinositol 4-phosphate dynamics in living cells. RSC Chem Biol 2024;5. https://doi.org/10.1039/d3cb00232b.

[161] Massengill CI, Day-Cooney J, Mao T, Zhong H. Genetically encoded sensors towards imaging cAMP and PKA activity *in vivo*. J Neurosci Methods 2021;362:109298. https://doi.org/10.1016/j.jneumeth.2021.109298.

[162] Subramaniam G, Schleicher K, Kovanich D, Zerio A, Folkmanaite M, Chao Y-C, et al. Integrated Proteomics Unveils Nuclear PDE3A2 as a Regulator of Cardiac Myocyte Hypertrophy. Circ Res 2023;132:828–48. https://doi.org/10.1161/CIRCRESAHA.122.321448.

[163] Kayser C, Lohse MJ, Bock A. Real-Time Measurements of Intracellular cAMP Gradients Using FRET-Based cAMP Nanorulers. Methods Mol Biol Clifton NJ 2022;2483:1–13. https://doi.org/10.1007/978-1-0716-2245-2_1.

[164] Prakash A, Markham A. Metoprolol: a review of its use in chronic heart failure. Drugs 2000;60:647–78. https://doi.org/10.2165/00003495-200060030-00011.

[165] Chen Y, Li T. Early metoprolol use in ICU patients with congestive heart failure is associated with increased 30-day mortality: a causal machine learning study. Front Pharmacol 2026;17:1771969. https://doi.org/10.3389/fphar.2026.1771969.

[166] Fujimaki M. Stereoselective disposition and tissue distribution of carvedilol enantiomers in rats. Chirality 1992;4:148–54. https://doi.org/10.1002/chir.530040304.

[167] Stahl E, Mutschler E, Baumgartner U, Spahn-Langguth H. Carvedilol Stereopharmacokinetics in Rats: Affinities to Blood Constituents and Tissues. Arch Pharm (Weinheim) 1993;326:529–33. https://doi.org/10.1002/ardp.19933260907.

[168] Zhou Q, Xiao J, Jiang D, Wang R, Vembaiyan K, Wang A, et al. Carvedilol and its new analogs suppress arrhythmogenic store overload-induced Ca2+ release. Nat Med 2011;17:1003–9. https://doi.org/10.1038/nm.2406.

[169] van der Krogt GNM, Ogink J, Ponsioen B, Jalink K. A Comparison of Donor-Acceptor Pairs for Genetically Encoded FRET Sensors: Application

to the Epac cAMP Sensor as an Example. PLoS ONE 2008;3:e1916. https://doi.org/10.1371/journal.pone.0001916.

[170] Lin T-Y, Mai QN, Zhang H, Wilson E, Chien H-C, Yee SW, et al. Cardiac contraction and relaxation are regulated by distinct subcellular cAMP pools. Nat Chem Biol 2024;20:62–73. https://doi.org/10.1038/s41589-023-01381-8.

[171] Liccardo F, Morstein J, Lin T-Y, Pampel J, Lang D, Shokat KM, et al. Subcellular activation of β-adrenergic receptors using a spatially restricted antagonist. Proc Natl Acad Sci 2024;121:e2404243121. https://doi.org/10.1073/pnas.2404243121.

[172] Shen A, Chen D, Kaur M, Bartels P, Xu B, Shi Q, et al. β-blockers augment L-type Ca2+ channel activity by targeting spatially restricted β2AR signaling in neurons. eLife 2019;8:e49464. https://doi.org/10.7554/eLife.49464.

[173] Baker JG, Hall IP, Hill SJ. Agonist Actions of "β-Blockers" Provide Evidence for Two Agonist Activation Sites or Conformations of the Human β1-Adrenoceptor. Mol Pharmacol 2003;63:1312–21. https://doi.org/10.1124/mol.63.6.1312.

[174] Smart NA, Kwok N, Holland DJ, Jayasighe R, Giallauria F. Bucindolol: A Pharmacogenomic Perspective on Its Use in Chronic Heart Failure. Clin Med Insights Cardiol 2011;5:55–66. https://doi.org/10.4137/CMC.S4309.

[175] Liggett SB, Mialet-Perez J, Thaneemit-Chen S, Weber SA, Greene SM, Hodne D, et al. A polymorphism within a conserved β1-adrenergic receptor motif alters cardiac function and β-blocker response in human heart failure. Proc Natl Acad Sci 2006;103:11288–93. https://doi.org/10.1073/pnas.0509937103.

[176] Rochais F, Vilardaga J-P, Nikolaev VO, Bünemann M, Lohse MJ, Engelhardt S. Real-time optical recording of β_1-adrenergic receptor activation reveals supersensitivity of the Arg389 variant to carvedilol. J Clin Invest 2007;117:229–35. https://doi.org/10.1172/JCI30012.

[177] Galandrin S, Oligny-Longpré G, Bonin H, Ogawa K, Galés C, Bouvier M. Conformational Rearrangements and Signaling Cascades Involved in Ligand-Biased Mitogen-Activated Protein Kinase Signaling through the β1-Adrenergic Receptor. Mol Pharmacol 2008;74:162–72. https://doi.org/10.1124/mol.107.043893.

[178] Marwood JF, Stokes GS. Studies on the vasodilator actions of bucindolol in the rat. Clin Exp Pharmacol Physiol 1986;13:59–68. https://doi.org/10.1111/j.1440-1681.1986.tb00316.x.

[179] Hershberger RE, Wynn JR, Sundberg L, Bristow MR. Mechanism of action of bucindolol in human ventricular myocardium. J Cardiovasc Pharmacol 1990;15:959–67. https://doi.org/10.1097/00005344-199006000-00014.

[180] Subcellular activation of β-adrenergic receptors using a spatially restricted antagonist | PNAS n.d. https://www.pnas.org/doi/10.1073/pnas.2404243121 (accessed July 11, 2026).

[181] Warne T, Edwards PC, Leslie AGW, Tate CG. Crystal Structures of a Stabilized β1-Adrenoceptor Bound to the Biased Agonists Bucindolol and Carvedilol. Struct England1993 2012;20–540:841–9. https://doi.org/10.1016/j.str.2012.03.014.

[182] Yao A, Kohmoto O, Oyama T, Sugishita Y, Shimizu T, Harada K, et al. Characteristic effects of alpha1-beta1,2-adrenergic blocking agent, carvedilol, on [Ca2+]i in ventricular myocytes compared with those of timolol and atenolol. Circ J Off J Jpn Circ Soc 2003;67:83–90. https://doi.org/10.1253/circj.67.83.

[183] Maack C, Böhm M, Vlaskin L, Dabew E, Lorenz K, Schäfers H-J, et al. Partial agonist activity of bucindolol is dependent on the activation state of the human beta1-adrenergic receptor. Circulation 2003;108:348–53. https://doi.org/10.1161/01.CIR.0000080325.94345.8B.

[184] Lattion A-L, Abuin L, Nenniger-Tosato M, Cotecchia S. Constitutively active mutants of the β1-adrenergic receptor. FEBS Lett 1999;457:302–6. https://doi.org/10.1016/S0014-5793(99)01064-9.

[185] England PJ, Shahid M. Effects of forskolin on contractile responses and protein phosphorylation in the isolated perfused rat heart. Biochem J 1987;246:687–95. https://doi.org/10.1042/bj2460687.

[186] Hohl CM, Li QA. Compartmentation of cAMP in adult canine ventricular myocytes. Relation to single-cell free Ca2+ transients. Circ Res 1991;69:1369–79. https://doi.org/10.1161/01.RES.69.5.1369.

[187] Fink M, Noble PJ, Noble D. Ca2+-induced delayed afterdepolarizations are triggered by dyadic subspace Ca2+ affirming that increasing SERCA reduces aftercontractions. Am J Physiol - Heart Circ Physiol 2011;301:H921–35. https://doi.org/10.1152/ajpheart.01055.2010.

[188] Kenakin T. Functional Selectivity through Protean and Biased Agonism: Who Steers the Ship? Mol Pharmacol 2007. https://doi.org/10.1124/mol.107.040352.

[189] Wedemeyer MJ, Chavera TS, Berg KA, Clarke WP. Insurmountable antagonism of human mu opioid receptors by buprenorphine is due to hemi-equilibrium. Eur J Pharmacol 2025;987:177192. https://doi.org/10.1016/j.ejphar.2024.177192.

[190] Riddy DM, Valant C, Rueda P, Charman WN, Et. A. Label-Free Kinetics: Exploiting Functional Hemi-Equilibrium to Derive Rate Constants for Muscarinic Receptor Antagonists. Mol Pharmacol 2015. https://doi.org/10.1124/mol.115.100545.

[191] Mika D, Richter W, Westenbroek RE, Catterall WA, Conti M. PDE4B mediates local feedback regulation of β_1-adrenergic cAMP signaling in a sarcolemmal compartment of cardiac myocytes. J Cell Sci 2014;127:1033–42. https://doi.org/10.1242/jcs.140251.

[192] Devic E, Xiang Y, Gould D, Kobilka B. Beta-adrenergic receptor subtype-specific signaling in cardiac myocytes from beta(1) and beta(2) adrenoceptor knockout mice. Mol Pharmacol 2001;60:577–83.

[193] Leroy J, Abi-Gerges A, Nikolaev VO, Richter W, Lechêne P, Mazet J-L, et al. Spatiotemporal dynamics of beta-adrenergic cAMP signals and L-type Ca2+ channel regulation in adult rat ventricular myocytes: role of phosphodiesterases. Circ Res 2008;102:1091–100. https://doi.org/10.1161/CIRCRESAHA.107.167817.

[194] Kuschel M, Zhou YY, Cheng H, Zhang SJ, Chen Y, Lakatta EG, et al. G(i) protein-mediated functional compartmentalization of cardiac beta(2)-adrenergic signaling. J Biol Chem 1999;274:22048–52. https://doi.org/10.1074/jbc.274.31.22048.

[195] Bartel S, Krause E-G, Wallukat G, Karczewski P. New insights into beta2-adrenoceptor signaling in the adult rat heart. Cardiovasc Res 2003;57:694–703. https://doi.org/10.1016/s0008-6363(02)00720-4.

[196] Su M, Paknejad N, Zhu L, Wang J, Do HN, Miao Y, et al. Structures of β1-adrenergic receptor in complex with Gs and ligands of different efficacies. Nat Commun 2022;13:4095. https://doi.org/10.1038/s41467-022-31823-1.

[197] Manglik A, Kim TH, Masureel M, Altenbach C, Yang Z, Hilger D, et al. Structural insights into the dynamic process of β2-adrenergic receptor signaling. Cell 2015;161:1101–11. https://doi.org/10.1016/j.cell.2015.04.043.

[198] Lieu DK, Liu J, Siu C-W, McNerney GP, Tse H-F, Abu-Khalil A, et al. Absence of Transverse Tubules Contributes to Non-Uniform Ca2+ Wavefronts in Mouse and Human Embryonic Stem Cell–Derived Cardiomyocytes. Stem Cells Dev 2009;18:1493–500. https://doi.org/10.1089/scd.2009.0052.

[199] Xiao S, Shaw RM. Cardiomyocyte Protein Trafficking: Relevance to Heart Disease and Opportunities for Therapeutic Intervention. Trends Cardiovasc Med 2015;25:379–89. https://doi.org/10.1016/j.tcm.2014.12.012.

[200] Chen EC, Matsson P, Azimi M, Zhou X, Handin N, Yee SW, et al. High Throughput Screening of a Prescription Drug Library for Inhibitors of Organic Cation Transporter 3, OCT3. Pharm Res 2022;39:1599–613. https://doi.org/10.1007/s11095-022-03171-8.

[201] Butler S, Wang R, Wunder SL, Cheng H-Y, Randall CS. Perturbing effects of carvedilol on a model membrane system: role of lipophilicity and chemical structure. Biophys Chem 2006;119:307–15. https://doi.org/10.1016/j.bpc.2005.09.004.

[202] Khanppnavar B, Maier J, Herborg F, Gradisch R, Lazzarin E, Luethi D, et al. Structural basis of organic cation transporter-3 inhibition. Nat Commun 2022;13:6714. https://doi.org/10.1038/s41467-022-34284-8.

[203] Ablorh N-AD, Thomas DD. Phospholamban phosphorylation, mutation, and structural dynamics: a biophysical approach to understanding and treating cardiomyopathy. Biophys Rev 2015;7:63–76. https://doi.org/10.1007/s12551-014-0157-z.

[204] Neubauer S. The Failing Heart — An Engine Out of Fuel. N Engl J Med 2007;356:1140–51. https://doi.org/10.1056/NEJMra063052.

[205] Greenberg B, Butler J, Felker GM, Ponikowski P, Voors AA, Desai AS, et al. Calcium upregulation by percutaneous administration of gene therapy in patients with cardiac disease (CUPID 2): a randomised, multinational, double-blind, placebo-controlled, phase 2b trial. The Lancet 2016;387:1178–86. https://doi.org/10.1016/S0140-6736(16)00082-9.

[206] Marx SO, Reiken S, Hisamatsu Y, Jayaraman T, Burkhoff D, Rosemblit N, et al. PKA phosphorylation dissociates FKBP12.6 from the calcium release channel (ryanodine receptor): defective regulation in failing hearts. Cell 2000;101:365–76. https://doi.org/10.1016/s0092-8674(00)80847-8.

[207] Podbregar M, Voga G. Effect of selective and nonselective beta-blockers on resting energy production rate and total body substrate utilization in chronic heart failure. J Card Fail 2002;8:369–78. https://doi.org/10.1054/jcaf.2002.130238.

[208] Wallhaus TR, Taylor M, DeGrado TR, Russell DC, Stanko P, Nickles RJ, et al. Myocardial Free Fatty Acid and Glucose Use After Carvedilol Treatment in Patients With Congestive Heart Failure. Circulation 2001;103:2441–6. https://doi.org/10.1161/01.CIR.103.20.2441.

[209] Messer AE, Jacques AM, Marston SB. Troponin phosphorylation and regulatory function in human heart muscle: dephosphorylation of Ser23/24 on troponin I could account for the contractile defect in end-stage heart failure. J Mol Cell Cardiol 2007;42:247–59. https://doi.org/10.1016/j.yjmcc.2006.08.017.

[210] Kuznetsov V, Pak E, Robinson RB, Steinberg SF. Beta 2-adrenergic receptor actions in neonatal and adult rat ventricular myocytes. Circ Res 1995;76:40–52. https://doi.org/10.1161/01.res.76.1.40.

[211] Louch WE, Koivumäki JT, Tavi P. Calcium signalling in developing cardiomyocytes: implications for model systems and disease. J Physiol 2015;593:1047–63. https://doi.org/10.1113/jphysiol.2014.274712.

[212] Kontogiannis C, Kosmopoulos M, Georgiopoulos G, Spartalis M, Paraskevaidis I, Chatzidou S. Mitochondria in β-adrenergic signaling: emerging therapeutic perspectives in heart failure and ventricular arrhythmias. J Thorac Dis 2018;10:S4183–5. https://doi.org/10.21037/jtd.2018.11.01.

[213] Tate KM, Briend-Sutren MM, Emorine LJ, Delavier-Klutchko C, Marullo S, Strosberg AD. Expression of three human beta-adrenergic-receptor subtypes in transfected Chinese hamster ovary cells. Eur J Biochem 1991;196:357–61. https://doi.org/10.1111/j.1432-1033.1991.tb15824.x.